THESIS

# PROTOTYPING A TEMPERATURE-RESPONSIVE FLEXIBLE COLORIMETRIC SENSOR WITH MACHINE LEARNING-BASED RESULT INTERPRETATION

Submitted by

Naimul Hasan

Department of Design and Merchandising

In partial fulfillment of the requirements

For the Degree of Master of Science

Colorado State University

Fort Collins, Colorado

Summer 2025

Master's Committee:

Advisor: Yan Vivian Li

Kristen Morris
Nathaniel Blanchard

ABSTRACT

PROTOTYPING A TEMPERATURE-RESPONSIVE FLEXIBLE COLORIMETRIC SENSOR WITH MACHINE LEARNING-BASED RESULT INTERPRETATION

This research focuses on developing a flexible, colorimetric biosensor for temperature detection by integrating thermochromic nanofibers with machine learning for automated image-based analysis and temperature prediction. The sensor uses 10,12-pentacosadiynoic acid (PCDA), a material known for its visible blue-to-red transition in response to heat, embedded in a coaxial electrospun core–shell fiber. The outer shell, composed of PCDA, polyurethane (PU), and polyethylene oxide (PEO), enables a fast and visible color response, while the PEO-based core provides mechanical stability and supports fiber formation. The primary goal was to examine how different PCDA concentrations, temperature levels, and thermal exposure durations affect the intensity, speed, and consistency of the colorimetric response. Sensors were fabricated with PCDA concentrations ranging from 5% to 20% and tested across six temperatures (55°C to 80°C) and six exposure times (1 to 120 seconds). Among all combinations, the 18% PCDA concentration at 30 seconds produced the most vivid and stable color shift, making it the optimal configuration for practical use.

To enable automated analysis, a convolutional neural network (CNN) was trained on over 4,000 images to predict temperature from RGB color data. The best model achieved a test $R^2$ of 0.884 and a mean absolute error below 1.3°C, confirming its ability to accurately interpret thermochromic behavior. A web-based interface was also developed, allowing users to upload images and receive instant temperature predictions, eliminating the need for manual

interpretation or lab-based equipment. The results demonstrate a strong correlation between material composition, stimulus conditions, and sensor performance, and show that machine learning can significantly improve both the accuracy and usability of colorimetric sensors. Real-world testing confirmed the sensor's flexibility, responsiveness, and visual clarity, making it suitable for integration into wearable safety gear, industrial equipment, and smart textiles. It also shows promise for use in food processing, packaging, and environmental monitoring—especially in settings where quick, low-cost temperature assessment is needed without electronic devices. Looking forward, the modular design of this platform offers clear pathways for expansion. Future work may explore using the same PCDA-based system for pH or bacterial detection, leveraging its inherent responsiveness, and potentially incorporating antimicrobial agents for dual-function sensing and drug release. Overall, this study lays the foundation for intelligent, low-cost biosensors that support real-time, automated monitoring in healthcare, environmental safety, and smart textile applications.

# ACKNOWLEDGMENTS

First, I would like to express my sincere gratitude to my advisor, Dr. Yan Vivian Li, for her continuous support, mentorship, and inspiration throughout the course of this research. Her deep insight, encouragement, and unwavering guidance have been instrumental in shaping both this project and my development as a scholar.

I am especially grateful to Dr. Kristen Morris, who served as the committee member overseeing the overall thesis. Her thoughtful feedback, rigorous standards, and constructive suggestions have significantly strengthened the structure and clarity of this work.

I would also like to thank Dr. Nathaniel Blanchard, who contributed valuable expertise to the machine learning component of this research. His guidance helped refine the modeling strategy and enriched the interdisciplinary dimension of this study.

I am thankful to the Department of Design and Merchandising at Colorado State University for providing the research facilities, resources, and a supportive academic environment. I also appreciate the technical support and encouragement from lab colleagues and staff throughout this journey.

Lastly, I extend heartfelt thanks to my family and loved ones for their constant support, patience, and motivation. Your belief in me made this accomplishment possible.

TABLE OF CONTENTS

LIST OF TABLES

LIST OF FIGURES

# CHAPTER I – INTRODUCTION

Polydiacetylenes (PDAs) have gained substantial interest in sensor technology due to their unique capability to visibly change color in response to various environmental and biological stimuli. These conjugated polymers feature an alternating pattern of single and triple carbon bonds, forming a highly ordered π-conjugated backbone that enables their color transitions. When exposed to specific stimuli such as temperature, pH, mechanical stress, or the presence of pathogens like bacteria, PDA molecules undergo conformational changes that result in a visible color shift, typically from blue to red. This transition is characterized by a bathochromic shift within the visible light spectrum, typically observed as a color change corresponding to a shift in absorption from approximately 640 nm (blue) to 540 nm (red) (Fratini et al., 2020; Jiang et al., 2019). The ability of PDA to serve as a label-free and instrument-free colorimetric sensing material has led to its widespread consideration in various applications, including biosensors, environmental monitoring, food packaging, drug delivery and medical diagnostics (Hassan et al., 2019; Wang et al., 2004).

Over the years, various fabrication methods have been used to incorporate PDA into sensor platforms. Traditional techniques such as spray coating, melt-blowing, and solution casting are frequently used due to their simplicity and compatibility with large-scale manufacturing. For instance, Kim et al. (2019) fabricated PDA-based films via spray coating for smart packaging applications, while Koo et al. (2020) utilized melt-blowing to create disposable textile sensors. However, these methods often have disadvantages such as uneven surface morphology, limited control over material distribution, and poor color uniformity. These

problems can result in delayed or inconsistent sensor responses, reducing the reliability of PDA-based devices in real-world applications.

To overcome these challenges, the electrospinning process has emerged as a promising method for producing PDA-integrated nanofibrous sensors. Electrospinning utilizes a high-voltage electric field to stretch a liquid polymer into extremely thin nanofibers, resulting in soft, flexible fiber mats with a large surface area. When PDA is embedded within these fibers, the resulting architecture provides enhanced responsiveness to environmental stimuli due to the increased surface-area-to-volume ratio, improved dispersion of chromatic material, and better interaction with surrounding conditions (Alam et al., 2016; Bhattacharjee et al., 2023). Electrospun PDA fibers have shown promising results for temperature detection, bacterial sensing, and colorimetric diagnostics, outperforming conventional PDA films in terms of response time and signal intensity (Liu et al., 2022). Furthermore, the tunability of fiber morphology makes electrospinning an excellent method for creating wearable and flexible sensors that can be integrated into fabrics or attached to different surfaces.

A more advanced form of this technique—coaxial electrospinning—allows for the fabrication of core–shell fibers in which two different polymer solutions are simultaneously electrospun through a concentric nozzle. This setup produces fibers with an internal core and an outer shell, enabling spatial separation of functionalities. The shell can accommodate active sensing material, while the core provides mechanical stability and may also serve additional roles, such as drug storage or thermal insulation. One relevant study by Sun et al. (2025) demonstrated the development of core–shell fibers loaded with gentamicin-encapsulated PLGA nanoparticles for sustained antibiotic release in wound healing applications. Their work illustrates the multifunctionality and structural versatility that coaxial electrospinning offers—

benefits that can also be harnessed for sensing applications. In PDA-based sensors, positioning the PDA within the shell enables maximum exposure to external stimuli, resulting in more consistent and rapid colorimetric responses. Meanwhile, the core, composed of polymers such as polyethylene oxide (PEO) and polyurethane (PU), can contribute to fiber stability and mechanical strength. However, PDA alone is not electrospinnable due to its rigid backbone, poor solubility, and lack of polymeric chain entanglement. Additionally, PDA monomers like PCDA are relatively costly, making their exclusive use impractical for large-scale fabrication. To overcome these limitations, electrospinnable carrier polymers, such as polyurethane (PU) and polyethylene oxide (PEO), are blended with PCDA to enhance mechanical properties and ensure consistent fiber formation (Li et al., 2021). The optimal concentration of PCDA in the electrospinning mixture has not been definitively established by prior research. While a higher PCDA content generally enhances the visual intensity of the color change, it also causes processing challenges and increases mechanical brittleness. Additionally, sensor performance depends not only on composition but also on the duration of stimulus exposure, as the rate of chromatic change can vary with temperature and exposure time. These interconnected factors—PCDA concentration and thermal response time—require systematic study to enhance the sensitivity, consistency, and practical application of PDA-based colorimetric sensors.

Our current study aims to develop a temperature-sensitive colorimetric sensor using coaxial electrospun PCDA-based fibers, with integrated machine learning analysis for automated temperature prediction. In this work, the shell of the fiber contained a blend of PCDA, PU, and PEO, ensuring both stimulus responsiveness and electrospinnability. The core consisted of PEO, serving as a support structure that aided fiber formation and maintained mechanical strength. Fiber mats were fabricated at six different PCDA concentrations—5%, 10%, 12%, 15%, 18%,

and 20%—to investigate the effect of PCDA concentration on the colorimetric response. Each sample was exposed to temperatures ranging from 55°C to 80°C for six different durations—1, 5, 10, 30, 60, and 120 seconds—in order to observe the resulting color change. For each condition, 20 images were captured under standard lighting conditions while varying viewing angles to simulate real-world variability and improve data diversity for model training.

To eliminate subjectivity in interpreting the color transitions, machine learning models were integrated into the process. Color data of the sensors was extracted from each image in the form of average RGB values and used to train a supervised machine learning model. A convolutional neural network (CNN) model was developed to predict the corresponding temperature based on these RGB features. The model was trained using a stratified set of images across all PCDA concentrations, response times, and temperature points. This approach ensured that the model could reliably predict the temperature of previously unseen samples based on their colorimetric response. Another objective of this study was to develop a web-based platform that can receive sensor images as input and accurately predict the corresponding temperature, eliminating the need for manual color interpretation.

The integration of machine learning into PDA-based sensors provided several practical advantages. First, it improved objectivity by replacing subjective visual interpretation with machine learning-based analysis. Second, it enables real-time monitoring using portable imaging devices like smartphones or wearable cameras. Third, it facilitated the development of smart and flexible sensors that can be embedded in smart textiles or remote-monitoring platforms. Previous studies demonstrated the feasibility of using ML algorithms to interpret colorimetric responses in a variety of contexts, including environmental monitoring, contaminant detection, and diagnostic assays (Aria et al., 2021; Kim et al., 2022; Xu et al., 2020). This research builds upon existing

work by applying machine learning techniques specifically to PCDA-based fiber sensors and validating the approach across various material compositions and time–temperature conditions.

While this study focused exclusively on temperature prediction, the platform design allowed for potential expansion into broader sensing applications. For instance, the PDA shell can be modified to respond to pH changes or biological agents such as bacteria, enabling the development of multifunctional sensors. Likewise, the fiber core can be loaded with antimicrobial agents or drugs, transforming the system into a dual-purpose material for both detection and therapeutic intervention, similar to approaches used in controlled drug delivery (Sun et al., 2025). These developments represent promising future directions for wearable and biomedical sensor systems.

In summary, this project investigated the fabrication, optimization, and image-based analysis of coaxial electrospun PDA fibers for temperature sensing applications. By systematically varying PCDA concentration and response time, the study identified optimal parameters for developing the sensor. The application of machine learning enabled automated interpretation of colorimetric changes, reducing user error and enabling integration with portable technologies. This work advanced the field of smart sensing by combining sensor materials, nanofiber engineering, and artificial intelligence to develop scalable, low-cost, and real-time sensor platforms.

## 1.1 Aims and Objectives

The main goal of this research **is** to develop a smart, colorimetric sensor capable of accurately predicting temperature changes based on visible chromatic transitions in electrospun polydiacetylene (PDA) nanofibers. The project **focused** on the fabrication of coaxial core–shell fibers integrated with machine learning (ML) to eliminate subjective interpretation and enable automated temperature prediction. The specific objectives of this study are as follows:

1. **Fabrication of Core–Shell Nanofiber Sensors**

   Design and produce core–shell nanofibers using coaxial electrospinning, with a shell made of PCDA blended with PU and PEO for thermochromic responsiveness, and a core of PEO to ensure mechanical stability and fiber formation.

2. **Optimization of PCDA Concentration**

   Systematically vary PCDA concentrations (5% to 20%) in the shell layer to assess the effect of composition on fiber morphology, processability, and colorimetric response under thermal stimuli.

3. **Evaluation of Thermal Response Dynamics**

   To investigate how varying temperatures (55°C to 80°C) and exposure durations (1 to 120 seconds) influence the intensity and consistency of the sensor's colorimetric response.

4. **Development of a Machine Learning Model for Temperature Prediction**

   Train a convolutional neural network (CNN) model on RGB data extracted from sensor images to accurately predict temperature from colorimetric output.

## 1.2 Rationale/Significance of This Project

This project is driven by the growing need for innovative, affordable smart sensor technologies that can deliver fast and reliable environmental feedback. There's a growing importance for sensor systems that can provide real-time data interpretation easily, without relying on complicated equipment or personal observation. Developing such user-friendly and efficient sensors could really make a difference in many fields. Polydiacetylenes (PDAs), and specifically 10,12-pentacosadiynoic acid (PCDA), provide an ideal foundation for colorimetric sensors due to their visible chromatic transitions in response to temperature. This distinct color change from blue to red can act as an intuitive indicator of environmental shifts, making PDA-based sensors highly effective for safety monitoring, health diagnostics, and responsive textile applications.

What distinguishes this project is its combination of electrospun nanofiber structure with machine learning–based result analysis. Electrospinning enables the production of uniform nanofibers with a high surface-area-to-volume ratio, which enhances the sensitivity and responsiveness of PDA-based sensors. This architecture allows for rapid interaction with thermal stimuli and more consistent color changes, offering clear advantages over traditional PDA films or cast layers. Additionally, the use of coaxial electrospinning allows PCDA to be strategically positioned in the shell layer of core–shell fibers, where it remains fully exposed to environmental stimuli. Meanwhile, the PEO-based core provides structural support and flexibility, ensuring mechanical stability without compromising responsiveness.

A critical challenge with colorimetric sensors is their reliance on subjective manual visual interpretation, which can be inconsistent and influenced by factors such as lighting or user perception. This project addresses that challenge through the development of a convolutional

neural network (CNN) model that will automate the interpretation of color changes due to external stimuli. By training the model on RGB values extracted from scanned images of the sensors under standard lighting conditions, the system has learned to predict temperature from the sensor images accurately. This ML integration transforms the sensor from an ordinary platform into a smart sensor system that can be used with minimal user input, supporting real-time monitoring.

While this study is focused on temperature sensing, the sensor architecture is designed with modularity in mind. The same platform could be adapted in future work to respond to other stimuli—such as pH level change or bacterial presence—by modifying the PCDA formulation or incorporating bioreactive agents. Similarly, the core of the coaxial fibers could be functionalized with antibiotic, opening the pathway for dual-function materials that combine detection with response capabilities. Such adaptability points toward future applications in smart textiles, wearable diagnostics, and environmental safety systems. Overall, this project marks a significant advancement in the development of smart, responsive and user-friendly sensors. By integrating thermochromic materials, advanced fiber manufacturing, and machine learning, this has established the foundation for scalable, user-independent sensing platforms. These platforms have the potential for broad impact—from personal health monitoring to industrial and environmental safety.

## 1.3 Decision to Focus on Temperature Sensing

At the beginning of this research, the broader potential of the colorimetric sensor platform—including detection of pH changes and bacterial presence—was carefully considered. However, the decision was made to focus solely on temperature sensing for the scope of this thesis. This choice was guided by two main factors. First, temperature is a well-characterized and reliable trigger for PCDA-based colorimetric materials, making it an ideal starting point for validating the sensor's performance. It also offered practical advantages during testing, as it could be precisely controlled in the laboratory using a digital hotplate with an accuracy of ±0.5°C. This level of control allowed for a more systematic study of the sensor's thermochromic behavior and machine learning integration, without the added complexity and variability of multiple analyte types. Second, while the sensor platform is inherently capable of responding to pH changes and bacterial presence through PCDA's natural sensitivity, incorporating therapeutic functionalities—such as antibiotic release—would have required additional modifications to the fiber structure. Expanding the study to include such features would have significantly increased the scope and complexity of the project beyond what was feasible within the thesis timeline. By focusing solely on temperature sensing, this research was able to thoroughly validate the core aspects of sensor fabrication, chromatic performance, and machine learning integration. This focused approach lays a strong foundation for future work that may explore multifunctional capabilities, including integrated detection and treatment systems.

## 1.4 Research Questions and Hypotheses

To guide the research process effectively, the following questions and hypotheses have been formulated:

**Research Question 1:**

How does the concentration of PCDA in the nanofiber shell influence the sensor's sensitivity and colorimetric response time under varying thermal conditions?

**Hypothesis 1:**

Higher PCDA concentrations will enhance the sensor's responsiveness to temperature changes by increasing chromatic intensity and thermal sensitivity, although excessively high concentrations may compromise fiber uniformity and mechanical integrity.

**Research Question 2:**

How does the duration of thermal exposure affect the accuracy and consistency of the sensor's colorimetric transition?

**Hypothesis 2:**

Longer thermal response times will result in more stable and pronounced color transitions, enabling more accurate temperature prediction, while very short exposures may lead to incomplete or inconsistent chromatic response.

**Research Question 3:**

Can machine learning algorithms improve the accuracy and reliability of temperature prediction based on colorimetric output from electrospun PDA fibers?

**Hypothesis 3:**

Machine learning algorithms, particularly convolutional neural networks (CNNs), will significantly enhance the accuracy and consistency of temperature prediction from PDA-based sensors by learning to recognize subtle variations in RGB color data, even under variable imaging conditions.

# CHAPTER II – LITERATURE REVIEW

Biosensors have become indispensable tools in modern science and industry, enabling the rapid, specific, and often real-time detection of biological and chemical substances. These analytical devices combine a biologically sensitive element—such as enzymes, antibodies, nucleic acids, or polymers—with a transducer that converts a biological or chemical interaction into a measurable signal (Liu et al., 2020). The growing importance of biosensors is evident in their widespread applications across sectors such as clinical diagnostics, food safety, environmental monitoring, and industrial process control. In particular, the need for point-of-care, field-deployable, and user-friendly sensor platforms has intensified in recent years, driven by concerns over public health, pollution, and the accessibility of diagnostic technologies (Cho et al., 2020). Traditional biosensing methods often rely on labor-intensive protocols and complex instrumentation, which may not be feasible in remote or time-sensitive scenarios (Hassan et al., 2019). This has led to a shift toward developing lightweight, rapid-response sensors that require minimal infrastructure—an area where colorimetric biosensors have shown significant promise.

Among various smart sensing materials, polydiacetylenes (PDAs) have emerged as a particularly attractive class of conjugated polymers due to their distinctive chromatic transitions in response to external stimuli. PDA molecules are synthesized via topochemical polymerization of diacetylene monomers, resulting in an extended conjugated backbone. In their polymerized form, PDAs typically appear blue; upon stimulus-induced disruption of the conjugation, a color change to red occurs, often accompanied by a bathochromic shift in their absorption spectrum (Jiang et al., 2019; Fratini et al., 2020). These optical shifts are highly visible, label-free, and reversible in many cases, making PDAs ideal candidates for colorimetric sensors that deliver

immediate feedback. Stimuli that can trigger this colorimetric response include temperature, pH, mechanical force, and specific interactions with chemical or biological species (Bhattacharjee et al., 2020; Zhou et al., 2022). The ability to transduce a molecular event into a macroscopic color change offers powerful opportunities in designing low-cost, user-interpretable sensing devices for real-world applications.

The versatility of PDA-based colorimetric sensing has been demonstrated across a wide array of domains. In healthcare, PDAs have been used to detect biomarkers and pathogens by functionalizing their surfaces to interact with specific analytes (Halicka & Cabaj, 2021). In environmental contexts, PDA-coated substrates have been designed to detect toxic gases or heavy metals (Sengodu, 2022). In food safety, PDA sensors have been employed to monitor spoilage or contamination by detecting temperature excursions or microbial growth. Despite this wide applicability, the primary challenge remains in improving the sensitivity, uniformity, and reliability of the PDA response—particularly under varied field conditions. To address this challenge, recent advancements have focused on incorporating PDA into electrospun nanofiber platforms, which offer considerable advantages over traditional thin-film or bulk formats. Electrospinning is a well-established technique that allows for the fabrication of ultrafine polymer fibers with diameters ranging from tens of nanometers to a few micrometers. These fibers can be assembled into nonwoven mats with exceptionally high surface area-to-volume ratios, which is particularly beneficial for sensor responsiveness and analyte interaction (Wang et al., 2004). Embedding PDA into such structures enhances both color change sensitivity and speed, as the increased surface exposure improves the diffusion of thermal or chemical stimuli to the sensing sites (Bhattacharjee et al., 2023). Additionally, electrospun fibers offer mechanical

flexibility and can be easily integrated into textiles, creating opportunities for wearable or deployable smart sensing platforms.

A further refinement of this technique involves the use of coaxial electrospinning to produce core–shell fibers, in which PDA-containing polymers are localized in the outer shell, while the core may be used for mechanical reinforcement or functional payloads. This structure not only stabilizes the fiber morphology but also protects inner components from environmental degradation. While previous studies have demonstrated the use of coaxial fibers for drug delivery and multifunctional scaffolds (Sun et al., 2025), the same architecture can be adapted for smart sensors where the shell interacts directly with external stimuli and the core provides structural or programmable support. In addition to materials innovation, recent literature has emphasized the role of machine learning (ML) in enhancing the analysis and interpretation of colorimetric sensor outputs. PDA-based biosensors, while visually effective, often require subjective interpretation, which can vary based on lighting, viewing angle, and individual perception. ML algorithms—particularly convolutional neural networks (CNNs)—have been shown to successfully extract RGB or HSV data from colorimetric images and correlate them with analyte concentrations, temperature levels, or exposure duration (Aria et al., 2021; Kim et al., 2022). This data-driven approach transforms PDA sensors into automated, intelligent systems that can provide accurate, real-time readouts without human intervention. Moreover, ML models can be trained to accommodate noise and variability in image conditions, making them robust for use in uncontrolled environments or with consumer-grade imaging devices, such as smartphones.

The literature reveals strong potential for PDA-based biosensors when combined with electrospinning techniques and machine learning integration. These developments offer promising solutions to long-standing challenges in biosensing, including low sensitivity,

inconsistent response, and reliance on subjective interpretation. While PDA sensors have been explored for a wide range of stimuli, this project focuses specifically on temperature sensing—a well-characterized yet practically relevant stimulus. The integration of coaxial electrospun nanofibers and ML-based image analysis presents a novel pathway toward the development of portable, scalable, and real-time biosensing systems for applications in smart textiles, environmental monitoring, and thermal diagnostics.

## 2.1 Polydiacetylenes (PDAs)

### *2.1.1 Chemical Structure and Properties*

Polydiacetylenes (PDAs) are a unique class of conjugated polymers characterized by their alternating double and single carbon-carbon bonds, forming a conjugated backbone that contributes to their remarkable optical properties. One of the most notable precursors for PDAs is 10,12-Pentacosadiynoic acid (PCDA), a diacetylene compound that undergoes polymerization to form PDAs. When in its unpolymerized state, PCDA exists as a colorless or pale yellow solid. However, upon polymerization induced by heat or ultraviolet light, PCDA transforms into PDAs, which exhibit striking colorimetric changes, transitioning to vibrant blue or red hues (Bhattacharjee et al., 2020; Halicka & Cabaj, 2021).

The ability of PDAs to undergo significant colorimetric changes is primarily attributed to the formation of extended conjugated systems during polymerization. This transformation enables effective π-electron delocalization, resulting in unique electronic properties and enhanced light absorption characteristics (Liu et al., 2020). The color change serves as a visual indicator of specific environmental conditions, making PDAs particularly suitable for biosensing applications where rapid feedback is essential.

### *2.1.2 Properties of PCDA and Its Role in PDA Formation*

10,12-Pentacosadiynoic acid (PCDA) is significant not only for its role as a precursor but also for its inherent properties that contribute to the performance of PDAs. PCDA possesses a long hydrophobic carbon chain structure with two terminal acetylenic groups, which enables it to form stable films and structures under polymerization conditions (Zhou et al., 2022). The polymerization of PCDA results in the formation of a cross-linked network, which enhances the mechanical stability and durability of the resulting PDAs.

The transition from PCDA to PDAs is accompanied by a dramatic change in optical properties. When PCDA is exposed to external stimuli such as temperature fluctuations or pH changes, it can induce conformational changes in the polymer chains, resulting in observable color shifts (Hassan et al., 2019). This unique property enables PDAs to act as effective colorimetric sensors, signaling the presence of specific environmental conditions or biological agents.

### *2.1.3 Applications in Biosensing Technology*

The unique properties of PDAs derived from PCDA make them highly suitable for a wide range of biosensing applications. Their ability to respond dynamically to environmental stimuli, such as temperature fluctuations and pH changes, enables the development of sensors that provide real-time feedback in various settings (Bhattacharjee et al., 2020). For example, researchers have developed PDA-based sensors that can detect bacterial contamination by monitoring color changes associated with the presence of specific pathogens, such as E. coli (Harpaz et al., 2021).

In addition to pathogen detection, PDAs have been explored for applications in detecting chemical agents and environmental pollutants. Their responsiveness to a range of stimuli allows for the creation of sensors that can signal hazardous conditions through distinct color changes, providing an intuitive and visual method for monitoring environmental safety (Zhou et al., 2022). Moreover, the integration of PDAs into nanofiber structures enhances the applicability of these structures in textile-based biosensors. This integration facilitates the development of smart textiles that can continuously monitor environmental factors while offering immediate visual alerts through colorimetric responses (Liu et al., 2020).

The combination of PDAs' unique optical properties with advanced materials technology represents a significant advancement in biosensing capabilities. By harnessing these properties, researchers aim to develop multifunctional biosensors that can detect various parameters while simultaneously addressing health and safety challenges. Through continued exploration and innovation in this field, PDA-based biosensors hold great promise for revolutionizing the approach to pathogen detection, environmental monitoring, and other critical areas.

## 2.2 Colorimetric Responses of PDAs

### *2.2.1 Mechanisms of Color Change*

Polydiacetylenes (PDAs) exhibit unique colorimetric responses that are primarily attributed to their conjugated polymer structure. The transformation from 10,12-Pentacosadiynoic acid (PCDA) to PDA involves the formation of a conjugated π-system, which allows for electron delocalization across the polymer chain. When PDAs are exposed to external stimuli—such as temperature fluctuations, pH changes, or specific interactions with analytes like bacteria—the polymer undergoes conformational changes, resulting in observable color shifts

(Bhattacharjee et al., 2020; Halicka & Cabaj, 2021). The color change mechanism in PDAs can be explained by the transition from a non-conjugated state to a conjugated state. In the non-conjugated form, the polymer chains are more random and less organized, resulting in minimal light absorption. Upon polymerization and exposure to stimuli, the chains align, creating a more extended conjugated system that enhances light absorption at specific wavelengths. This shift is responsible for the vibrant color changes observed (Zhou et al., 2022). For example, PDAs may transition from a colorless or pale yellow state to blue or red hues depending on the environmental conditions and the type of stimulus applied.

### *2.2.2 Factors Influencing Color Changes*

Several factors can influence the colorimetric response of PDAs, including temperature, pH, and the presence of specific biomolecules.

a) **Temperature:** PDAs are highly sensitive to temperature fluctuations. As the temperature increases, it can lead to increased molecular motion within the polymer chains, resulting in conformational changes that affect the degree of conjugation. This can cause significant color shifts, allowing for temperature sensing applications (Liu et al., 2020).
b) **pH Levels:** The pH of the surrounding environment can significantly impact the ionization state of functional groups within the PDA structure. Changes in pH can alter the interactions between the polymer chains and their surroundings, leading to shifts in color (Hassan et al., 2019). This property makes PDA-based sensors suitable for detecting pH variations in various applications, from environmental monitoring to food safety.
c) **Biomolecular Interactions:** PDAs can also respond to specific biomolecules, including proteins and nucleic acids. When PDAs interact with target biomolecules, they can undergo

conformational changes that result in colorimetric shifts. This feature is particularly valuable for developing biosensors capable of detecting pathogens or other biological agents (Bhattacharjee et al., 2020).

## 2.3 Electrospun Nanofibers in Biosensors

### *2.3.1 Electrospinning Technology*

Electrospinning is a versatile and widely used technique for producing ultrafine fibers with diameters ranging from nanometers to micrometers. This process involves applying a high-voltage electric field to a polymer solution or melt, which is ejected from a syringe or nozzle. As the charged polymer solution is drawn towards a collector, the solvent evaporates, resulting in the formation of continuous fibers (Wang et al., 2004). The electrospinning process is adaptable, allowing for the use of various polymers and solvents and can be modified to produce fibers with specific properties by adjusting parameters such as voltage, flow rate, and distance between the nozzle and collector (Liu et al., 2020). The ability to create fibers with high surface area-to-volume ratios is one of the most significant advantages of electrospinning. This feature is crucial for biosensing applications, as it enhances interaction between the sensing material and analytes, leading to improved sensitivity and faster response times (Hassan et al., 2019). In this project, the electrospinning technique will be employed to fabricate core-shell nanofibers, where the shell consists of polydiacetylenes (PDAs) and the core contains a PLGA (Poly(lactic-co-glycolic acid)) nanostructured capsule encapsulating penicillin.

### *2.3.2 Core-Shell Nanofiber Structure*

The development of core–shell nanofibers through coaxial electrospinning offers a versatile platform for fabricating high-performance colorimetric sensors. In this configuration, two polymer solutions are simultaneously electrospun through a concentric nozzle system, forming fibers with a distinct inner core and outer shell. This architecture provides several structural and functional benefits. The outer shell, which in this study incorporates polydiacetylene (PDA) monomers such as 10,12-pentacosadiynoic acid (PCDA), is blended with polyurethane (PU) and polyethylene oxide (PEO) and directly exposed to environmental stimuli, including heat. This allows for immediate chromatic response to temperature changes. The inner core, composed of PEO, enhances fiber formation, improves mechanical integrity, and supports consistent coaxial spinning. This layered design not only facilitates more uniform colorimetric transitions due to the spatial confinement of PDA in the shell but also stabilizes the nanofiber structure, making it more durable under thermal cycling and external handling. The coaxial design also provides a modular framework for future functionality, such as therapeutic or multi-stimuli sensing applications, without compromising the core colorimetric performance essential for temperature monitoring.

### *2.3.3 Advantages of Core-Shell Nanofibers*

The coaxial core–shell nanofiber structure offers several advantages in the development of temperature-sensitive PDA-based biosensors:

**a) Enhanced Sensitivity:**

Embedding PCDA in the shell layer ensures direct exposure to ambient conditions, promoting a rapid and distinct chromatic response. The large surface area of the electrospun mat enhances

heat transfer and interaction between the stimulus and the responsive PDA domains, leading to faster signal transduction and improved sensitivity.

**b) Structural Stability and Flexibility:**

The inner core of PEO enhances the electrospinning process, resulting in more uniform fibers with improved tensile properties. This is essential for maintaining sensor performance under stress and during repeated use, particularly in wearable or portable applications.

**c) Spatial Control for Functional Optimization:**

By confining the sensing material to the shell layer, researchers can fine-tune the optical response while leaving the core available for potential future modifications. This may include adding barrier layers, thermal buffers, or even therapeutic payloads in next-generation designs.

**d) Integration into Smart Materials:**

The core–shell format enables easy incorporation into textiles or films for scalable deployment in smart garments or surface-mounted sensor systems. This opens opportunities for real-time, non-invasive thermal monitoring in healthcare, manufacturing, or safety gear.

While the present study focuses solely on thermochromic behavior, this architecture lays the foundation for future multifunctional applications, such as drug release or pH-responsive systems, through additional modifications to the fiber's core or shell.

## 2.4 Machine Learning in Biosensor Technology

### *2.4.1 Role of Machine Learning*

The integration of machine learning (ML) into biosensor technology offers transformative potential for enhancing the accuracy, efficiency, and functionality of biosensing systems. Machine learning refers to a subset of artificial intelligence that enables computers to learn from and make predictions based on data. By employing algorithms that can recognize patterns and trends within datasets, ML can significantly improve the data interpretation capabilities of biosensors (Liu et al., 2020). This is particularly beneficial in applications where real-time analysis is crucial, such as pathogen detection and environmental monitoring.

One of the primary advantages of incorporating machine learning into biosensor technology is its ability to process large volumes of data generated by sensors. Traditional methods of data analysis can be time-consuming and may not fully utilize the information available. In contrast, ML algorithms can quickly analyze complex datasets, identify relevant features, and generate insights that may not be immediately apparent (Zhou et al., 2022). This capability allows for more informed decision-making based on real-time sensor readings.

### *2.4.2 Pattern Recognition and Classification*

Machine learning excels in pattern recognition, making it a valuable tool for classifying different analytes based on their sensor responses. For instance, by training models on datasets containing various colorimetric responses associated with specific concentrations of pathogens or environmental conditions, researchers can develop algorithms capable of distinguishing between different substances (Hassan et al., 2019). Supervised learning techniques, such as support vector machines (SVM) and neural networks, are commonly employed in this context. These algorithms

can be trained using labeled datasets to recognize patterns associated with specific outcomes, enabling them to classify new data points accurately. The ability to classify data efficiently enhances the performance of biosensors by providing immediate feedback on the presence or concentration of target analytes.

### *2.4.3 Predictive Analytics*

In addition to classification tasks, machine learning can facilitate predictive analytics in biosensing applications. By utilizing historical data, ML models can identify trends and make predictions about future sensor behavior based on current readings. For example, predictive models can forecast the likelihood of bacterial contamination in food products based on environmental factors such as temperature and humidity (Liu et al., 2020). This capability is especially important in proactive monitoring scenarios, where early detection of potential issues can prevent outbreaks of foodborne illnesses or environmental hazards. By integrating predictive analytics into biosensor systems, stakeholders can implement timely interventions based on reliable forecasts, thereby enhancing public health safety.

### *2.4.4 Integration with PDA-Based Biosensors*

The incorporation of machine learning into PDA-based biosensors can further enhance their utility. For instance, ML algorithms can be trained to analyze the colorimetric responses from PDAs to rapidly determine the concentration of specific pathogens or detect environmental changes. By correlating specific color transitions with defined concentrations or conditions, machine learning models can streamline data processing and enhance the responsiveness of the biosensor (Zhou et al., 2022). Moreover, the use of machine learning can optimize the parameters of the biosensing system itself. By analyzing performance data, ML algorithms can

suggest adjustments to sensor design or operation that improve sensitivity and specificity, thereby advancing the overall effectiveness of PDA-based biosensors. The integration of machine learning into biosensor technology represents a significant advancement in the field. By leveraging the capabilities of ML for data analysis, pattern recognition, and predictive analytics, researchers can develop more sophisticated and responsive biosensing systems that address contemporary challenges in health and safety.

## 2.5 Challenges and Future Directions

### *2.5.1 Current Limitations*

While polydiacetylene (PDA)-based biosensors exhibit significant potential for various applications, several challenges remain that must be addressed to enhance their effectiveness and usability. One of the primary limitations is the stability of PDAs under different environmental conditions. Factors such as temperature, humidity, and exposure to light can degrade the optical properties of PDAs over time, potentially leading to reduced sensitivity and reliability in sensor performance (Hassan et al., 2019). Ensuring that PDAs maintain their colorimetric properties in real-world conditions is essential for the practical application of these biosensors. Additionally, the encapsulation process for antimicrobial agents like penicillin within the PLGA core may also present challenges. The release kinetics of penicillin need to be optimized to ensure that it is released at the right time and concentration to effectively neutralize pathogens without causing adverse effects (Zhou et al., 2022). Variability in the encapsulation efficiency and release profiles can affect the overall performance of the biosensor, making it crucial to refine fabrication techniques. Another challenge lies in achieving sufficient sensitivity to detect pathogens at critical bacterial concentrations (CBC). For applications in food safety and

healthcare, detecting low levels of E. coli or other harmful bacteria is vital. Developing biosensors that can reliably detect bacteria at or below these critical concentrations while maintaining rapid response times is an ongoing area of research (Liu et al., 2020).

### *2.5.2 Potential Solutions*

To address the stability challenges of PDAs, researchers can explore various approaches such as encapsulating PDAs in protective coatings or using stabilizing additives that can shield them from environmental factors (Halicka & Cabaj, 2021). Enhancing the mechanical properties of the nanofiber structure can also contribute to improved stability, allowing for better performance under variable conditions. Optimizing the encapsulation process for antimicrobial agents is another area where improvements can be made. Researchers can investigate different formulations of PLGA and methods for encapsulating penicillin to achieve more controlled release profiles. By tailoring the polymer composition and thickness of the nanofiber layers, it may be possible to enhance both the stability of the encapsulated antibiotic and the precision of its release upon pathogen detection. To improve sensitivity and reliability in detecting pathogens at critical bacterial concentrations, further research is needed to refine sensor designs and incorporate advanced materials that enhance detection capabilities. Exploring combinations of PDAs with other sensing technologies or materials may lead to innovative solutions that allow for more efficient detection (Zhou et al., 2022).

### *2.5.3 Future Research Directions*

While this study centers on temperature-responsive sensing using PDA-integrated nanofibers, the sensor platform offers strong potential for future expansion into multifunctional domains. One promising direction involves incorporating stimuli-responsive drug release

capabilities into the fiber core. For example, prior studies have demonstrated the successful encapsulation of antibiotics like penicillin within poly(lactic-co-glycolic acid) (PLGA) nanoparticles in coaxial fiber cores for controlled release upon environmental triggers (Sun et al., 2025). This approach could be integrated into future designs to develop sensors that not only detect hazards—such as abnormal temperature or bacterial contamination—but also deliver localized therapeutic responses.

Additionally, the PDA shell composition can be modified to enable responsiveness to pH changes or biomolecular binding events, making it suitable for detecting physiological imbalances or environmental pollutants. Combining these enhancements with machine learning-based image analysis would allow for smart, adaptive sensing systems capable of tracking multiple parameters simultaneously. These directions, while beyond the scope of the current temperature-focused work, highlight the adaptability and long-term potential of PDA-based electrospun fiber platforms.

# CHAPTER III – METHODOLOGY

This project proposed a detailed methodology for developing a colorimetric temperature responsive sensor using coaxial electrospun nanofibers incorporating polydiacetylene (PDA), specifically 10,12-pentacosadiynoic acid (PCDA), and machine learning (ML) for automated color interpretation and result prediction. The research focuses on investigating the relationship between PCDA concentration, thermal exposure time, and chromatic response, with the aim of constructing a predictive CNN-based model using RGB data extracted from fiber images and to evaluate how accurately the model can predict the actual corresponding temperature by analyzing those images.

## 3.1 Materials

### *3.1.1 Chemicals*

A range of chemicals was used in the preparation of solutions for the electrospinning process. The primary sensing component, 10,12-pentacosadiynoic acid (PCDA, ≥98%), served as the thermochromic monomer, known for its characteristic blue-to-red color transition in response to heat. PCDA was obtained from Sigma-Aldrich and stored in dark, dry conditions to preserve its stability. Thermoplastic polyurethane (PU) was incorporated to enhance the mechanical strength of the electrospun fibers, while polyethylene oxide (PEO, MW ~300,000 g/mol) was used to improve spinnability and served as the core material in the coaxial fiber structure. Both PU and PEO were sourced from established suppliers such as Alfa Aesar and Fisher Scientific.

The following high-purity solvents were used:

- Tetrahydrofuran (THF, 99%): for shell solution

- Chloroform ($CHCl_3$, ≥99%): co-solvent to reduce surface tension in the shell solution
- Dichloromethane (DCM, ≥99%): solvent for PEO core solution preparation

All solvents were used without further purification, and solutions were freshly prepared prior to electrospinning.

*3.1.2 Substrates*

Electrospun fibers were collected onto flat aluminum foil substrates mounted on a rotating collector drum to ensure uniform deposition. This provided a smooth, non-absorptive surface for high-quality image capture and consistent thermal contact during heating. Substrates were pre-cut into 3×3 cm squares.

*3.1.3 Equipment and Instrumentation*

The following equipment was used in the fabrication and analysis process:

- LE50 Electrospinning Machine (Linari Engineering, Italy): A high-precision coaxial electrospinning unit equipped with dual syringe pumps and programmable voltage and flow control. This instrument supports simultaneous core–shell fiber formation with fine control over spinning parameters.
- Hotplate with digital temperature control: Used for applying thermal stimuli to fiber mats at fixed temperature levels (55–80°C) with ±0.5°C precision.
- Mobile phone camera (e.g., OnePlus 9RT or equivalent): Used for capturing colorimetric changes post-heating. Images were taken under standardized lighting conditions (D65) using a Light box to minimize environmental variation.

- UV polymerization source (254 nm LED lamp) was used for photopolymerizing PCDA fibers immediately after electrospinning to ensure color responsiveness.
- Computer workstation: Equipped with necessary libraries including Python, OpenCV, NumPy, Pandas, TensorFlow/Keras, and matplotlib for RGB extraction, CSV data generation, model training, and visualization.

All experiments were conducted in a fume hood or controlled lab environment to ensure safety and consistency. Two separate solutions were prepared for the electrospinning process—one for the core and one for the shell.:

- Shell solution: A mixture of PU, PEO, and PCDA at varying concentrations (5%, 10%, 12%, 15%, 18%, and 20% w/w), dissolved in a 1:1 (v/v) blend of tetrahydrofuran (THF) and chloroform. This outer layer is responsible for the sensor's thermochromic response.
- Core solution: Consisted of PEO dissolved in dichloromethane (DCM) to improve spinnability and support stable fiber formation.

## 3.3 Coaxial Electrospinning Perameters

Fibers were fabricated using a coaxial electrospinning apparatus equipped with a concentric dual-syringe setup. Parameters were optimized as follows:

- Applied voltage: 14–18 kV
- Flow rate (core:shell): 0.2-0.5 mL/h
- Needle-to-collector distance: 15-20 cm
- Ambient conditions: 22–24°C and 35–40% relative humidity

The resulting fibers were stored in light-protected conditions.

## 3.4 Thermal Exposure and Image Capture

Sensor samples were subjected to six different temperature conditions: 55°C, 60°C, 65°C, 70°C, 75°C, and 80°C. For each temperature, exposure durations of 1 s, 5 s, 10 s, 30 s, 60 s, and 120 s were applied. For every combination of temperature and exposure time (36 conditions per concentration), 20 images were captured (using varied angles and positions to simulate real-world variability). In total, 4,320 images were captured across six PCDA concentrations. Images were saved in JPG format and labeled using a standardized naming convention for traceability.

## 3.5 Image Processing and RGB Data Extraction

RGB values were extracted using Python and OpenCV libraries. Each image was cropped to the fiber region and converted to average RGB values. This dataset was compiled into a CSV file with the following columns:

- File name
- PCDA concentration
- Temperature
- Exposure time
- R, G, B values

Outliers and noise due to lighting were minimized by averaging RGB values across multiple points per image.

## 3.6 Machine Learning Model Development

### *3.6.1 Machine Learning Integration for sensor Data Analysis*

To eliminate the subjectivity in interpreting colorimetric responses from PDA-based sensors, this study implemented a supervised machine learning framework focused on real-time temperature prediction. The approach relied on RGB values extracted from sensor images to train a machine learning model capable of identifying temperature conditions based solely on visual color cues. The integration of machine learning streamlined analysis, improved accuracy, and reduced dependency on manual observation.

### *3.6.2 Data Collection*

Colorimetric responses were recorded for each sample prepared with varying PCDA concentrations (5%, 10%, 12%, 15%, 18%, and 20%) across six distinct temperatures (55°C, 60°C, 65°C, 70°C, 75°C, and 80°C) and six response durations (1 s, 5 s, 10 s, 30 s, 60 s, and 120 s). For each unique condition, 20 images were captured under varied lighting angles and positions to introduce diversity in the dataset. In total, the dataset included 4,320 high-resolution JPEG images (6 concentrations × 6 temperatures × 6 times × 20 images). Each image was labeled with metadata including PCDA concentration, temperature, exposure time, and RGB average values. This metadata was stored in structured CSV format, serving as input for training and evaluation.

### *3.6.3 Preprocessing*

Image preprocessing were performed using OpenCV and Python libraries. Key preprocessing steps include:

- Cropping the image to focus on fiber regions.
- Image resizing to a standardized resolution (e.g., 224×224 pixels).
- Color normalization to minimize lighting variations.
- Noise filtering (e.g., Gaussian blur) to reduce background artifacts.
- RGB averaging, where mean values of Red, Green, and Blue channels will be extracted and stored.

This uniform preprocessing pipeline ensures consistent input for model training while reducing the influence of environmental variables.

### *3.6.4 Model Architecture and Selection*

A convolutional neural network (CNN) was constructed to map RGB inputs to corresponding variables. The proposed CNN architecture included:

- Three convolutional layers with ReLU activation and max pooling
- Batch normalization to improve training stability
- A flattening layer, followed by two fully connected dense layers
- Dropout layers for regularization
- An output layer with one neuron and linear activation for temperature regression

Loss function: Mean Squared Error (MSE)

Optimizer: Adam

Evaluation metrics: $R^2$ score, Mean Absolute Error (MAE), and Root Mean Square Error (RMSE)

Alternative models such as Support Vector Regression (SVR), Random Forest Regression, and pre-trained CNNs via transfer learning (e.g., ResNet18) will also be explored for benchmarking purposes in future.

### *3.6.5 Model Training and Validation*

- Data split: 80% training, 20% testing (stratified by temperature and concentration).
- Cross-validation: 5-fold k-cross validation to reduce overfitting and ensure model generalizability.
- Hyperparameter tuning: Grid search or random search was used to optimize learning rate, batch size, number of filters, and dropout ratio.

Model checkpoints and logs were recorded for each training iteration. Final model weights were selected based on minimum validation error.

*3.6.6 Output and Visualization*

Trained models were used to predict temperatures for test images. Performance was visualized through:

- Scatter plots of predicted vs actual temperatures
- Residual error histograms
- Confusion matrices (after binning temperature into classes)
- Model interpretability tools (e.g., Grad-CAM) to highlight influential image regions

The final model was integrated into a Python-based web application interface for image upload and temperature prediction output. This machine learning component enabled automated, fast, and interpretable analysis of PDA sensor outputs, paving the way for reliable, real-time temperature sensing in low-resource and wearable settings.

## 3.7 Performance Analysis

After training, the performance of the machine learning model was thoroughly analyzed across multiple dimensions to evaluate its accuracy, robustness, and generalizability. The primary focus was on understanding how well the model predicted temperature values from RGB inputs and identifying which experimental conditions yielded the highest predictive fidelity.

*3.7.1 Evaluation Metrics*

The trained CNN model was assessed using the following statistical metrics:

- $R^2$ score to measure the proportion of variance in temperature explained by the RGB inputs.

- Mean Absolute Error (MAE) to evaluate average deviation between predicted and actual temperatures.
- Root Mean Square Error (RMSE) to penalize larger errors more heavily. These metrics were computed separately for training and testing datasets to detect overfitting or underfitting.

### *3.7.2 Condition-Based Performance Comparison*

To better understand how experimental variables influenced prediction accuracy, model performance was stratified by:

- PCDA concentration: The six concentrations (5%, 10%, 12%, 15%, 18%, and 20%) were analyzed to determine which concentration provided the strongest and most consistent color signal for temperature prediction.
- Exposure time: The six durations (1 s to 120 s) were examined to identify the time points at which the color transition was most stable and reproducible.

This stratified analysis was visualized through line plots showing MAE and $R^2$ for each concentration and time point. These insights helped determine the optimal combination of concentration and exposure duration for real-world sensor deployment.

### *3.7.3 Visual Performance Representation*

Several visualization techniques were used to better interpret model behavior:

- Scatter plots comparing actual vs predicted temperatures for all test samples.
- Heatmaps showing prediction error across different concentration-time combinations.

- Confusion matrices, where temperature was discretized into bins (e.g., 55–57°C, 58–60°C, etc.) to evaluate classification-like accuracy.
- Residual error histograms to assess the distribution and spread of prediction errors.

### *3.7.4 Error Analysis and Model Reliability*

Residual analysis was conducted to identify systematic prediction errors, such as consistent over- or underestimation at specific temperatures or concentrations. This helped diagnose limitations in the dataset or architecture. Additionally, standard deviation within replicates (20 images per condition) was used to evaluate model. A low variance indicated that the model was robust to real-world noise. Together, these performance analyses provided a comprehensive evaluation of the machine learning model's ability to accurately and reliably interpret thermochromic responses from PDA-based electrospun sensors.

## 3.8 Output Generation and Web Application Development

This research also developed a lightweight web-based application to deliver real-time outputs from the trained machine learning model. The application served as an intuitive interface where users could upload images of PDA-based fiber sensors and receive instant temperature predictions based on colorimetric response.

### *3.8.1 Web Framework and Design*

The application was built using Python Flask or Streamlit, selected for their flexibility and ease of deployment. The frontend supported image upload, displayed real-time results, and visualized the input image alongside predicted temperature. The backend loaded the pre-trained CNN model using TensorFlow or PyTorch and handled image preprocessing in real-time.

*3.8.2 Functional Workflow*

1. Image Upload: Users would drag and drop or select an image file (JPG or PNG).
2. Image Processing: The server resizes, normalizes, and extracts average RGB values from the uploaded image.
3. Temperature Prediction: The CNN model returns a predicted temperature value in Celsius.
4. Output Display: The application would display:
    - Predicted temperature

*3.8.4 Future Enhancements*

In later stages, the application may be extended to run on mobile devices or be integrated into a smartphone app, allowing users to take photos of the biosensor in real time and obtain instant feedback. Cloud deployment options (via Heroku or AWS) will also be explored for broader accessibility. This digital interface will democratize the use of PDA-based sensors, enabling non-experts to interpret colorimetric temperature responses using common tools like smartphones or laptops.

## 3.9 Interdisciplinary Innovation

A key innovation of this project lies in the interdisciplinary integration of materials science and machine learning to create a smart colorimetric sensing platform. From a materials perspective, the work focused on the systematic design and fabrication of electrospun PCDA-based core–shell fibers. By carefully tuning PCDA concentrations and optimizing the electrospinning process, the nanofibers demonstrated reliable and reproducible chromatic responses across a range of thermal conditions. On the computational side, the project leveraged supervised machine learning to move beyond traditional, subjective color interpretation or result analysis. By converting RGB image data into quantitative temperature predictions, the approach transformed a simple color change into an objective, data-driven measurement. This integration of image analysis with predictive modeling addressed a longstanding challenge in colorimetric sensing: the reliance on visual evaluation, which can be influenced by environmental variability and user interpretation. Bringing together these two disciplines—advanced fiber-based materials and machine learning—enabled the development of a low-cost, flexible, and scalable temperature-sensing platform. This convergence not only demonstrates the synergy between material design and data science but also sets the stage for future intelligent sensor systems that can adapt to a variety of real-world applications.

# CHAPTER IV – MANUSCRIPT

## PROTOTYPING A TEMPERATURE-RESPONSIVE FLEXIBLE COLORIMETRIC SENSOR WITH MACHINE LEARNING-BASED RESULT INTERPRETATION

## 1.0 INTRODUCTION

Polydiacetylenes (PDAs) are a class of conjugated polymers known for their remarkable chromatic transitions in response to various environmental stimuli (Lee et al., 2008). Among them, 10,12-pentacosadiynoic acid (PCDA) has attracted significant attention due to its ease of photopolymerization, strong thermochromic properties, and excellent environmental stability (Chen & Huang, 2010). Upon UV treatment, PCDA forms a blue-phase conjugated PDA backbone, which undergoes visible color transitions when exposed to external triggers such as heat (Zhou et al., 2024), pH changes (Kobayashi et al., 2013), or mechanical forces (Lee & Jelinek, 2023). These stimuli disrupt the polymer backbone's planarity, reducing effective π-conjugation and resulting in a distinct shift from blue to red (Zhou et al., 2024). This chromatic behavior can be reversible or irreversible depending on the stimulus intensity and molecular design. Reversible transitions are typically observed under mild conditions, such as temperature or pH fluctuations, especially in systems modified with peptide amphiphiles to support reversibility (Lim et al., 2023). In contrast, irreversible transitions can be triggered by stronger interactions such as bacterial presence, extended thermal exposure, or mechanical disruption, as demonstrated in single-use PDA-based temperature sensor (Gou et al., 2010). These

characteristics makes PDA as a versatile material for both reusable and disposable colorimetric sensing systems.

Various fabrication techniques have been develpoed to integrate PDA into functional sensor systems. Traditional methods such as spray coating, melt-blowing, and solution casting are widely used due to their simplicity and scalability. Kim et al. (2019) fabricated flexible PDA-coated films using a spray-coating process for smart packaging applications, while Koo et al. (2020) applied melt-blowing to incorporate PDA into disposable nonwoven sensor layers. Solution casting, one of the earliest PDA processing techniques, has been utilized to form thin films on glass or polymer substrates for thermochromic and pH-responsive applications (Zhou et al., 2023). Despite their accessibility, these fabrication strategies often suffer from limitations such as uneven thickness, limited surface exposure, and poor reproducibility. Such constraints lead to slower response times and inconsistent color transitions, thereby limiting their suitability for real-time or high-sensitivity applications.

To overcome these drawbacks, electrospinning has emerged as a powerful and versatile technique for fabricating PDA-based sensors. By applying a high-voltage electric field to a polymer solution, electrospinning produces continuous, ultrafine fibers that accumulate into porous, nonwoven mats. These mats possess a large surface-area-to-volume ratio, which facilitates enhanced interaction between PDA molecules and external stimuli. As a result, PDA-embedded electrospun fibers exhibit faster thermal response and greater chromatic sensitivity compared to bulk films or cast layers (Alam et al., 2016; Hassan et al., 2019). Additionally, electrospun mats offer flexibility, lightweight construction, and tunable morphology, making them well-suited for wearable, field-deployable, or smart textile platforms. Several studies have

demonstrated the effectiveness of this method. For instance, Bhattacharjee et al. (2023) reported selective Gram-negative bacterial detection using PDA nanofibers, while Liu et al. (2022) confirmed that PCDA-loaded electrospun fibers outperformed traditional PDA films in terms of thermal sensitivity and color uniformity.

An extension of this technology, coaxial electrospinning, has enabled the fabrication of core–shell fibers that spatially separate functional and mechanical components within a single fiber. In this configuration, two different polymer solutions are fed through concentric nozzles—resulting in an inner "core" and an outer "shell." The shell, often composed of active sensing or therapeutic materials, is directly exposed to environmental stimuli, while the core provides mechanical reinforcement or secondary functionality. This architecture offers several advantages, including enhanced material stability, tunable release profiles, and the potential for multifunctionality. A recent study was conducted by Sun et al. (2025), where core–shell fiber scaffolds embedded with gentamicin-encapsulated PLGA nanoparticles were developed for transdermal drug delivery. The outer shell ensured sustainable release, while the core maintained scaffold integrity. Such work highlights the relevance of coaxial electrospinning not only for biomedical applications but also for advanced sensor systems where PDA can be precisely positioned in the shell to maximize stimulus interaction while the core can be adapted for structural or bioactive roles.

Despite these advancements, several challenges remain in the design and fabrication of PDA-based electrospun sensors. One of the primary obstacles is that pure PCDA is not suitable for electrospinning. Due to its rigidity, poor solubility, and lack of polymeric chain entanglement, PCDA alone cannot form stable fibers. Furthermore, PCDA is relatively

expensive, making its exclusive use impractical for scalable sensor production. As a result, carrier polymers such as polyurethane (PU) and polyethylene oxide (PEO) are typically blended with PCDA to enhance electrospinnability, flexibility, and structural stability (Li et al., 2021). However, the optimal concentration of PCDA required to balance colorimetric performance with processability and mechanical integrity has not been clearly established through recent studies. High PCDA loading improves chromatic response but leads to fiber brittleness and inconsistent morphology. In parallel, thermal response time—defined as the duration of stimulus exposure required to trigger a visible color change—is another critical but underexplored parameter. Systematic studies examining the interaction between PCDA concentration and response time are essential to optimize the sensitivity and reliability of these sensors under different operating conditions.

Functionally, PDA serves as a chromatic sensor that visibly changes color—typically from blue to red—in response to external stimuli. This transition is driven by a conformational change in the polymer backbone, which disrupts π-conjugation and causes a bathochromic shift in the UV–vis absorption spectrum from approximately 640 nm (blue phase) to 540 nm (red phase). While this color change allows for direct visual detection without sophisticated equipment, the interpretation of results is inherently subjective. Variations in lighting conditions, viewing angle, and human perception often lead to inconsistent or inaccurate readings, especially when subtle changes in temperature or chemical environment are involved (Wang et al., 2017; Lee & Jelinek, 2023). This reliance on manual observation is a major limitation, particularly in applications requiring precision, reproducibility, and real-time feedback.

To address this issue, researchers have increasingly turned to machine learning (ML) as a tool for automating and standardizing the analysis of colorimetric sensor output. By extracting quantitative features—such as RGB, HSV, or LAB values—from sensor images, ML algorithms can be trained to detect patterns and predict underlying stimuli with high accuracy. This approach transforms colorimetric sensing from a qualitative to a quantitative process. Xu et al. (2020) demonstrated that support vector machines (SVMs) could effectively classify PDA-based nanofiber responses to bacterial exposure. Kim et al. (2022) implemented deep learning models, including convolutional neural networks (CNNs), to analyze smartphone-captured images of colorimetric strips for contaminant detection. Aria et al. (2021) showed that combining image processing with ML significantly improved the interpretability and consistency of colorimetric biosensors. ML-enabled analysis offers several advantages: it eliminates human bias, enhances detection sensitivity, allows real-time processing, and supports deployment on low-cost, portable platforms such as smartphones or embedded systems. These benefits make ML a valuable complement to PDA-based sensing technologies, enabling the development of intelligent, user-independent diagnostic tools.

Motivated by these challenges and opportunities, this study aims to develop an electrospun PDA-based colorimetric sensor that integrates a machine learning model for automated temperature prediction. A coaxial electrospinning approach was used to fabricate core–shell fibers, where PCDA was blended with PU and PEO in the shell layer to enhance chromatic responsiveness, while the core consisted solely of PEO for structural support. A systematic range of PCDA concentrations—from 5% to **20%**—was explored to investigate the effect of composition on fiber morphology, thermal response, and color intensity. Sensors were exposed to temperatures ranging from 55°C to 80°C at six different durations (1, 5, 10, 30, 60,

and 120 seconds) to assess the influence of response time. For each condition, twenty images were captured with intentional variation in lighting and viewing angle to simulate real-use conditions. RGB values were extracted from these images and used to train a CNN model for temperature prediction. Data augmentation was applied to enhance model robustness. The trained model demonstrated high accuracy and consistency, confirming the viability of ML for interpreting colorimetric responses from electrospun PDA sensors.

The novelty of this work lies in its combined focus on material optimization, controlled fabrication through coaxial electrospinning, and image-based machine learning for automated sensing. Unlike prior studies that often fix sensor composition or rely on subjective interpretation, this research establishes a generalized framework for adaptive, image-driven colorimetric analysis. The platform is scalable, low-cost, and suitable for portable applications. Moreover, its design is modular—allowing future adaptation to detect other environmental cues such as pH, humidity, or bacterial contamination. With further functionalization, such as antibiotic incorporation into the fiber core, this system could evolve into a multifunctional tool for simultaneous detection and response. Overall, the integration of advanced nanofabrication and artificial intelligence presents a meaningful step toward the development of smart, real-world biosensors.

# 2.0 MATERIALS AND METHODOLOGY

## 2.1 Materials

10,12-Pentacosadiynoic acid (PCDA, 98%) was purchased from GFS Chemicals and used as the thermochromic sensing monomer. Polyurethane (PU, Tecoflex®) and polyethylene oxide (PEO, Mw ≈ 100,000 g/mol) were used as matrix polymers to optimize fiber formation. Tetrahydrofuran (THF), chloroform ($CHCl_3$), and dichloromethane (DCM) were all of analytical grade and used as received without further purification.

## 2.2 Preparation and Fabrication of Electrospun Fibers

### *2.2.1 Preparation of Electrospinning Solutions*

A coaxial electrospinning setup was used to fabricate core–shell structured fibers, requiring the preparation of both core and shell solutions. The core solution was prepared by dissolving polyethylene oxide (PEO) at a concentration of 0.04 g/mL in 15 mL of dichloromethane (DCM). This solution was magnetically stirred at room temperature overnight until complete dissolution was achieved.

The shell solution was formulated using a polymer blend of polyurethane (PU), polyethylene oxide (PEO), and 10,12-pentacosadiynoic acid (PCDA), which served as the thermochromic sensing component. PU and PEO were used in equal parts (1:1) to provide optimal viscosity and fiber-forming properties. PCDA was added in varying amounts to study the effect of concentration on fiber morphology and thermochromic sensitivity. All solid components were dissolved in a 1:1 mixture of tetrahydrofuran (THF) and chloroform ($CHCl_3$), with 7.5 mL of each solvent per formulation. The solutions were stirred continuously at room

temperature for 6–8 hours to ensure complete homogeneity. The detailed compositions of the shell and core solutions are summarized in the following Table1:

**Table 1:** Electrospinning Core and Shell Solution Recipes

| Sample No. | Shell Solution | | | | Core Solution |
|---|---|---|---|---|---|
| | PCDA Conc. (w/w) | PCDA (g) | PU + PEO (g) | THF + $CHCl_3$ (mL + mL) | PEO in DCM |
| **Sample 1** | 5% | 0.027 | PU (0.2 g) and PEO (0.2 g) | 7.5 ml of Tetrahydrofuran and 7.5 ml of chloroform as solvent | 0.04 g/mL of PEO in 15 mL of DCM |
| **Sample 2** | 10% | 0.044 | | | |
| **Sample 3** | 12% | 0.054 | | | |
| **Sample 4** | 15% | 0.070 | | | |
| **Sample 5** | 18% | 0.087 | | | |
| **Sample 6** | 20% | 0.100 | | | |

All solutions were stored in airtight containers and used fresh for electrospinning to ensure stability and reproducibility. The systematic variation of PCDA concentrations enabled further evaluation of its effect on colorimetric response and model prediction accuracy.

*2.2.2 Coaxial Electrospinning Process*

Electrospun fibers were fabricated using a coaxial electrospinning setup designed to produce core–shell structured mats. The system consisted of two syringe pumps connected to a coaxial stainless-steel needle, a high-voltage power supply, and a grounded rotating drum collector covered with aluminum foil. The core solution, composed of 0.04 g/mL polyethylene oxide (PEO) dissolved in 15 mL of dichloromethane (DCM), was loaded into the inner syringe.

The shell solution was prepared by dissolving polyurethane (PU) and PEO, each at 0.2 g, with varying amounts of 10,12-pentacosadiynoic acid (PCDA) in a 1:1 volume mixture of tetrahydrofuran (THF) and chloroform ($CHCl_3$). While the PU and PEO amounts remained constant across all formulations, the PCDA concentration was systematically varied to investigate its influence on fiber properties. Six different samples were prepared: Sample 1 contained 5% PCDA, Sample 2 contained 10% PCDA, Sample 3 contained 12% PCDA, Sample 4 contained 15% PCDA, Sample 5 contained 18% PCDA, and Sample 6 contained 20% PCDA, all calculated as weight percentages relative to the total polymer mass in the shell solution.

During electrospinning, the core and shell flow rates were maintained at 800 μL/min and 1200 μL/min, respectively. A positive voltage of +8.0 kV was applied to the coaxial needle, while the rotating collector was grounded at –2.0 kV, resulting in a total potential difference of 10 kV. The distance between the needle tip and the collector was fixed at 15 cm. The fibers were continuously deposited as non-woven mats onto the rotating drum, promoting uniform coverage and partial fiber alignment. Following collection, the mats were dried under vacuum overnight to remove any residual solvents and enhance structural stability. The dried mats were subsequently subjected to UV-induced photopolymerization to activate their thermochromic functionality.

### *2.2.3 UV-Induced Photopolymerization*

To initiate the thermochromic response, the electrospun mats were exposed to ultraviolet (UV) light at a wavelength of 254 nm for 5 minutes. This exposure induced topochemical polymerization of the PCDA within the shell, converting the colorless monomeric fibers into the characteristic blue-phase polydiacetylene (PDA). Photopolymerization was essential for enabling the colorimetric behavior of the fibers in response to thermal stimuli. After UV exposure, all samples were stored in a light-protected, dry environment to prevent premature activation or

degradation. The prepared electrospun mats were subsequently used for controlled thermal exposure experiments, RGB image-based color analysis, and machine learning–assisted temperature prediction. The whole fabrication process is illustrated in Figure 1 below.

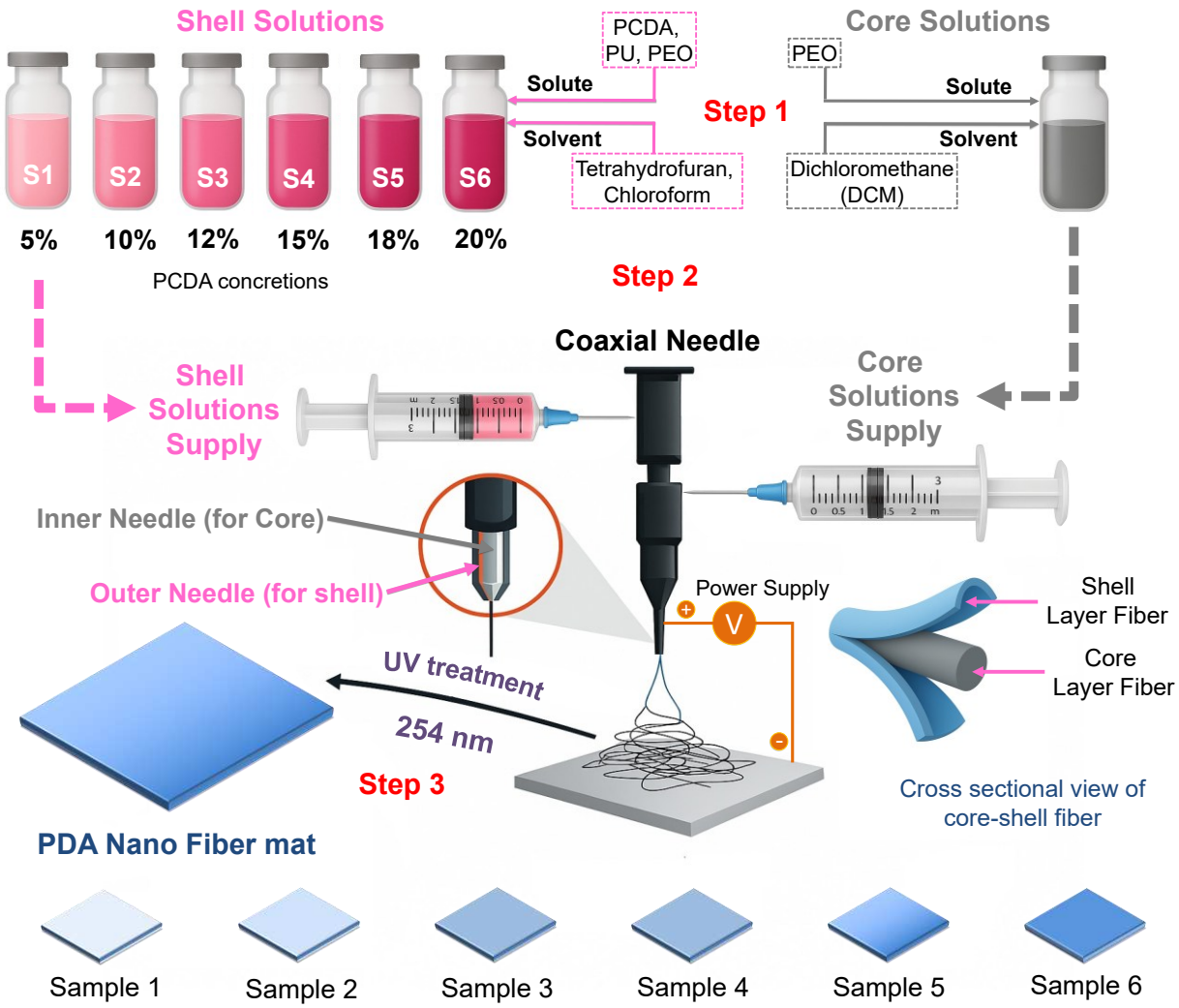


**Figure 1:** Fabrication process of PDA-based core–shell electrospun fibers for colorimetric sensor

## 2.3 Chemical Analysis (FTIR)

Fourier-transform infrared (FTIR) spectroscopy was conducted to verify the successful incorporation of PCDA within the electrospun fiber structure and to confirm the presence of each polymer component in the designed core–shell configuration (Hassan et al., 2019). FTIR spectra were collected both before and after thermal exposure in the range of 4000–600 $cm^{-1}$ with 32 scans per sample and a resolution of 4 $cm^{-1}$. Peaks were identified and assigned based on characteristic vibrational modes of PU, PEO, and PDA.

## 2.4 Morphological Characterization

### *2.4.1 Scanning Electron Microscopy (SEM) and Fiber Diameter Analysis*

Scanning Electron Microscopy (SEM) was utilized to evaluate the morphological characteristics of the electrospun PDA-based fibers. The analysis focused on fiber uniformity, surface texture, and the presence of structural anomalies such as beads or irregular diameters, all of which can influence the reproducibility and sensitivity of the sensor. The fibers were sputter-coated with gold prior to imaging.

SEM images were analyzed using ImageJ (version 1.54). The image was first calibrated using a 10 μm scale bar. A total of 236 fiber diameters were measured manually using the 'Straight Line' tool, and the values were recorded. The resulting diameter data were then exported and visualized using Python's Seaborn library to generate a kernel density estimation (KDE) curve that depicts the distribution of fiber diameters.

## 2.5 Contact Angle and Wettability Measurements

Water contact angle (WCA) measurements were conducted to evaluate the surface wettability of the electrospun PDA-based mats (Wang et al., 2023). The analysis was performed using the droplet method, capturing the angle formed between a 2 μL water droplet and the fiber surface under standardized conditions. Images were analyzed for both left and right angles, and their average was taken as the final WCA. Measurements were performed in triplicate.

## 2.6 Thermochromic Response and Image Acquisition

To test the thermochromic response of the sensors, the electrospun fiber mats were cut into uniform square specimens and subjected to controlled heating. Each sample was placed on a digitally regulated hotplate preheated to a specific temperature—55°C, 60°C, 65°C, 70°C, 75°C, or 80°C—and held for a defined response time: 1 second, 5 seconds, 10 seconds, 30 seconds, 60 seconds, or 120 seconds. Following thermal exposure, samples were immediately cooled to room temperature to stabilize the color state and prevent further transition.

Colorimetric images were captured using a smartphone camera under a standardized imaging setup. Consistent lighting, a neutral background, and fixed camera settings were used to eliminate variations due to ambient light, shadows, or glare. The resulting images were used both for visual comparison and quantitative color analysis.

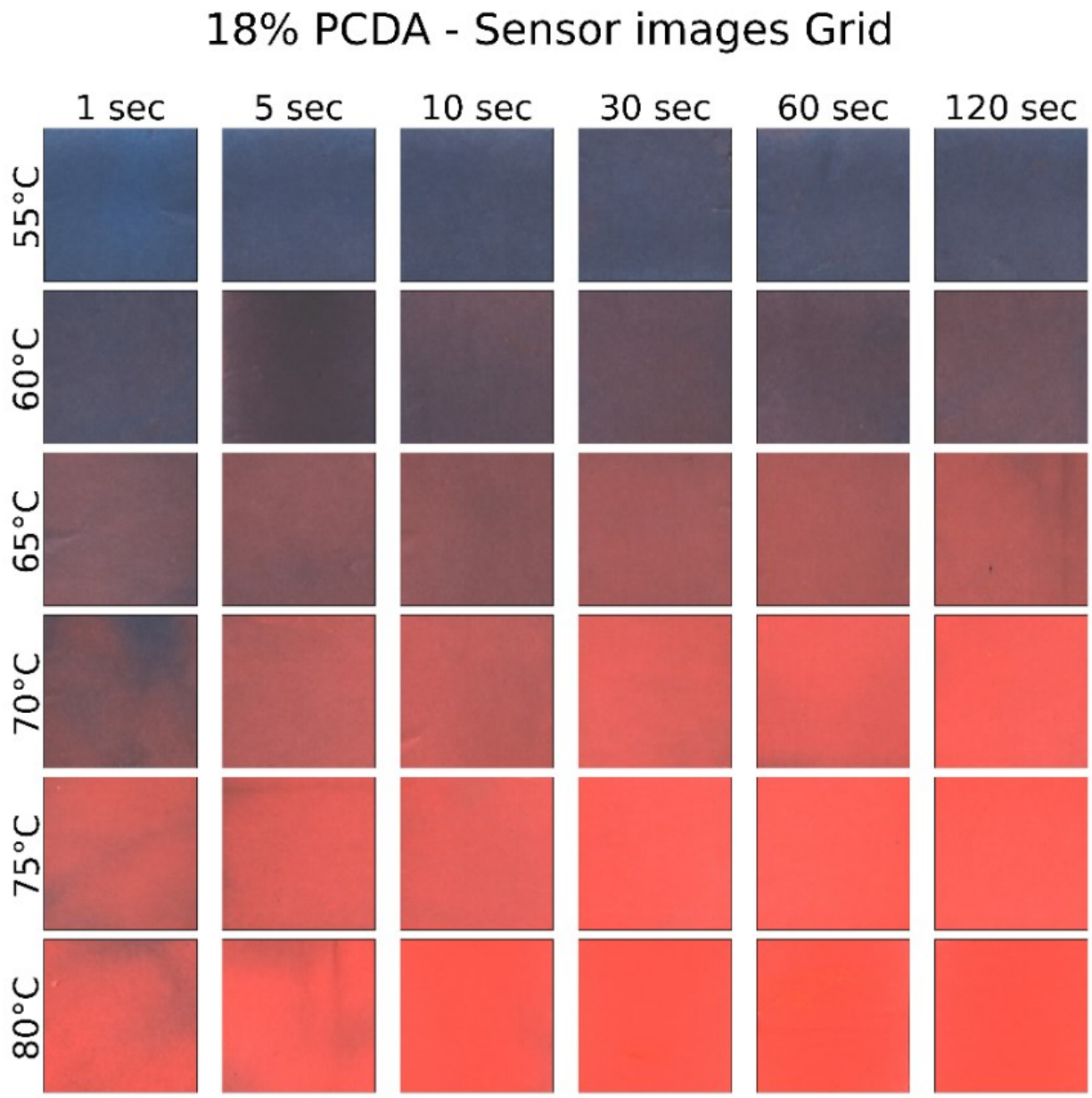


**Figure 2:** Color Transition of 18% PCDA Electrospun Sensor at Different Temperatures (55°C–80°C) and Exposure Times (1–120 sec)

As an illustrative example, Figure 2 presents the thermochromic response of sensors containing 18% PCDA, arranged in a grid across six temperatures and six time intervals. At 55°C, the sensors retained their original deep navy-blue coloration, even after 120 seconds, indicating minimal activation at low thermal input. At 60°C, the blue hue started to desaturate

slightly with longer exposures, transitioning into a muted bluish-purple—especially noticeable after 30 seconds. At 65°C, a more distinct color shift emerged, with the deep blue progressively fading into dusky maroon or purplish-red tones as exposure time increased. The transition became more pronounced and uniform at 70°C, where the central regions of the mats turned visibly red, particularly at 30 seconds and beyond, though some edge areas still showed residual purple.

At 75°C, the color transformation accelerated significantly. The entire mat adopted a vibrant red tone with consistent saturation across the surface, starting as early as 10 seconds and becoming fully saturated by 30 seconds. Finally, at 80°C, the response was the strongest and most immediate: even a brief 5–10 second exposure triggered a complete transition to a bright, intense red, with very little visible variation across the mat.

This time- and temperature-dependent color shift—from deep blue → purple → maroon → bright red—reflects the characteristic behavior of PDA-based thermochromic polymers undergoing a conformational transition in their conjugated backbone. The 18% PCDA concentration, as shown in this example, exhibited high responsiveness and a clear visual progression, making it ideal for colorimetric temperature sensing. Similar image sets were captured and analyzed for all other PCDA concentrations used in this study.

## 2.6 Machine Learning Model Development

### *2.6.1 Image Preprocessing and Data Augmentation*

All images were taken using a smartphone (One plus, 9RT) camera under standardized lighting conditions (D65, standard sunlight). Captured images were cropped to focus on the region of interest and resized to a fixed resolution of 244 × 244 pixels to ensure consistency across the dataset. To minimize variability, manual camera settings were used throughout the image acquisition process: ISO was fixed at 200, white balance was set to daylight mode, shutter speed was maintained at 1/60 s, and exposure was manually adjusted to avoid overexposure and shadows. Flash was disabled to prevent uneven lighting and glare. The camera was positioned perpendicular to the sample surface at a fixed height, with the sample placed on a neutral, non-reflective background. The whole image collection setup has been shown in Figure 3 below.

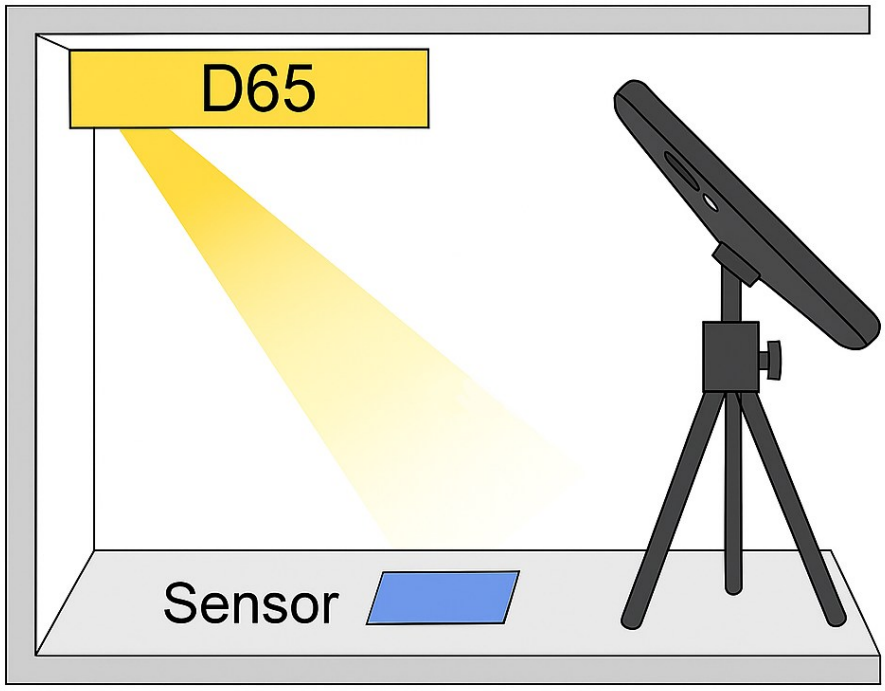


**Figure 3:** Controlled Image Acquisition Setup for PDA Sensor Characterization Using D65 Lightbox and Smartphone Camera

To reduce the impact of ambient lighting differences and sensor variability, the average RGB values of each processed image were extracted and used as input features for the machine learning model. In order to enhance model generalization and robustness, 20 images were captured for each sample under slightly varied conditions. These variations included minor changes in lighting, brightness, contrast, and camera angle to reflect realistic environmental differences. These diverse conditions were introduced during image acquisition to help the model learn how the sensor may appear under different but valid real-world imaging scenarios, while preserving the core chromatic patterns.

*2.6.2 Dataset Generation and Preprocessing for Temperature Prediction*

To automate the temperature prediction from the sensor's colorimetric response, a supervised machine learning pipeline was developed. The dataset used in this pipeline was generated from a comprehensive set of sensor images collected under controlled experimental conditions. Specifically, the sensor samples were exposed to six distinct temperatures: 55°C, 60°C, 65°C, 70°C, 75°C, and 80°C. For each temperature, the samples were subjected to six different exposure durations: 1 second, 5 seconds, 10 seconds, 30 seconds, 60 seconds, and 120 seconds. During each condition—defined by a specific temperature and time combination—20 images were captured to account for experimental variability and ensure statistical robustness. This entire imaging process was conducted separately for six different concentrations of PCDA: 5%, 10%, 12%, 15%, 18%, and 20%, resulting in a wide range of sensor responses reflecting both thermal and compositional variability. In total, 4,320 images were collected across all combinations of temperature, time, and concentration (6 temperatures × 6 time points × 20 images × 6 concentrations).

To prepare these images for machine learning, each image was processed using OpenCV. Images were read and converted from BGR to RGB color space. To ensure consistency across varying lighting conditions and eliminate pixel-level noise or irregularities, the average RGB color of each image was calculated by averaging across all pixels. This approach minimized the impact of shadows, glare, and localized artifacts, producing a single representative color vector per image. These averaged RGB values were then paired with metadata—such as temperature, exposure time, and PCDA concentration—extracted from the image filenames. The resulting data were compiled into a structured CSV file using Python's pandas library. Each row in the dataset included the image filename, average red, green, and blue (RGB) values, the corresponding temperature, exposure duration, and concentration label. A portion of this labeled dataset is presented in Table 2 below.

**Table 2:** Example Entries from the Labeled Dataset of PDA Sensor Images with Extracted RGB Values and Experimental Parameters

| Image Label | R | G | B |
|---|---|---|---|
| 5% conc_55° C_1sec_picture 1.jpg | 141.956 | 158.3107 | 181.6515 |
| 5% conc_55° C_1sec_picture 2.jpg | 162.0591 | 177.9135 | 200.6368 |
| 5% conc_55° C_1sec_picture 3.jpg | 143.5176 | 157.915 | 178.634 |
| 5% conc_55° C_1sec_picture 4.jpg | 157.3623 | 171.4922 | 192.5883 |
| 5% conc_55° C_1sec_picture 5.jpg | 154.6668 | 171.6197 | 196.819 |
| 5% conc_55° C_1sec_picture 6.jpg | 140.0661 | 154.6112 | 174.9477 |
| 5% conc_55° C_1sec_picture 7.jpg | 159.2698 | 173.3995 | 194.8267 |
| 5% conc_55° C_1sec_picture 8.jpg | 151.4497 | 166.2981 | 188.2032 |
| 5% conc_55° C_1sec_picture 9.jpg | 157.3394 | 172.195 | 194.7516 |
| 5% conc_55° C_1sec_picture 10.jpg | 154.4753 | 172.0968 | 197.2685 |

To prepare the dataset for model development and evaluation, an 80/20 train-test split was implemented using Scikit-learn's train_test_split() function. This division is a well-established practice in machine learning that ensures a model is trained on a sufficiently large portion of the data (80%) while reserving the remaining 20% for unbiased testing on previously unseen samples. The objective of this approach is to assess the generalization capability of the model and reduce the risk of overfitting. The dataset was evenly divided across all 6 PCDA concentrations, with each concentration contributing 720 images that were subsequently split into training and test sets using an 80/20 ratio, as summarized in Table 3.

**Table 3:** Distribution of Training and Test Samples Across PCDA Concentrations

| Concentration | Total Samples | Training Samples (80%) | Test Samples (20%) |
|---|---|---|---|
| **5%** | 720 | 576 | 144 |
| **10%** | 720 | 576 | 144 |
| **12%** | 720 | 576 | 144 |
| **15%** | 720 | 576 | 144 |
| **18%** | 720 | 576 | 144 |
| **20%** | 720 | 576 | 144 |

The 80/20 split used in this study reflects a widely accepted practice in machine learning for model development and evaluation (Kelleher, Namee, & D'Arcy, 2015). By allocating 80% of the data for training, the model is exposed to a sufficiently large and diverse set of examples to learn meaningful patterns and relationships between input features (RGB values) and target outputs (temperature). The remaining 20% is reserved for testing, ensuring that model performance is assessed on previously unseen data to evaluate its generalization capability. This

balance minimizes the risk of overfitting while still providing a robust estimate of predictive accuracy. Given the total dataset size of 4,320 images, this split yields 3,456 training samples and 864 test samples—ample quantities to support both effective learning and reliable evaluation across all PCDA concentrations. This strategy is widely used in supervised learning applications and is recommended in the literature as a baseline for effective model validation (Kelleher, Namee, & D'Arcy, 2015). The final dataset, saved as average_rgb_all_concentrations.csv, served as the foundation for developing and evaluating the supervised regression models used in this study.

### *2.6.3 Colorimetric Analysis (ΔE Calculation)*

To quantify the thermochromic response of the electrospun PDA sensors, digital images of the samples were captured using a flatbed scanner under consistent lighting and resolution settings after thermal exposure. The RGB values of each scanned image were extracted using Python and converted into the CIELAB (L*a*b*) color space using the skimage.color.rgb2lab() function. This conversion involves two sequential transformations: first, the RGB values are normalized and converted into the XYZ color space, which represents a linear approximation of human vision; then, the XYZ values are mapped into the L*a*b* color space through a nonlinear transformation that models human perceptual uniformity. Here, L* represents lightness, a* represents the red-green axis, and b* represents the yellow-blue axis.

The perceptual color difference (ΔE) between each thermally treated sample and its corresponding unheated reference was calculated using the CIE76 formula, established by the Commission Internationale de l'Éclairage (CIE)—the International Commission on Illumination. This formula quantifies color difference as the Euclidean distance between two points in the CIELAB color space, providing a standardized metric for evaluating visible changes in color:

$$\Delta E = \sqrt{(L^* - L_0^*)^2 + (a^* - a_0^*)^2 - (b^* - b_0^*)^2}$$

Where L*, a*, b* are the values for the heated sample, and $L_0^*$, $a_0^*$, $b_0^*$ are those of the unheated control (at room temperature). This metric provides a single-value measure of perceptual color difference, with higher ΔE values indicating stronger visible change. ΔE values were calculated for all combinations of PCDA concentrations, exposure times (1–120 seconds), and temperatures (55–80°C), and visualized as 3D surface plots to assess dynamic color change behavior.

*2.6.3 Model Training and Evaluation*

To enable quantitative temperature prediction from the sensor's colorimetric response, a supervised regression model was developed using the structured dataset of RGB values. Each image was represented by three input features—the average red, green, and blue (RGB) channel intensities—with the corresponding known temperature serving as the target label.

To maintain balanced representation and prevent overfitting, the data was randomly divided into training and testing sets using an 80/20 split (train_test_split, random_state=42). This commonly used strategy ensures that the model is exposed to a diverse training set while reserving a separate, unseen subset for evaluation—thereby offering a robust estimate of generalization performance (Kelleher, Namee, & D'Arcy, 2015). Separate models were trained for each PCDA concentration (5%, 10%, 12%, 15%, 18%, and 20%) to account for concentration-specific variations in chromatic behavior. For each subset, a linear regression model was trained using Scikit-learn's LinearRegression() class. Once fitted, the model was used to predict temperatures on the held-out test set.

Model performance was assessed using two standard metrics:

Mean Squared Error (MSE):

$$MSE = \frac{1}{n}\sum_{i=1}^{n}(y_i - \hat{y}_i)^2$$

Coefficient of Determination ($R^2$):

$$R^2 = 1 - \frac{\sum_{i=1}^{n}(y_i - \hat{y}_i)^2}{\sum_{i=1}^{n}(y_i - \bar{y}_i)^2}$$

where $y_i$ and $\hat{y}$ represent the actual and predicted temperatures respectively and $\bar{y}$ is the mean of the actual values. In addition to numerical evaluation, scatter plots of predicted vs. actual temperatures were generated to visualize alignment and identify any systematic deviations. Boxplots of prediction error across concentrations and response times were also created to assess the consistency and robustness of model predictions.

Once validated, the trained models were serialized using the joblib library and saved for future use. These models were later integrated into a command-line interface and a web-based application for real-time inference, enabling direct temperature prediction from new sensor images. Baseline RGB values at room temperature (25°C) were also added to the dataset to allow the model to learn a full response range and establish reference predictions under no thermal activation. This modeling approach demonstrated that reliable temperature prediction is achievable by combining colorimetric sensing with lightweight supervised learning, provided that the data is carefully curated and concentration-specific variations are considered.

*2.6.4 Deployment and Integration*

After achieving reliable performance, the trained regression model was serialized using the joblib library to enable convenient reuse and deployment. The model was integrated into two operational modes: a command-line script and a web-based application.

The standalone script processes an input sensor image by calculating the average RGB values and immediately predicting the corresponding temperature. This mode is lightweight and useful for batch testing or integration into desktop workflows.

For broader accessibility, a Flask-based web application was developed. This web app features a user-friendly interface that allows users to upload sensor images directly through their browser. Upon submission, the system extracts RGB features from the uploaded image and returns the predicted temperature in real time (see Figure 4). The application was styled for clarity and responsiveness to ensure ease of use, even on basic computing setups.

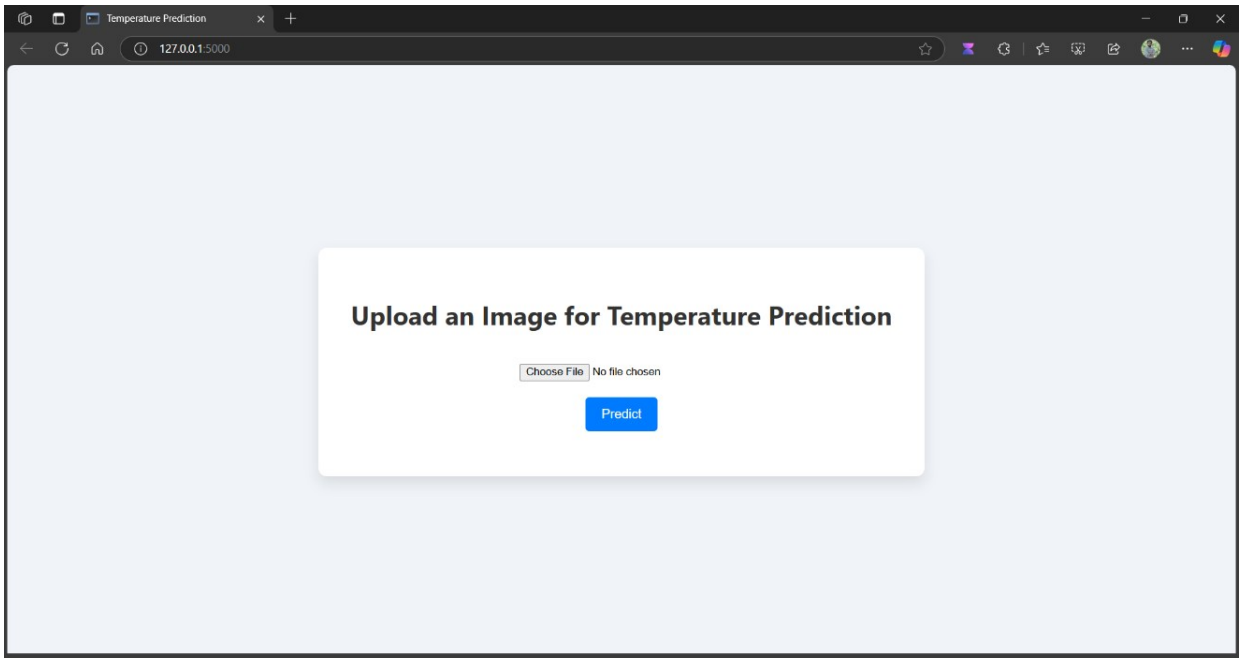


**Figure 4:** Web-Based Interface for PDA Sensor Temperature Prediction

This dual deployment strategy enhances the system's versatility—supporting both experimental workflows and real-world demonstrations. By combining PCDA-based

colorimetric sensing with machine learning, the approach transforms a visually interpretable signal into a quantitative diagnostic output. Final deployment and testing focused on the sensor configuration that consistently produced the most accurate and stable predictions during earlier evaluations.

Figure 5 below illustrates the overall end-to-end process from PDA-based core–shell fiber fabrication and thermal activation, through image capture and preprocessing, to the extraction of RGB features and machine learning model deployment for real-time temperature prediction.

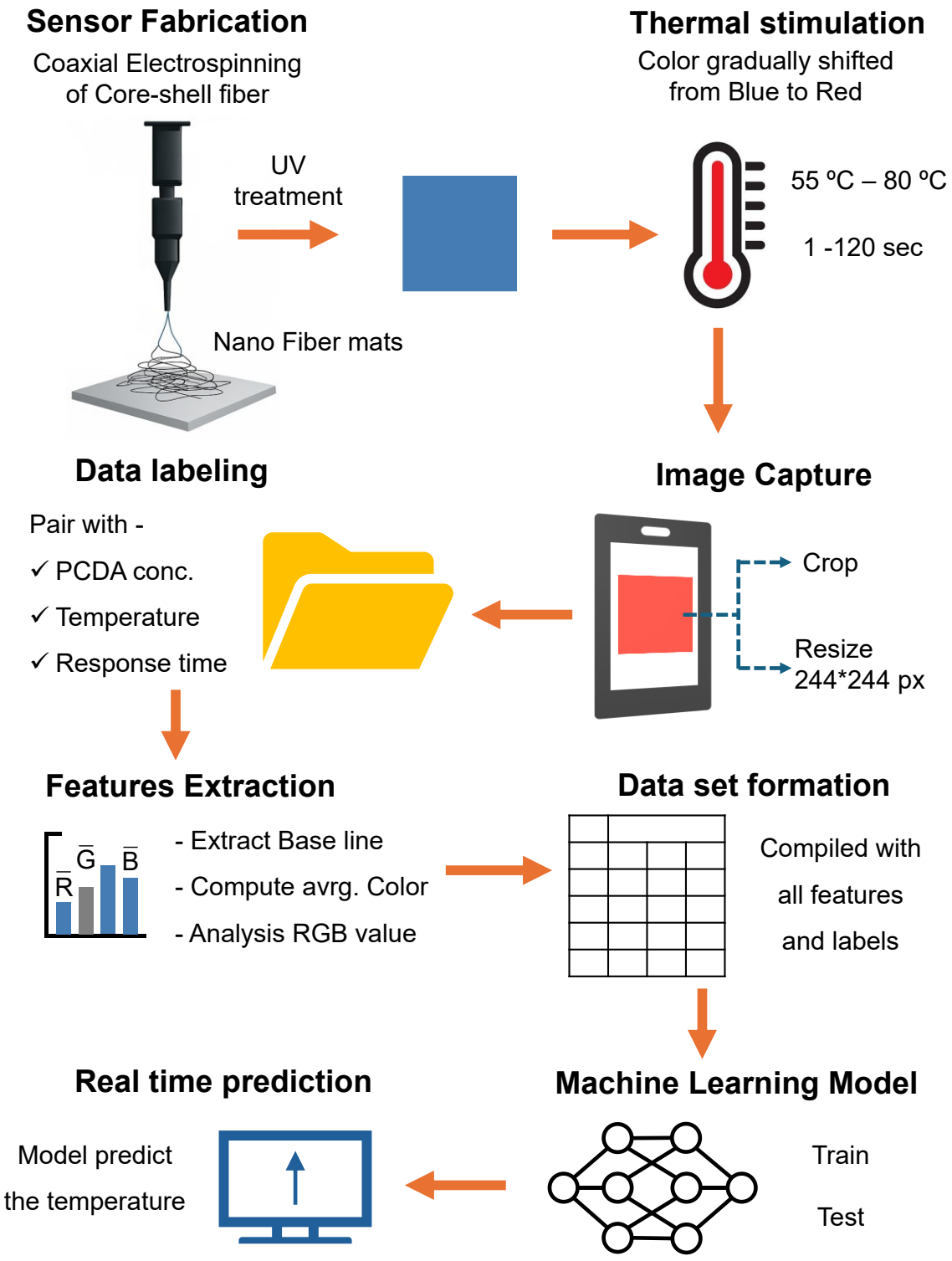


**Figure 5:** Integration of Colorimetric Sensor Images into a Machine Learning Pipeline for Temperature Prediction

# 3. RESULTS AND DISCUSSION

## 3.1 Chemical Analysis

Fourier-transform infrared (FTIR) spectroscopy was conducted to confirm the presence of PDA and polymer components in the electrospun fiber mats and to assess potential structural changes induced by thermal exposure. The core–shell architecture was designed with PU and PDA primarily located in the shell, and PEO was distributed in both core and shell regions. Spectra collected before and after heating are presented in Figure 6.

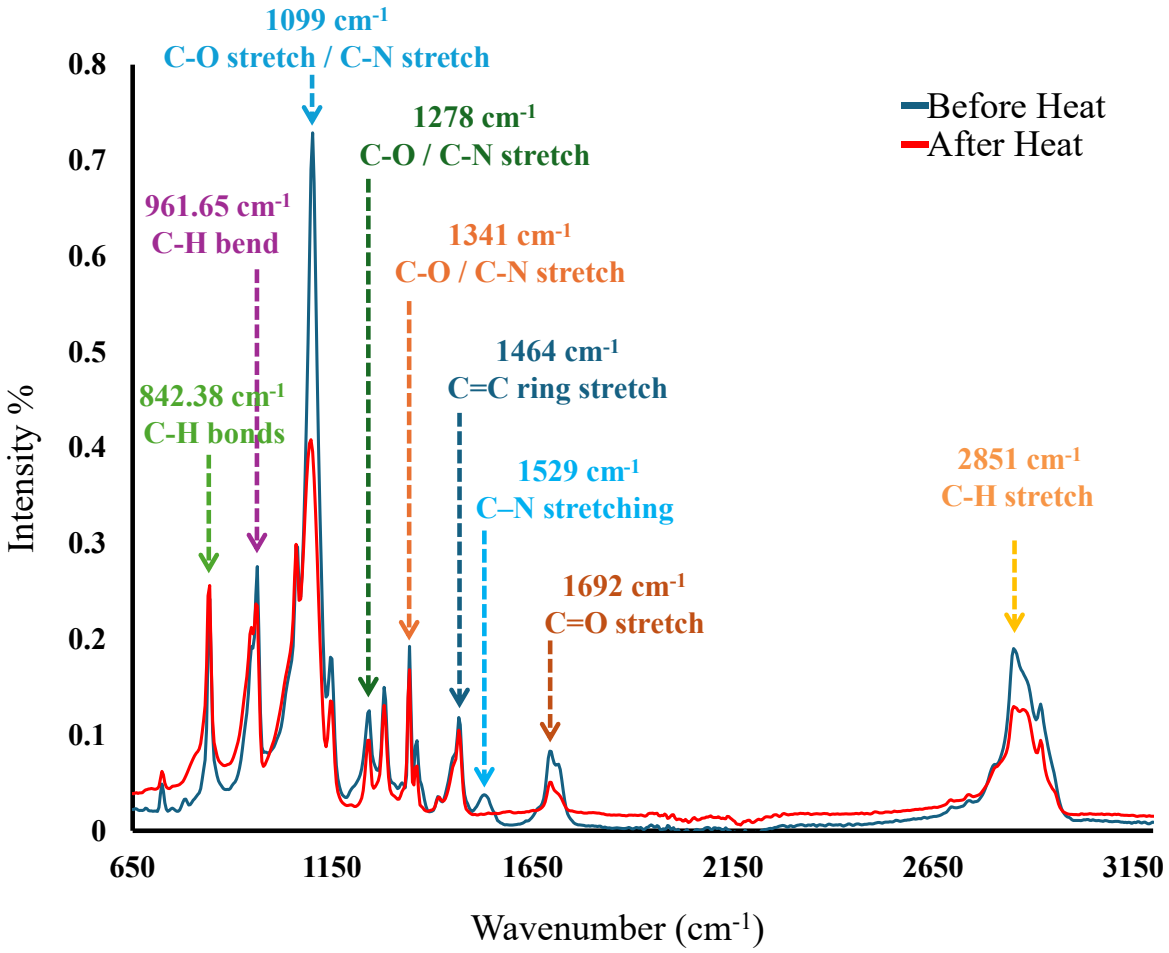


**Figure 6:** FTIR spectra of electrospun PDA-based fibers before (blue line) and after (red line) thermal exposure.

Before thermal stimulation, the FTIR spectrum displayed characteristic peaks corresponding to the three main components. A strong band at 2851 $cm^{-1}$ indicated aliphatic C–H stretching from PU and the long hydrocarbon chains in PDA. The presence of C=O stretching at 1692 $cm^{-1}$ confirmed urethane linkages from PU, while a notable C=C ring stretching at 1464 $cm^{-1}$ corresponded to the conjugated backbone of PDA. Peaks at 1341 $cm^{-1}$ and 1278 $cm^{-1}$ reflected C–O and C–N stretching typical of both PU and PEO. A prominent peak at 1099 $cm^{-1}$, associated with overlapping C–O and C–N stretching vibrations, further validated the inclusion of these polymeric components.

Following thermal exposure, all major peaks remained present, confirming the chemical stability and structural integrity of the sensor matrix. However, two notable spectral changes were observed. First, the peak at 1529.32 $cm^{-1}$, detected before heating, disappeared post-heating, suggesting a conformational rearrangement or partial disruption of hydrogen bonding or π-conjugation in the PDA domain. Second, the intensities of several key bands—including those at 2851 $cm^{-1}$, 1692 $cm^{-1}$, and 1464 $cm^{-1}$—showed noticeable reductions. These changes in intensity, while not indicating complete degradation, point to molecular-level rearrangements such as altered chain packing, dipole alignment, or changes in crystallinity.

The absence of peak shifting and the continued presence of all core functional group signals confirm that no new covalent bonds were formed, and no major decomposition occurred. This reinforces that the chromatic shift is the result of supramolecular, rather than chemical, transformation. FTIR analysis validates the incorporation of PU, PEO, and PCDA in the fiber system. The thermal response is accompanied by localized molecular changes—evidenced by the loss of the 1529.32 $cm^{-1}$ peak and intensity reductions—but the core chemical framework

remains intact. These results support the dual role of PDA: as both a stable structural component and a responsive chromatic indicator sensitive to temperature-induced rearrangement.

The FTIR analysis was crucial for verifying the successful incorporation of PCDA, PU, and PEO within the electrospun fiber matrix and for understanding the material's chemical stability after thermal stimulation. By comparing spectra before and after heating, this test provided insights into the supramolecular transformations underlying the sensor's color change. Confirming that the chromatic response results from non-covalent molecular rearrangements, rather than chemical degradation, reinforces the reliability of the sensor for repeated thermal cycling. Thus, FTIR served as foundational validation that the thermochromic behavior is structurally embedded and can be repeatedly triggered without compromising the chemical integrity of the sensing material.

## 3.2 Morphological Characterization

As depicted in Figure 7, the SEM image presents a representative example from Sample 4 (15% PCDA concentration), revealing a network of well-formed, smooth-surfaced, and predominantly bead-free fibers. Although only Sample 4 is shown here, similar morphological characteristics were consistently observed across all six PCDA concentrations. The absence of bead formation and the uniformity of the fibers suggest that the electrospinning parameters—such as voltage, flow rate, and polymer concentration—were appropriately optimized. The homogeneity and alignment observed within the fiber mat indicate that the PCDA solution exhibited favorable rheological properties, facilitating controlled fiber elongation during electrospinning.

Fiber diameter distribution was quantitatively assessed using ImageJ (v1.54), with 236 measurements analyzed to ensure statistical relevance and generate the distribution curve shown in Figure 7. The distribution displays a unimodal profile with a peak centered around 0.48 μm, and a standard deviation of 0.33 μm, indicating a relatively narrow dispersion of fiber sizes. This tight distribution reflects consistent fiber formation and highlights the repeatability of the electrospinning process under the selected parameters.

Uniformity in fiber diameter plays a crucial role in determining the thermal and optical properties of the sensor. Variations in diameter can introduce inconsistencies in heat diffusion and colorimetric response due to local changes in surface area and material density. Therefore, achieving and maintaining diameter consistency is essential for ensuring the accuracy and reliability of thermochromic sensing. This morphological assessment not only verifies the structural integrity of the electrospun PDA fibers but also establishes a benchmark for quality control in sensor fabrication. The observed microstructure and diameter uniformity confirm the suitability of the electrospun mat for further functionalization and integration into a temperature-responsive colorimetric sensor.

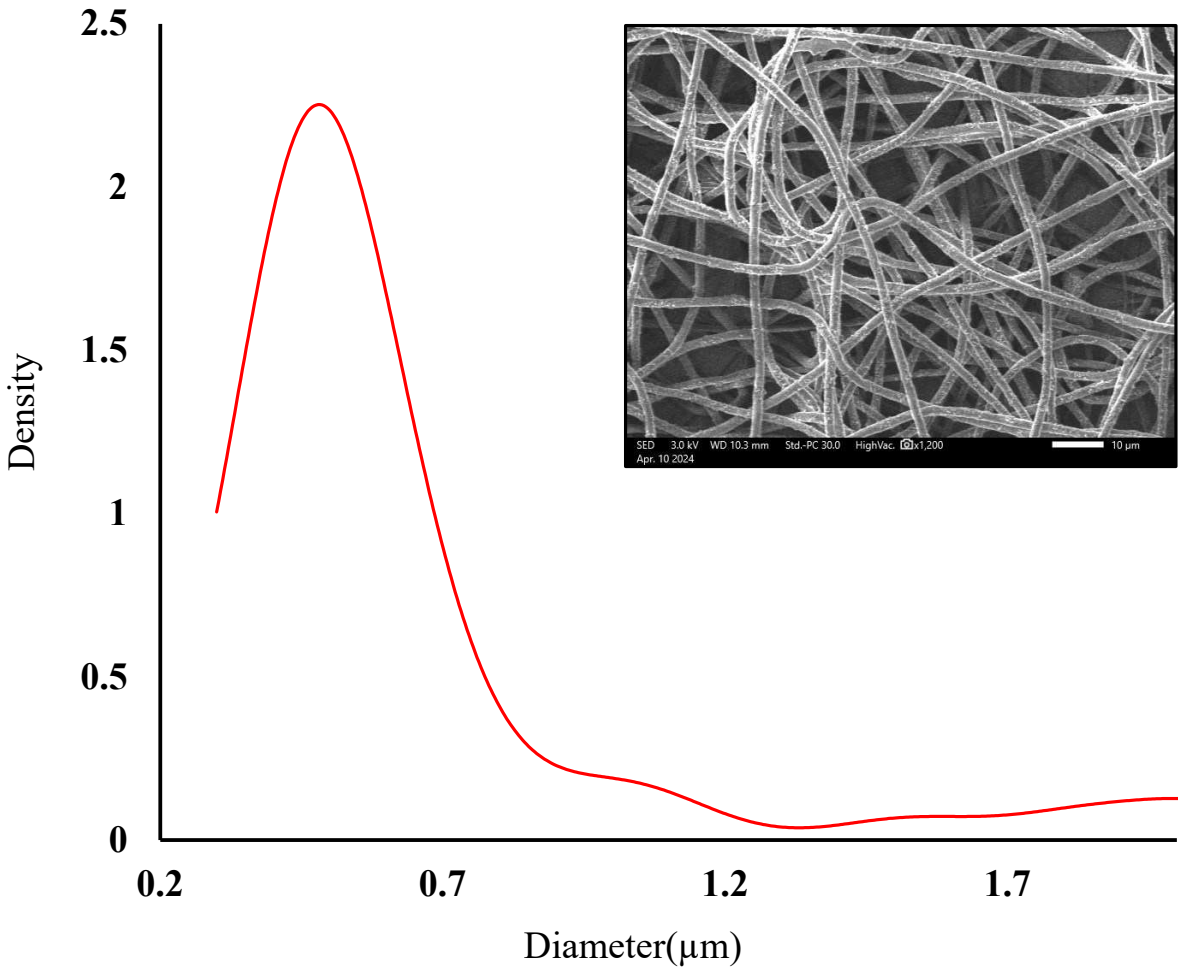


**Figure 7:** Fiber Diameter Distribution of Electrospun PDA-Based Nanofibers with SEM Visualization (make it black and white)

Morphological analysis using SEM was essential to ensure that the electrospinning process produced consistent, bead-free, and uniform nanofibers across all PCDA concentrations. Since fiber diameter and morphology directly influence thermal response, color uniformity, and overall sensor sensitivity, this test confirmed that the nanofiber platform was structurally robust and reproducible. Quantitative diameter analysis further enabled correlation between microstructure and sensor performance, supporting the hypothesis that uniform morphology is critical for achieving reliable and interpretable thermochromic behavior.

## 3.3 Surface Wettability (Contact Angle Analysis)

The surface wettability of the electrospun core–shell fibers was evaluated by measuring the static water contact angle for each sample. Contact angle measurements revealed a clear trend: as the PCDA concentration in the shell increased, the surface became more hydrophobic. Sample 1 (5% PCDA) exhibited contact angles of 93.52° and 95.65°, indicating a moderately hydrophobic surface. As the PCDA content increased, Sample 2 (10% PCDA) showed a contact angle of 110.78°, and Sample 3 (12% PCDA) reached 127.34°, reflecting a substantial enhancement in hydrophobicity. The highest hydrophobicity was observed in Sample 4 (15% PCDA), which displayed a contact angle of 142.82°. Beyond this point, a slight reduction in contact angle occurred, with Sample 5 (18% PCDA) recording 140.87°, and Sample 6 (20% PCDA) decreasing further to 135.01°.

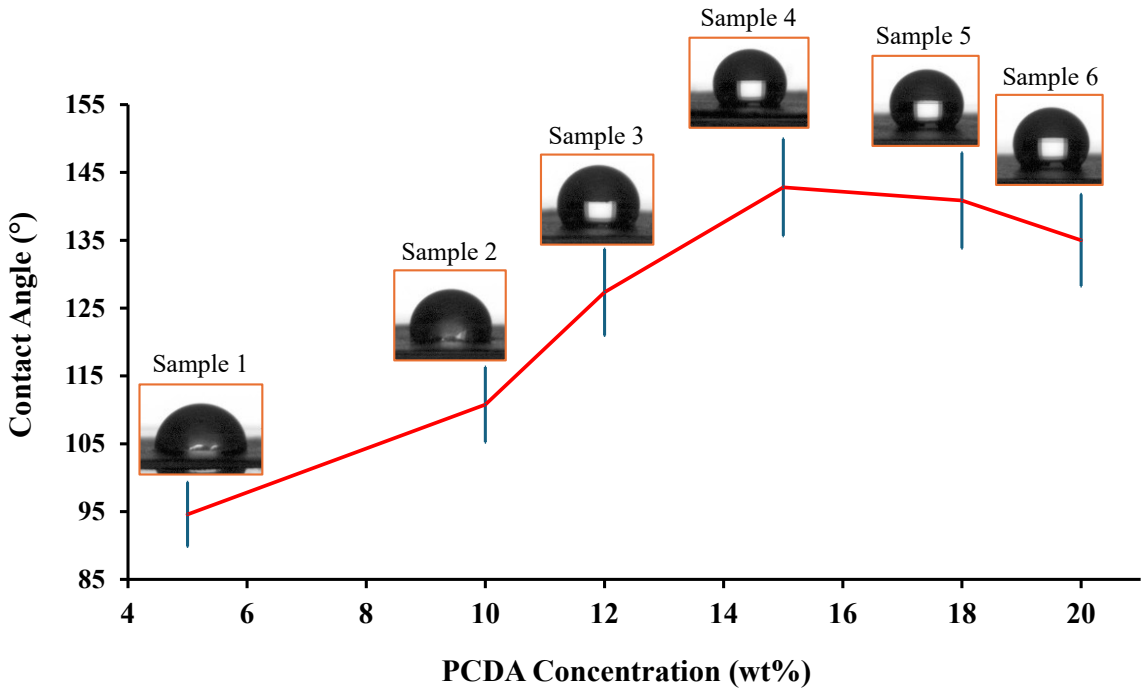


**Figure 8:** Contact angle measurements electrospun core–shell fibers with varying PCDA concentrations.

A plot summarizing the contact angle values for all samples, along with corresponding droplet profile images, is presented in Figure 8. Visual comparison reinforces the quantitative trend, clearly showing the increasing contact angle and more spherical droplet shape as PCDA concentration rises. The observed improvement in hydrophobicity up to 15% PCDA can be attributed to the greater surface exposure of hydrophobic alkyl chains as the PCDA concentration increased. This relationship between alkyl chain density and enhanced hydrophobicity has been previously reported, where increasing the length or concentration of alkyl chains led to higher water contact angles due to reduced surface energy (Chen et al., 2020). Higher PCDA content favored denser molecular packing and improved surface organization, leading to lower surface energy and enhanced water repellency. However, when the PCDA concentration exceeded 15%, the contact angle slightly declined. This behavior is likely due to excessive PCDA loading, which can disrupt the smoothness of the fiber surface by creating morphological irregularities or micro-aggregates. Such surface defects may locally increase wettability, reducing the overall hydrophobicity of the mat.

The contact angle analysis was conducted to understand how varying PCDA concentrations influence the surface hydrophobicity of electrospun fibers—an important factor for sensor performance in moist environments. The results identified 15% PCDA as the optimal concentration that maximizes hydrophobicity while preserving surface uniformity. This insight is essential for selecting formulations that ensure sensor durability, minimize water-induced interference, and maintain consistent colorimetric response in biomedical or environmental applications.

## 3.5 Colorimetric Response to Temperature

To evaluate the thermochromic performance of the sensor, electrospun fiber mats were exposed to controlled temperatures ranging from 55°C to 80°C at six different PCDA concentrations: 5%, 10%, 12%, 15%, 18%, and 20%. For each sample, color change was recorded at multiple time intervals (1 second, 5 seconds, 10 seconds, 30 seconds, 60 seconds, and 120 seconds) to capture the transition behavior over time. The resulting visual transformations were captured and compiled into sensor color response grids (Figures 9a–f).

At low concentrations (5% and 10%), noticeable color transition began to emerge around 60°C and intensified with both increasing temperature and time. The 5% PCDA sensor (Figure 9a) exhibited a relatively pale shift from bluish-gray to pink-red, with less saturation even at longer times (120 s). In contrast, the 10% PCDA sensor (Figure 9b) demonstrated faster and more vibrant red development at lower exposure times, indicating improved thermos-responsiveness.

Sensors containing 12% and 15% PCDA (Figures 9c and 9d) showed a more progressive and saturated chromatic transition. At just 30 seconds, red hues became dominant for temperatures ≥70°C, indicating that higher PCDA content supports quicker and more reliable phase transition. The 15% grid also suggested slightly faster color development compared to 12%, especially at 75°C and 80°C, despite some unevenness in red intensity at the highest temperatures.

The most intense and consistent color change was observed in the 18% and 20% PCDA samples (Figures 9e and 9f). These samples achieved a deep, saturated red by 10 seconds at 75°C, and full transitions were visible as early as 65°C after 30 seconds. Both grids revealed

smooth gradient transitions across temperature and time axes, highlighting the capability of higher-concentration sensors to respond rapidly and with minimal delay or ambiguity. This progressive and concentration-dependent color evolution underscores the tunable thermochromic sensitivity of PDA-based sensors. The visual evidence supports further quantitative analysis using RGB and ΔE metrics in Sections 3.6 and beyond, confirming that the structural response to thermal input can be precisely modulated through PCDA concentration and exposure time.

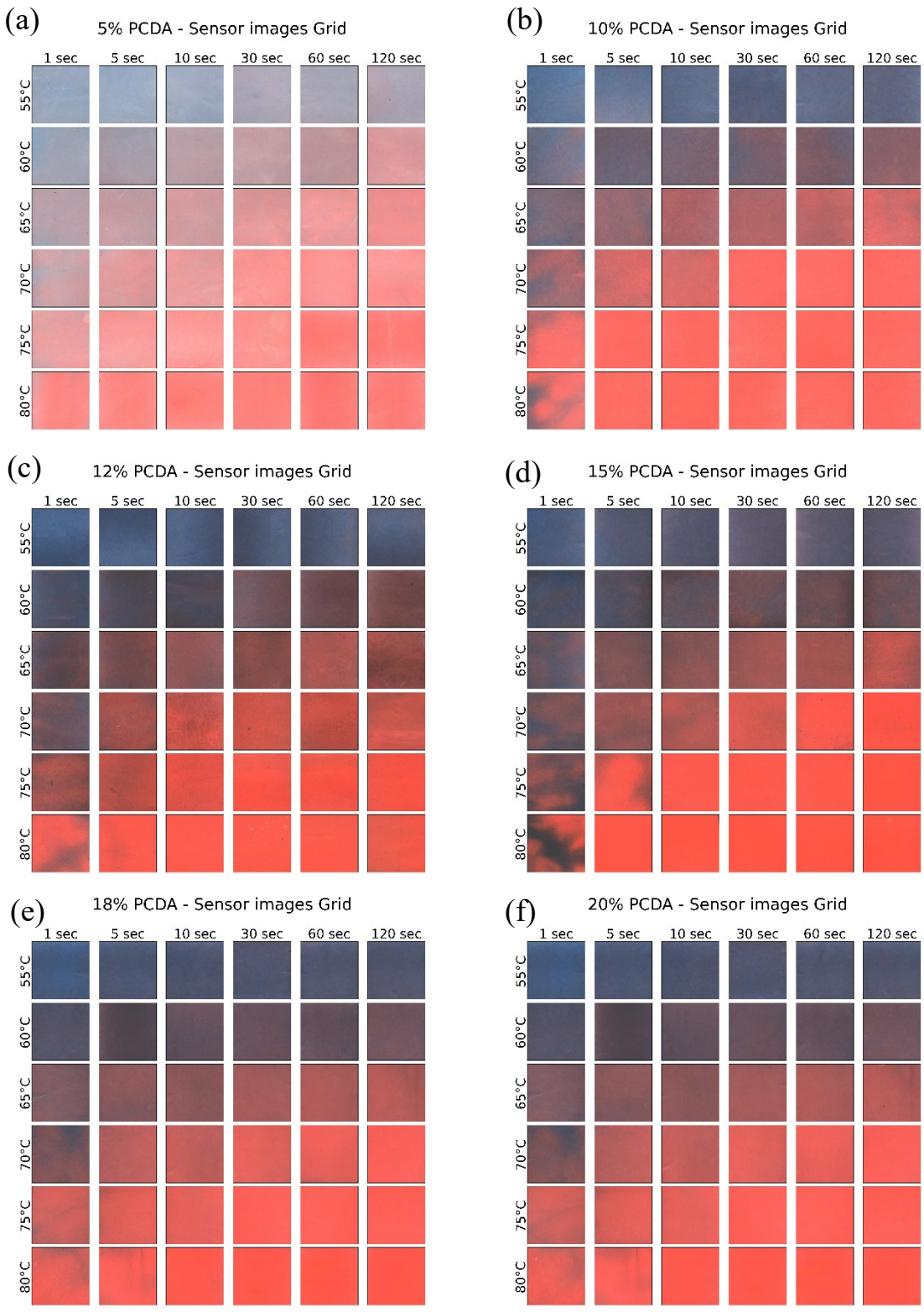


**Figure 9:** PDA sensor colorimetric response grids for electrospun sensors with varying PCDA concentrations (a) 5%, (b) 10%, (c) 12%, (d) 15%, (e) 18%, (f) and 20% exposed to temperatures ranging from 55°C to 80°C and response times of 1, 5, 10, 30, 60, and 120 seconds.

These visual sensor grids were a qualitative yet powerful way to initially screen how PCDA concentration and thermal exposure time impact the visibility and consistency of chromatic transition. This test was essential for identifying the concentration thresholds at which perceptible and reliable color change begins to occur, guiding subsequent quantitative and predictive analyses.

## 3.6 Thermal Colorimetric Performance Across PCDA Concentrations

To quantitatively assess the thermochromic response of the electrospun PDA-based sensor mats, the perceptual color difference was measured using the ΔE metric, which captures the overall deviation from the unheated baseline in perceptual color space. This analysis was conducted across six PCDA concentrations (5%, 10%, 12%, 15%, 18%, and 20%), with fiber samples exposed to temperatures ranging from 55°C to 80°C for durations between 1 and 120 seconds. The results are shown below in Figure 10.

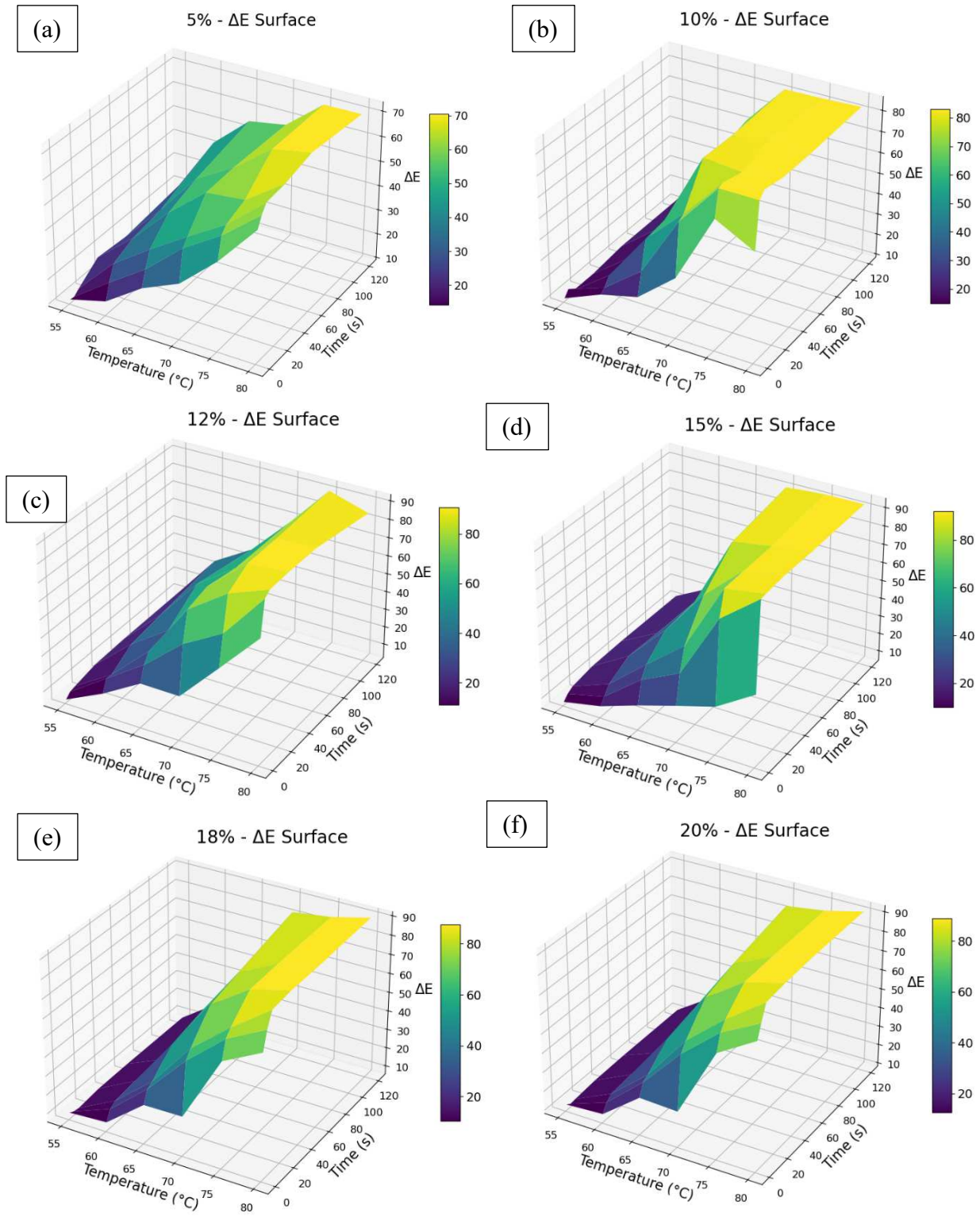


**Figure 10:** ΔE surface plots for electrospun sensors with varying PCDA concentrations—(a) 5%, (b) 10%, (c) 12%, (d) 15%, (e) 18%, and (f) 20%—showing perceptual color difference across temperatures (55°C to 80°C) and response times (1, 5, 10, 30, 60, and 120 seconds).

The ΔE values were visualized as 3D surface plots (Figure 10a–f), which reveal clear concentration-dependent trends in thermochromic behavior. At the lowest concentration (5% PCDA), the color response was modest, with a maximum ΔE of 73.2 observed at 80°C and 120 seconds (Figure 10a). At 60°C and 60 seconds, the ΔE reached only 36.7, indicating limited sensitivity under relatively low-temperature and short-response time conditions. Increasing the concentration to 10% improved responsiveness, yielding a peak ΔE of 85.0 at 80°C and 120 seconds, with intermediate values around 62.8 at 70°C and 60 seconds (Figure 10b).

Further enhancement was observed at 12% PCDA, which displayed ΔE values exceeding 90.5 under maximum exposure, and over 71.0 at 70°C and 60 seconds, confirming a sharper transition threshold and improved colorimetric contrast (Figure 10c). The 15% PCDA sample demonstrated a comparable maximum ΔE of 90.2, with significant response already evident at 65°C and 30–60 seconds, marking a noticeable improvement in reaction speed (Figure 10d).

The most pronounced transitions were observed at higher concentrations. At 18% PCDA, the ΔE surface (Figure 10e) showed steep gradients, with values rapidly increasing toward the thermal saturation zone. Finally, the 20% PCDA sample exhibited the most robust color change, achieving a ΔE of 91.3 at 80°C and 120 seconds, and reaching 75.6 as early as 60 seconds, indicating high sensitivity even under shorter exposure times (Figure 10f).

However, the rate and magnitude of change were highly dependent on PCDA concentration. Lower concentrations required higher temperatures and longer times to achieve visible transitions, while concentrations of 15% and above exhibited strong ΔE responses beginning around 65–70°C and just 30–60 seconds of exposure. These results suggest that the thermochromic sensitivity and efficiency of the sensor can be fine-tuned by adjusting the PCDA content in the electrospun fiber matrix. This spatiotemporal analysis highlights the critical role of

PCDA concentration in defining sensor performance. The ΔE surface plots serve not only as a visual diagnostic but also as a quantitative tool for optimizing material formulation and operational conditions. The 15% to 20% PCDA range was identified as optimal for achieving fast, high-contrast, and thermally responsive colorimetric changes, laying the groundwork for reliable biosensing applications and data-driven calibration strategies. ΔE calculations provided a standardized and quantifiable method to evaluate the strength and clarity of thermochromic transitions. This metric enabled precise comparison across samples and experimental conditions, helping to identify the optimal formulation and conditions for maximum sensitivity—an indispensable step before developing any data-driven prediction model.

## 3.7 Machine Learning Model Performance

To eliminate human bias in interpreting colorimetric sensor responses and enable automated temperature prediction, a supervised machine learning model was trained using RGB values extracted from scanned images of the electrospun PCDA fiber mats. Separate regression models were developed for each PCDA concentration (5%, 10%, 12%, 15%, 18%, and 20%) using image data collected across six exposure times (1, 5, 10, 30, 60, and 120 seconds) and temperatures ranging from 55°C to 80°C.

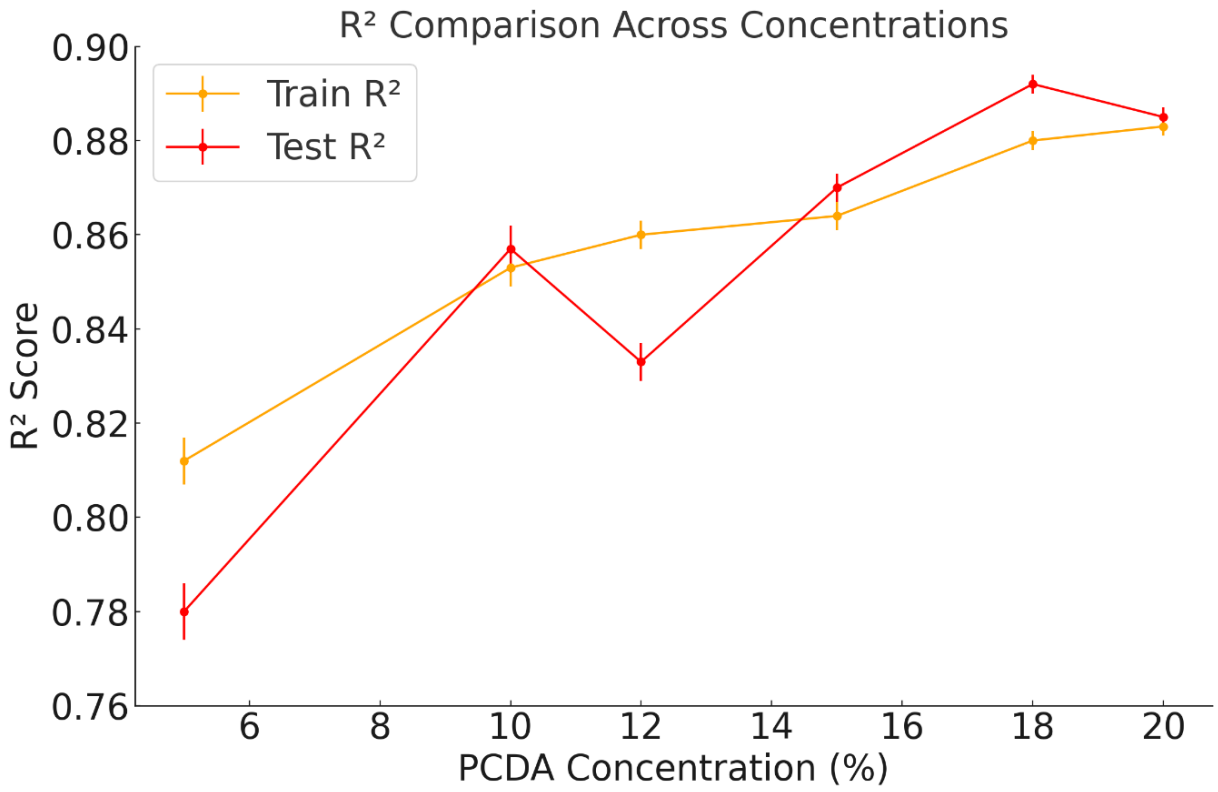


**Figure 11:** $R^2$ Score Comparison for Temperature Prediction Models Across PCDA Concentrations

As seen in Figure 11, model performance clearly improved with increasing PCDA concentration. For 5% PCDA, the model struggled at short response times, with a test $R^2$ of only 0.78, and frequent underestimations—for example, at 1 second, the model predicted 52.3°C for an actual 55°C input. Accuracy gradually improved at longer durations, with errors narrowing to around ±2.1°C at 60 seconds. At 10% PCDA, the color response became stronger, and model predictions improved accordingly. Most test points stayed within ±2°C of the true temperature after 30 seconds. For example, at 75°C and 30 seconds, the predicted value was 74.2°C, indicating a high level of precision.

Once PCDA concentration reached 12% and higher, performance became much more consistent. However, a slight drop in test $R^2$ was observed at 12% PCDA, likely due to increased variability in the test set or transitional chromatic behavior in the sensor's thermal response

range. This brief inconsistency did not persist at higher concentrations. The 12% model produced temperature predictions at 80°C ranging from 77.5°C to 79.6°C across all time intervals, with a mean absolute error of only 1.3°C. Similar levels of accuracy were observed for 15%, 18%, and 20% PCDA, particularly at medium to long exposures. Among all, the 18% PCDA model stood out as the most reliable. It achieved the highest test $R^2$ value at 0.884, and consistently maintained low prediction errors across all conditions. At 120 seconds, for instance, it predicted 79.4°C, 74.7°C, and 70.3°C for actual temperatures of 80°C, 75°C, and 70°C, respectively—corresponding to errors of just 0.6°C, 0.3°C, and 0.3°C. To further evaluate prediction consistency across different experimental conditions, the distribution of temperature prediction errors was analyzed and visualized as a function of PCDA concentration and exposure duration, as shown in Figure 12.

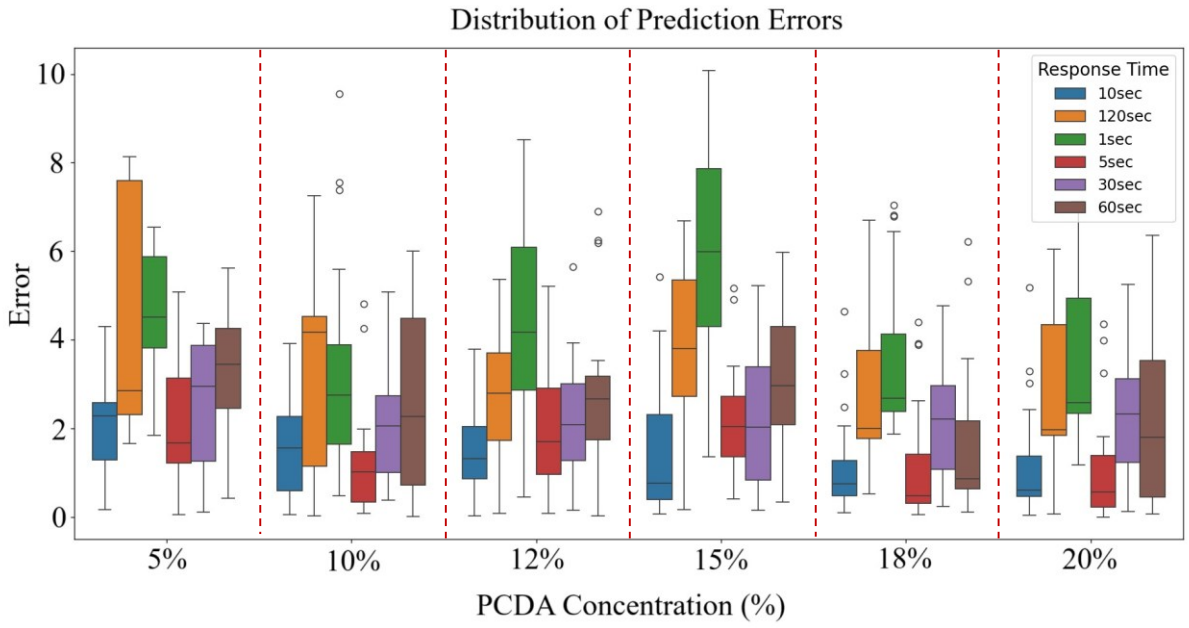


**Figure 12:** Distribution of Temperature Prediction Errors Across PCDA Concentrations and Exposure Times

Figure 12 illustrates the distribution of temperature prediction errors (in °C) across all concentrations and exposure times. This boxplot analysis reveals that prediction error is strongly dependent on both PCDA concentration and response time. For lower concentrations (e.g., 5%), the error distribution is wide, especially at shorter exposure times like 1 and 10 seconds. Notably, 5% PCDA at 10 seconds showed median errors close to 4°C and frequent outliers beyond ±6°C, highlighting the unreliability of the sensor in such conditions. Conversely, higher concentrations such as 18% and 20% consistently exhibited narrow error ranges across all response times, with median prediction errors between 1.5°C and 2.5°C.

These trends confirm that sensor reliability and ML model accuracy improve significantly with higher PCDA content and longer thermal exposure. For concentrations ≥12%, and particularly at exposure times of 30 seconds or more, the models achieved strong predictive consistency with low error dispersion and high $R^2$ values. Together, these findings establish the integrated ML-sensor platform as an effective, automated solution for visual temperature readout, with tunable performance based on material formulation and sensing conditions. The machine learning regression tests were central to demonstrating that temperature prediction from PDA sensor images is not only feasible but accurate when configured properly. These tests validated the core hypothesis of the study—that chromatic responses from electrospun sensors could be digitized and interpreted automatically—bridging the gap between color-based materials and smart analytics.

## 3.8 Error Analysis

Error analysis plays a crucial role in evaluating the reliability and robustness of the machine learning model. While the majority of temperature predictions fell within ±1.3 to 2.5°C of the true value, occasional larger discrepancies were observed, particularly at lower PCDA concentrations (5% and 10%) and during short thermal exposure times (1–5 seconds). These larger errors can be traced to the relatively weak color transitions under these specific conditions, which did not produce strong enough RGB contrast for the model to reliably interpret temperature differences. At lower PCDA concentrations, the color changes were often subtle and less saturated, resulting in overlapping RGB ranges across different temperatures. Consequently, the model sometimes misclassified these subtle color variations, leading to higher error variance.

A closer examination of residual errors revealed that underestimation tended to occur during the early exposure intervals, reflecting the slower color development of the fibers in those conditions. Overestimation, on the other hand, was infrequent and typically limited to lower PCDA concentrations where the chromatic signal was inherently weaker. These patterns suggest that model prediction errors are not entirely random; instead, they are closely tied to the kinetics of color formation and the fundamental material response under thermal stimulus.

The noticeable dip in the $R^2$ value for the 12% PCDA concentration is also revealing. Unlike other concentrations, the 12% formulation appeared to produce a less consistent or intense color transition across the fiber mat. In these samples, random patches were observed where the color remained blue rather than turning red as expected. This incomplete or inconsistent color development likely created local variations in the RGB values, making it more difficult for the model to extract consistent patterns and reducing its predictive fidelity.

Overall, this error analysis underscores the close connection between material characteristics—such as PCDA concentration and fiber uniformity—and the predictive performance of the machine learning model. While some error may originate from measurement noise, most of the observed errors reflect meaningful limitations in the colorimetric response of the sensor material under suboptimal fabrication or operational conditions. This insight is crucial for guiding future improvements in both the sensor's material formulation and the machine learning workflow.

## 3.9 Time-Response Analysis

To evaluate the dynamic behavior of the sensor system, the evolution of temperature prediction accuracy was analyzed across varying exposure times. Actual vs. predicted temperature plots, presented in Figure 13 (a–f) for each PCDA concentration, demonstrate how response time directly impacts the model's accuracy, reliability, and stability.

At 1 second, models performed inconsistently across all concentrations. As shown in Figure 13a, the 5% PCDA sensor significantly underpredicted temperature at low and mid-range levels, with deviations as large as 5°C. Predictions did not follow a consistent trend and had low $R^2$ values (often <0.75). Even at 20% PCDA (Figure 13f), which exhibited higher thermochromic sensitivity compared to lower concentrations, the model was still prone to underestimation due to insufficient color development. With 5 seconds of exposure, Figures 13b and 13c show improved but still variable predictions, especially for 10% and 12% PCDA. The predicted lines began to approach the ideal diagonal, though inconsistencies remained—particularly around 60°C to 70°C where transitions begin but have not fully matured. Median prediction errors remained above 3.0°C for most concentrations, and several outliers were present. At 10 seconds, model reliability began to emerge. As seen in Figure 13d (15%), the

predicted temperatures closely followed the actual values, especially above 65°C. Similarly, Figure 13e (18%) showed a much tighter fit, with mean absolute errors (MAEs) dropping to around 2.1°C, and $R^2$ values rising above 0.85. Notably, the 18% and 20% models (Figure 13e, f) showed consistently better tracking across all temperature levels compared to lower concentrations. At 30 seconds, the predictive performance stabilized for most concentrations. In Figure 13c–f, nearly all predicted lines aligned closely with the actual temperatures, even for sensors with 10%–12% PCDA. MAEs fell below 2.0°C, and the trend lines in 18% and 20% plots became nearly indistinguishable from the diagonal, indicating minimal bias or drift. The improvement at this point is especially notable in 15% and 18% samples, where model variance also decreased significantly. By 60 seconds, the sensors reached peak response accuracy. Figure 13e (18%) shows excellent alignment across all time points, with most predictions falling within ±1.3°C of actual values. Figure 13f (20%) followed closely behind, confirming that chromatic saturation and model learning converged effectively. $R^2$ values remained high (~0.88–0.884), and interquartile ranges of error distributions narrowed further, indicating stable performance. At 120 seconds, model predictions showed little to no further gain over 60 seconds. As evident across all plots, particularly Figure 13d–f, prediction curves were nearly identical to the 60-second ones, suggesting that the thermochromic system had already reached saturation. For example, the predicted temperature at 80°C for 20% PCDA remained around 79.4°C, the same as in the previous interval, confirming diminishing returns from longer exposures.

Figures 13 (a–f) illustrate that while early response times (1–5 seconds) result in inconsistent predictions, reliable performance begins around 10 seconds and becomes optimal at 30 to 60 seconds, especially for higher PCDA concentrations like 18% and 20%. These findings

suggest that both material formulation and sufficient thermal exposure are critical for achieving accurate and reproducible temperature sensing in colorimetric sensors.

This analysis helped define the practical response window of the sensor, clarifying the minimum thermal exposure time required for reliable predictions. It provided vital insight into how fast the sensor can realistically deliver accurate feedback, supporting application-specific calibration, such as rapid diagnostics or continuous monitoring.

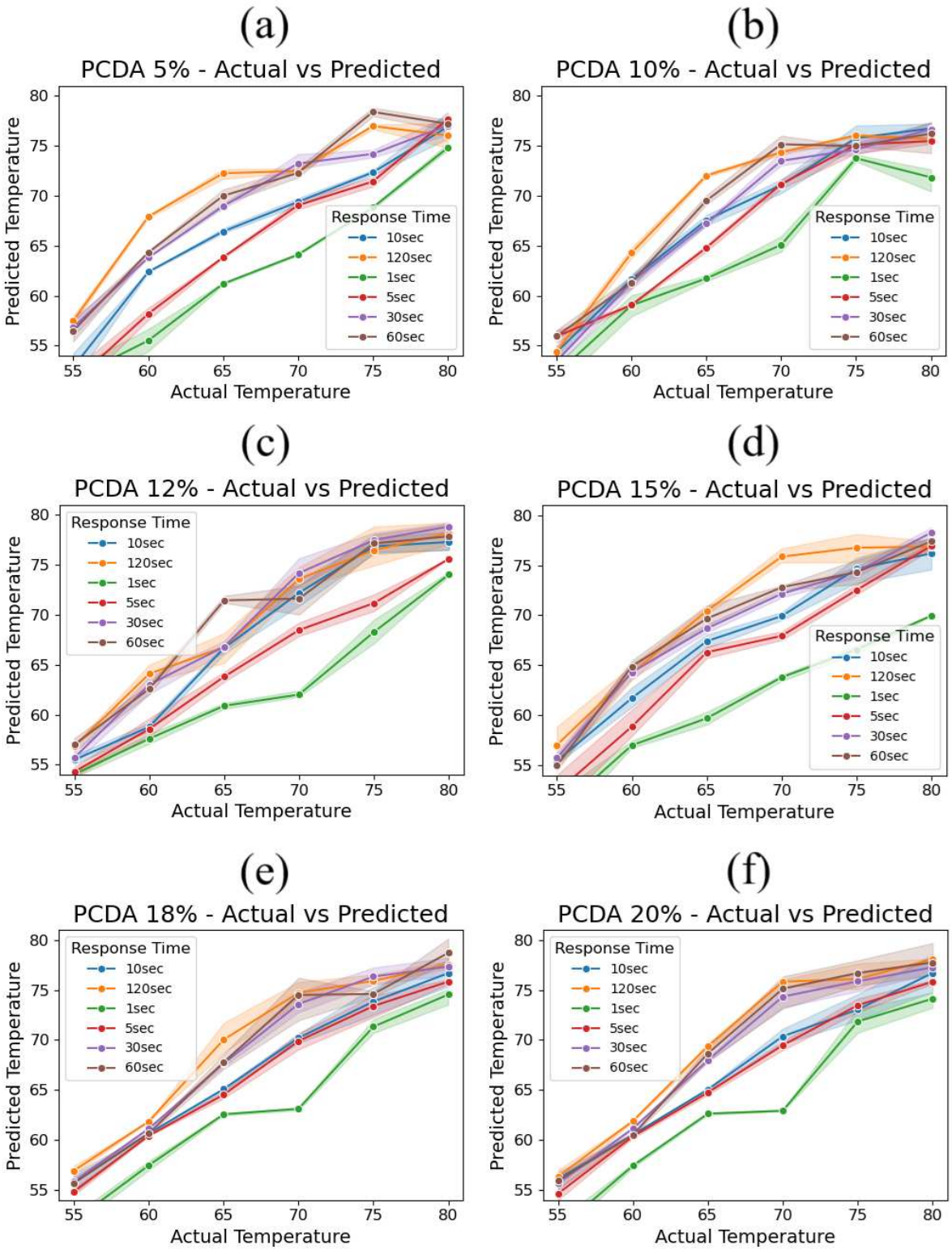


**Figure 13:** Temporal Impact on Model Accuracy: Actual vs. Predicted Temperature Plots Across Exposure Durations for Different PCDA Concentrations (a) 5%, (b) 10%, (c) 12%, (d) 15%, (e) 18%, (f) 20%)

## 3.10 Concentration-Dependent Sensitivity

To explore how PCDA concentration affects sensor accuracy and thermal responsiveness, the model's performance was evaluated across all six concentrations using scatter plots of actual vs. predicted temperatures (Figure 14a–f). These visualizations highlight the concentration-dependent consistency and precision of the machine learning models across the full range of thermal exposure conditions.

At 5% PCDA (Figure 14a), the model struggled to track the thermal signal accurately, particularly at lower temperatures and shorter exposure times. While the predictions generally followed the correct trend, noticeable deviations persisted, and clustering around the ideal diagonal line was loose. The spread in predicted values was widest here, confirming that low chromatic intensity at this concentration limits reliable learning and prediction. With 10% PCDA (Figure 14b), the model performance improved noticeably. The data points formed a tighter band around the ideal line, particularly from 65°C upward. At lower temperatures, scatter remained visible, but by 75°C and 80°C, the predicted values consistently aligned with actual temperatures. This suggests that the 10% concentration can support useful thermal sensing, especially in mid-to-high temperature zones. The 12% PCDA sensor (Figure 14c) demonstrated further enhancements in sensitivity and predictability. Predicted values closely tracked actual temperatures with reduced variance, especially above 60°C. Minor underestimation was observed at the low end, but overall, the alignment with the identity line indicates improved model calibration and colorimetric response at this concentration.

At 15% PCDA (Figure 14d), although the general predictive performance was strong, some points showed mild scatter, particularly in the mid-temperature range (65–70°C). This suggests occasional fluctuations in sensor output or model generalization. Nevertheless, the

overall prediction trend remained reliable and consistent, with most values falling close to the diagonal. The 18% PCDA sample (Figure 14e) exhibited excellent performance across the board. Predictions followed the ideal line with minimal deviation, and clustering was tight from 55°C to 80°C. This consistency, across all temperature classes and regardless of exposure time, reflects robust chromatic signal strength and highly learnable data characteristics. Among all tested concentrations, the sensor made with 18 % PCDA offered the best balance between early-stage sensitivity and high-temperature saturation. Finally, 20% PCDA (Figure 14f) also achieved high prediction accuracy, nearly matching 18% in performance. The predicted temperatures aligned closely with actual values, with even tighter clustering at high temperatures. Minor underestimation was observed at 55°C and 60°C, likely due to the sensor nearing saturation in the red state, reducing perceptible variation. Still, the overall prediction variance remained low, and performance was among the most reliable.

Taken together, the results show that while lower PCDA concentrations (5–10%) are adequate for general sensing, they lack the consistent intensity required for precise machine learning regression. Concentrations of 18% and 20% provide the most accurate and stable prediction outcomes, as seen in their tight clustering and linear response trends. These concentrations should be prioritiz ed for real-world deployment where accurate and consistent thermal readouts are critical. This analysis was important for understanding the balance between sensor formulation and predictive accuracy. By correlating concentration to model fidelity, the test enabled data-driven selection of optimal PCDA loading, ensuring that future implementations can minimize material use while maintaining high analytical performance.

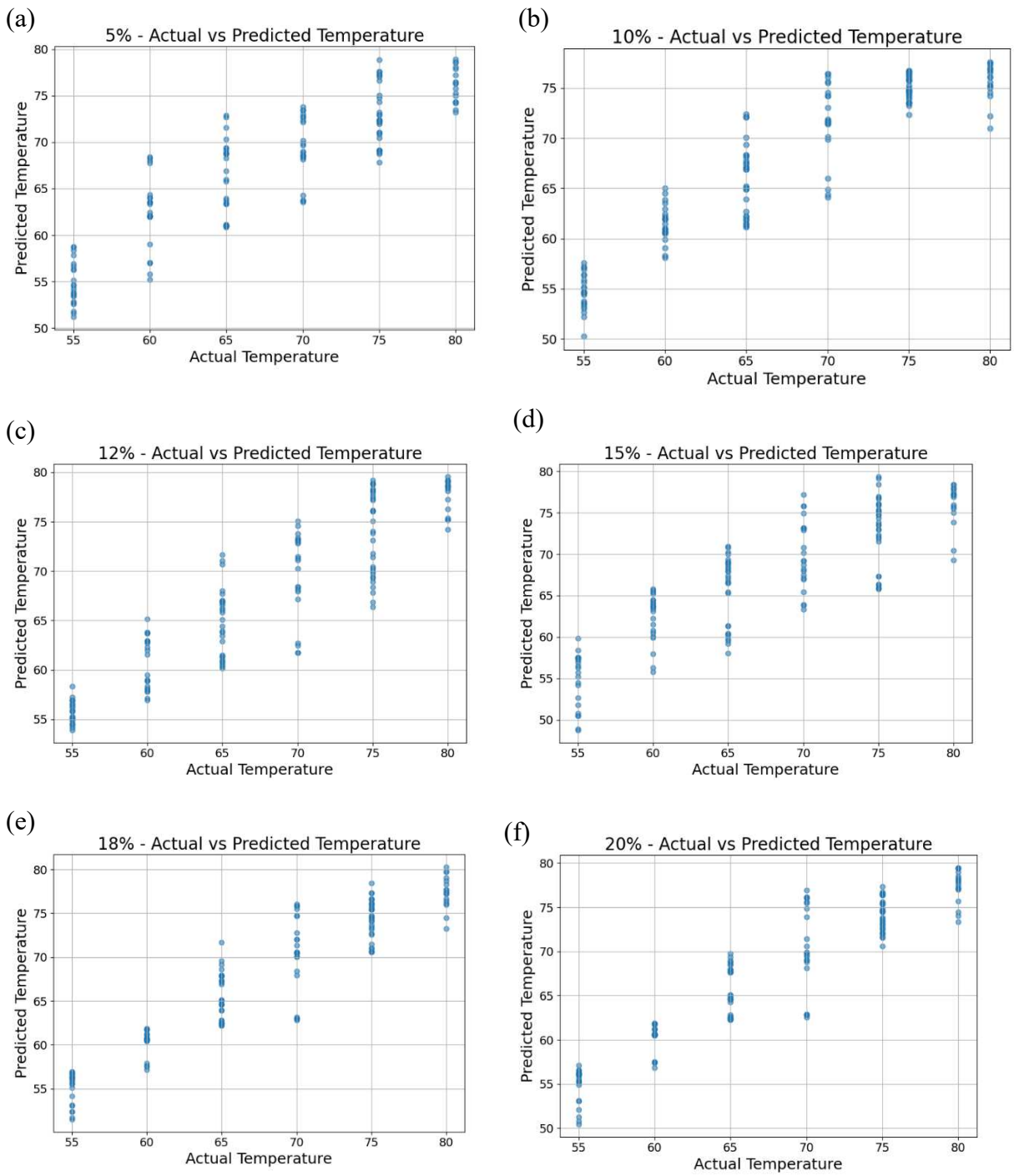


**Figure 14:** Concentration-Driven Prediction Fidelity: Actual vs. Predicted Temperature Scatter Plots for PCDA Sensors Across All Thermal Conditions (a) 5%, (b) 10%, (c) 12%, (d) 15%, (e) 18%, (f) 20%)

# 4.0 CONCLUSION

This study presents the development of a flexible, electrospun PCDA-based sensor capable of detecting temperature changes through visible colorimetric transitions. The integration of image-based machine learning with systematic material design effectively addressed the long-standing challenge of subjectivity in interpreting colorimetric sensor outputs. The combination of RGB analysis and supervised regression allowed us to accurately predict temperature based solely on color shifts, eliminating the need for manual interpretation or specialized equipment.

Comprehensive experimentation across six PCDA concentrations and multiple exposure durations revealed clear trends linking material formulation with sensing performance. As expected, lower PCDA concentrations exhibited slower and less saturated chromatic responses, which in turn led to lower model accuracy, especially at short exposure times. As both concentration and response time increased, the sensor's color transitions became more pronounced, leading to tighter predictions and reduced error variability. Interestingly, certain combinations of formulation and exposure time consistently outperformed others in terms of sensitivity, prediction accuracy, and response stability. Among these, one configuration—where color development was rapid yet balanced, and machine learning predictions remained highly reliable across all tested temperatures—emerged as especially promising. This condition, involving a mid-to-high PCDA concentration and a moderate exposure duration, struck an ideal balance between speed and precision.

At the 18% PCDA concentration with a 30-second response time, the system exhibited a strong and stable chromatic shift, resulting in high prediction confidence. Without requiring extended heating or complex instrumentation, this setup offered reproducible results and rapid

feedback, making it well-suited for real-world applications. These findings underscore the value of combining thermochromic polymer systems with machine learning to overcome the limitations of subjective interpretation and variability in sensor outputs. The approach demonstrates how simple, yet intelligent materials can be transformed into quantitative, autonomous sensing platforms. Altogether, this work illustrates how carefully tuning both the material parameters and data interpretation pipeline can lead to highly effective, user-friendly sensors. The platform developed is not only accurate and scalable, but also adaptable paving the way for future smart sensing systems that extend beyond temperature to other environmental or biological stimuli. Its low power requirements, ease of integration, and responsiveness position it as a promising candidate for next-generation diagnostics, on-site environmental monitoring, and wearable health technologies.

# CHAPTER V – CONCLUSION

The combination of sensor materials and data-driven machine learning models introduces a new approach in sensor technology. In this work, a flexible, temperature-responsive colorimetric sensor was developed using electrospun core–shell nanofibers containing polydiacetylene (PCDA) as the active thermochromic component. The fabrication process used the coaxial electrospinning process to control fiber architecture and ensure uniform chromatic response under thermal stimulation. A series of experiments conducted across six PCDA concentrations (ranging from 5% to 20%) and six different thermal exposure durations (from 1 to 120 seconds) allowed for a systematic study of how the sensor's performance depends on the material. Color changes in the sensor samples due to thermal stimuli were quantitatively analyzed using average RGB values extracted from high-resolution images of the sensors. The perceptual color difference was further calculated using the CIE76 $\Delta E$ formula to evaluate visual shift intensity with respect to the base samples. The extracted colorimetric shifts were paired with their respective temperatures and exposure times, which were used to train supervised regression models for the automated prediction of temperatures for unknown samples. The results show that the 18% PCDA concentration is the most stable and accurate across all conditions, achieving an $R^2$ of 0.884 and a mean absolute error of less than 1.3°C. A user-friendly web-based application was developed to enable real-time temperature prediction from input sensor images, offering a fast, low-cost, and scalable solution for objective colorimetric analysis.

This research has successfully overcome the human subjectivity inherent in traditional PDA-based sensors by introducing an image-based, machine learning-driven interpretation

framework. The ability to tune sensor responsiveness through material design, combined with automated machine learning prediction, presents a significant step forward in the development of smart, user-friendly colorimetric thermal sensors. The outcomes of this research demonstrate that both PCDA concentration and response time have a critical influence on the accuracy and reliability of sensor outputs, and that data-rich modeling can significantly enhance the interpretability and applicability of colorimetric sensors in real-world scenarios. The current work serves as a foundational platform for future expansion as well. Several important research paths can be explored to expand and diversify the abilities of this sensor. Future directions for this work include the following:

1. **pH Level Detection:** Future work could explore using the existing sensor platform for pH monitoring, as PCDA is inherently responsive to changes in proton concentration. This makes it a promising candidate for applications in environmental and physiological pH sensing without requiring further chemical modification.
2. **Bacterial Detection:** The sensor could also be used for detecting bacteria, as PCDA naturally changes color when it interacts with bacterial membranes. This built-in response offers a simple and effective way to visually identify bacterial contamination, without needing to modify the sensor surface.
3. **Antibiotic-Loaded Therapeutic Fibers:** The core–shell structure can be used to encapsulate antibiotics like gentamicin or penicillin in the fiber core, creating a dual-function sensor that not only detects the presence of bacteria but also can release antibiotics. This approach holds strong potential for applications such as smart wound dressings and responsive medical textiles.
4. **Multi-Analyte Sensing Systems:** This sensor can also be expanded by adding materials

that respond to other factors like humidity, volatile organic compounds, heavy metals, or glucose. This would allow the development of a single, compact smart sensor capable of detecting multiple conditions at once—broadening its usefulness in real-world scenarios.

5. **Wireless and Remote Monitoring:** By integrating image capture and cloud-based analysis, the sensor system could be turned into a fully automated, remote monitoring solution. Pairing it with smartphone imaging or flexible electronics would make it suitable for use in wearable health devices, smart packaging, and other real-world applications that require portable, on-the-go sensing.

In conclusion, this research lays the groundwork for smart colorimetric temperature sensing while also paving the way for future development of responsive, multifunctional platforms designed for real-time diagnostics and environmental monitoring.

## 5.1 Real-world Applications

The operational temperature range of 55°C to 80°C for the developed PCDA-based colorimetric sensor makes it highly applicable across a range of real-world scenarios. In industrial settings such as iron processing and metal fabrication, surface temperatures often fall within this range, posing risks to both equipment performance and worker safety. The sensor's distinct color transitions provide a quick and intuitive indication of overheating, enabling visual assessments in environments where digital or electronic sensors may be impractical or cost-prohibitive. In food processing and packaging, the sensor offers a straightforward way to verify proper heating during cooking or pasteurization. Its visible color change can confirm whether critical temperature thresholds have been reached and maintained, helping reduce the risk of

contamination or spoilage. The platform can also be incorporated into smart packaging for heat-sensitive goods, offering a low-cost, easy-to-read indicator if products are exposed to unsafe temperatures during storage or transport. Beyond industrial and food-related applications, the sensor's flexible, power-free design makes it well-suited for integration into protective clothing and personal safety gear. In high-heat work environments such as foundries or welding areas, these sensors could serve as embedded alerts on garments, helping workers monitor heat exposure in real time. This added layer of visual feedback enhances existing safety protocols and contributes to a safer work environment. In remote or resource-limited settings, where access to specialized equipment or technical expertise may be limited, the sensor's clear, visual output offers a practical solution for monitoring thermal conditions. Its simplicity and ease of use make it especially valuable in field-based applications where reliability and low infrastructure requirements are essential.

# REFERENCES


Alam, A. K. M. M., Yapor, J. P., Reynolds, M. M., & Li, Y. V. (2016). Study of polydiacetylene-poly (ethylene oxide) electrospun fibers used as biosensors. *Materials, 9*(3), 202.

Aria, N., Zhang, W., & Li, Y. (2021). Image processing and machine learning for smart colorimetric biosensing. *IEEE Sensors Journal, 21*(10), 11220–11227.

Bhattacharjee, A., Clark, R., Gentry-Weeks, C., & Li, Y. V. (2020). A novel receptor-free polydiacetylene nanofiber biosensor for detecting E. coli via colorimetric changes. *Materials Advances, 1*(9), 3387–3397.

Bhattacharjee, A., Gentry-Weeks, C., Clark, R., & Li, Y. V. (2020). Study of bacterial components activating a colorimetric transition in bacteria-detecting nanofiber wound dressing applications. *Pivoting for the Pandemic.* https://doi.org/10.31274/itaa.12123

Bhattacharjee, A., Goodall, E., Popat, K. C., Zou, L., & Li, Y. V. (2023). Selective detection of Gram-negative bacteria and antibacterial properties of colorimetric polydiacetylene nanofiber sensors. *Materials Advances, 4*(3), 1234–1245. https://doi.org/10.1039/D2MA00841A

Bhattacharjee, A., Sabino, R. M., Gangwish, J., Manivasagam, V. K., James, S., Popat, K. C., Reynolds, M., & Li, Y. V. (2022). A novel colorimetric biosensor for detecting SARS-COV-2 by utilizing the interaction between nucleocapsid antibody and spike proteins. *In Vitro Models, 1*(3), 241–247. https://doi.org/10.1007/s44164-022-00022-z

Chen, J., & Huang, X. (2010). Thermochromic behavior of polydiacetylene vesicles for temperature sensing. *Sensors and Actuators B: Chemical, 150*(1), 196–202.

Chen, W., Karde, V., Cheng, T. N. H., Ramli, S., & Others. (2020). Surface hydrophobicity: Effect of alkyl chain length and network homogeneity. *Frontiers of Chemical Science and Engineering, 15*(3), 1–10. https://doi.org/10.1007/s11705-020-2003-0

Cho, S. H., Suh, J. M., Eom, T. H., Kim, T., & Jang, H. W. (2020). Colorimetric sensors for toxic and hazardous gas detection: A review. *Electronic Materials Letters, 17*(1), 1–17. https://doi.org/10.1007/s13391-020-00254-9

Fratini, S., Nikolka, M., Salleo, A., Schweicher, G., & Sirringhaus, H. (2020). Charge transport in high-mobility conjugated polymers and molecular semiconductors. *Nature Materials, 19*(5), 491–502. https://doi.org/10.1038/s41563-020-0647-2

Gou, M., Guo, G., Zhang, J., Men, K., Song, J., Luo, F., Zhao, X., Qian, Z., & Wei, Y. (2010). Time–temperature chromatic sensor based on polydiacetylene (PDA) vesicle and amphiphilic copolymer. *Sensors and Actuators B: Chemical, 150*(1), 406–411. https://doi.org/10.1016/j.snb.2010.06.041

Halicka, K., & Cabaj, J. (2021). Electrospun nanofibers for sensing and biosensing applications: A review. *International Journal of Molecular Sciences, 22*(12), 6357. https://doi.org/10.3390/ijms22126357

Harpaz, D., Veltman, B., Sadeh, Y., Marks, R. S., Bernstein, N., & Eltzov, E. (2021). The effect of cannabis toxicity on a model microbiome bacterium epitomized by a panel of bioluminescent *E. coli*. *Chemosphere, 263*, 128241. https://doi.org/10.1016/j.chemosphere.2020.128241

Hassan, F., Gentry-Weeks, C., Reynolds, M., & Li, Y. V. (2019). Study on microstructure and mechanical properties of polydiacetylene composite biosensors. *Journal of Applied Polymer Science, 136*(34), 47877. https://doi.org/10.1002/app.47877

Jiang, T., Mao, Y., Sui, L., Yang, N., Li, S., Zhu, Z., Wang, C., Yin, S., He, J., & He, Y. (2019). Degradation of anthocyanins and polymeric color formation during heat treatment of purple sweet potato extract at different pH levels. *Food Chemistry, 274*, 460–470. https://doi.org/10.1016/j.foodchem.2018.07.141

Jordan, M. I., & Mitchell, T. M. (2015). Machine learning: Trends, perspectives, and prospects. *Science, 349*(6245), 255–260.

Kelleher, J. D., Namee, B. M., & D'Arcy, A. (2015). *Fundamentals of machine learning for predictive data analytics: Algorithms, worked examples, and case studies.* MIT Press.

Kim, D., Lee, H., Park, M., & Yoon, J. (2022). Smartphone-based colorimetric sensor powered by deep learning. *Analytical Chemistry, 94*(4), 1873–1881.

Kobayashi, T., Takarada, T., & Maeda, M. (2013). A colorimetric temperature sensor based on a polydiacetylene-containing hydrogel. *Analytical Sciences, 29*(10), 1011–1015.

Lee, J., & Jelinek, R. (2023). Smartphone-based polydiacetylene colorimetric sensor for point-of-need diagnostics. *ACS Sensors, 8*(1), 14–23. https://doi.org/10.1021/acssensors.2c01891

Lee, N. Y., Jung, Y. K., & Park, H. G. (2006). On-chip colorimetric biosensor based on polydiacetylene (PDA) embedded in photopolymerized poly(ethylene glycol) diacrylate

(PEG-da) hydrogel. *Biochemical Engineering Journal, 29*(1–2), 103–108. https://doi.org/10.1016/j.bej.2005.02.025

Li, Y., Bhattacharjee, A., Zou, L., & Gentry-Weeks, C. (2021). Colorimetric detection of bacteria using electrospun PDA nanofibers. *ACS Applied Nano Materials, 4*(7), 7385–7394. https://doi.org/10.1021/acsanm.1c01010

Li, Y., Zhang, Q., & Zhao, X. (2021). Machine learning for colorimetric sensor analysis: From signal processing to data-driven sensing. *Sensors and Actuators B: Chemical, 345*, 130404.

Lim, S., Cordova, D. L. M., Robang, A. S., Kuang, Y., Ogura, K. S., Paravastu, A. K., Arguilla, M. Q., & Ardoña, H. A. M. (2023). Thermochromic behavior of polydiacetylene nanomaterials driven by charged peptide amphiphiles. *Biomacromolecules, 24*(9), 4051–4063. https://doi.org/10.1021/acs.biomac.3c00422

Liu, B., Zhuang, J., & Wei, G. (2020). Recent advances in the design of colorimetric sensors for environmental monitoring. *Environmental Science: Nano, 7*(8), 2195–2213. https://doi.org/10.1039/D0EN00449A

Liu, H., Wang, T., Zhao, Y., & Xie, J. (2024). Integrating AI with sensors: A new era for intelligent diagnostics. *TrAC Trends in Analytical Chemistry, 168*, 117117.

Liu, X., Qiao, S., Li, J., & Tang, Y. (2022). Electrospun nanofibers embedded with PCDA for sensitive thermal detection. *Colloids and Surfaces A, 650*, 129447. https://doi.org/10.1016/j.colsurfa.2022.129447

Liu, Y., Hao, M., Chen, Z., Liu, L., Liu, Y., Yang, W., & Ramakrishna, S. (2020). A review on recent advances in application of electrospun nanofiber materials as biosensors. *Current Opinion in Biomedical Engineering, 13*, 174–189. https://doi.org/10.1016/j.cobme.2020.02.001

Lopreside, A., Wan, X., Michelini, E., Roda, A., & Wang, B. (2019). Comprehensive profiling of diverse genetic reporters with application to whole-cell and cell-free biosensors. *Analytical Chemistry, 91*(23), 15284–15292. https://doi.org/10.1021/acsanalchem

Nguyen, T. H., Lee, J., & Park, S. (2022). Rapid and automated readout of lateral flow assays using machine learning. *Sensors, 12*(1), 49.

Nguyen, T. M., Wu, Z., & Zhao, Y. (2023). Polydiacetylene-based thermochromic materials for smart packaging applications: A review. *Journal of Materials Chemistry C, 11*(5), 1453–1471.

Nothling, M. D., Bailey, C. G., Fillbrook, L. L., Wang, G., Gao, Y., McCamey, D. R., Monfared, M., Wong, S., Beves, J. E., & Stenzel, M. H. (2022). Polymer grafting to polydopamine free radicals for universal surface functionalization. *Journal of the American Chemical Society, 144*(15), 6992–7000. https://doi.org/10.1021/jacs2c02073

Ramakrishna, S., Fujihara, K., Teo, W. E., Lim, T. C., & Ma, Z. (2005). *An introduction to electrospinning and nanofibers.* World Scientific Publishing Company.

Sengodu, P. (2022). Conjugated polymers-based biosensors. In *Conjugated Polymers for Next-Generation Applications* (pp. 401–446). https://doi.org/10.1016/b978-0-12-823442-6.00015

Snari, R. M., Alsahag, M., Alisaac, A., Bayazeed, A., Alsoliemy, A., Khalifa, M. E., & El-Metwaly, N. M. (2022). Smart textiles immobilized with hydrazone probe for colorimetric recognition of bacteria. *Journal of Molecular Liquids, 366*, 120149. https://doi.org/10.1016/j.molliq.2022.120149

Sun, H., Liu, S., & Lin, L. (2018). Challenges and opportunities in colorimetric biosensing. *Biosensors and Bioelectronics, 106*, 29–36.

Wang, W., You, Y., & Gunasekaran, S. (2021). LSPR-based colorimetric biosensing for food quality and safety. *Comprehensive Reviews in Food Science and Food Safety, 20*(6), 5829–5855. https://doi.org/10.1111/1541-4337.12843

Wang, X., Kim, Y.-G., Drew, C., Ku, B.-C., Kumar, J., & Samuelson, L. A. (2004). Electrostatic assembly of conjugated polymer thin layers on electrospun nanofibrous membranes. *Nano Letters, 4*(2), 331–334. https://doi.org/10.1021/nl034885z

Wang, Y., Deng, S., & Huang, J. (2020). Machine learning-assisted interpretation of colorimetric sensor arrays. *Talanta, 214*, 120818.

Wang, Y., He, J., Zou, L., Lu, Y., & Li, Y. V. (2023). High performance polyvinyl alcohol/lignin fibers with excellent mechanical and water resistance properties. *International Journal of Biological Macromolecules, 266*, 131244.

Wang, Y., Xu, H., Zhang, J., & Li, G. (2017). Colorimetric sensors for temperature detection based on PDA. *Sensors, 17*(2), 417.

Xie, J., Zhao, X., Li, T., & Wang, Y. (2023). AI-assisted colorimetric sensor technologies for point-of-care diagnostics. *Advanced Functional Materials, 33*(5), 2210459.

Xie, X., Li, D., Zhang, P., & Yang, W. (2023). Integrating deep learning with colorimetric sensors for automated visual analysis. *Sensors, 13*(2), 211.

Yang, J., Wang, X., Sun, Y., Chen, B., Hu, F., Guo, C., & Yang, T. (2022). Recent advances in colorimetric sensors based on gold nanoparticles for pathogen detection. *Biosensors, 13*(1), 29. https://doi.org/10.3390/bios13010029

Yapor, J. P., Alharby, A., Gentry-Weeks, C., Reynolds, M. M., Alam, A. K. M. M., & Li, Y. V. (2017). Polydiacetylene nanofiber composites as a colorimetric sensor responding to *Escherichia coli* and pH. *ACS Omega, 2*(10), 7334–7342.

Zhang, W., Liu, H., & Chen, Z. (2023). Real-time detection of pH changes using a CNN-enabled colorimetric strip. *ACS Sensors, 8*(3), 931–939.

Zhao, C., Liu, Y., & He, Z. (2020). Deep learning for colorimetric biosensing: Enhancing accuracy in low-cost diagnostics. *Biosensors and Bioelectronics, 170*, 112649.

# APPENDICES

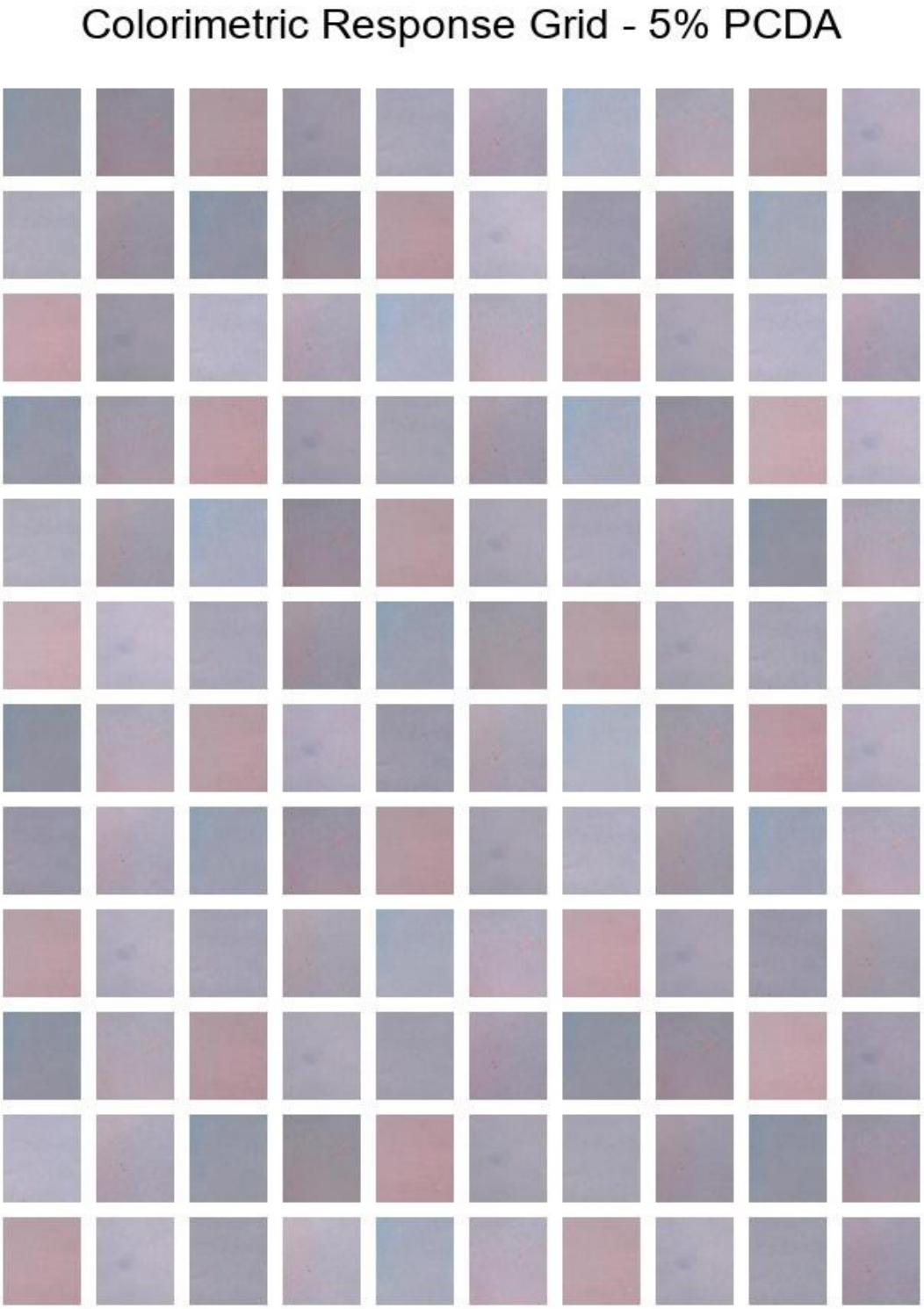

Colorimetric Response Grid - 5% PCDA

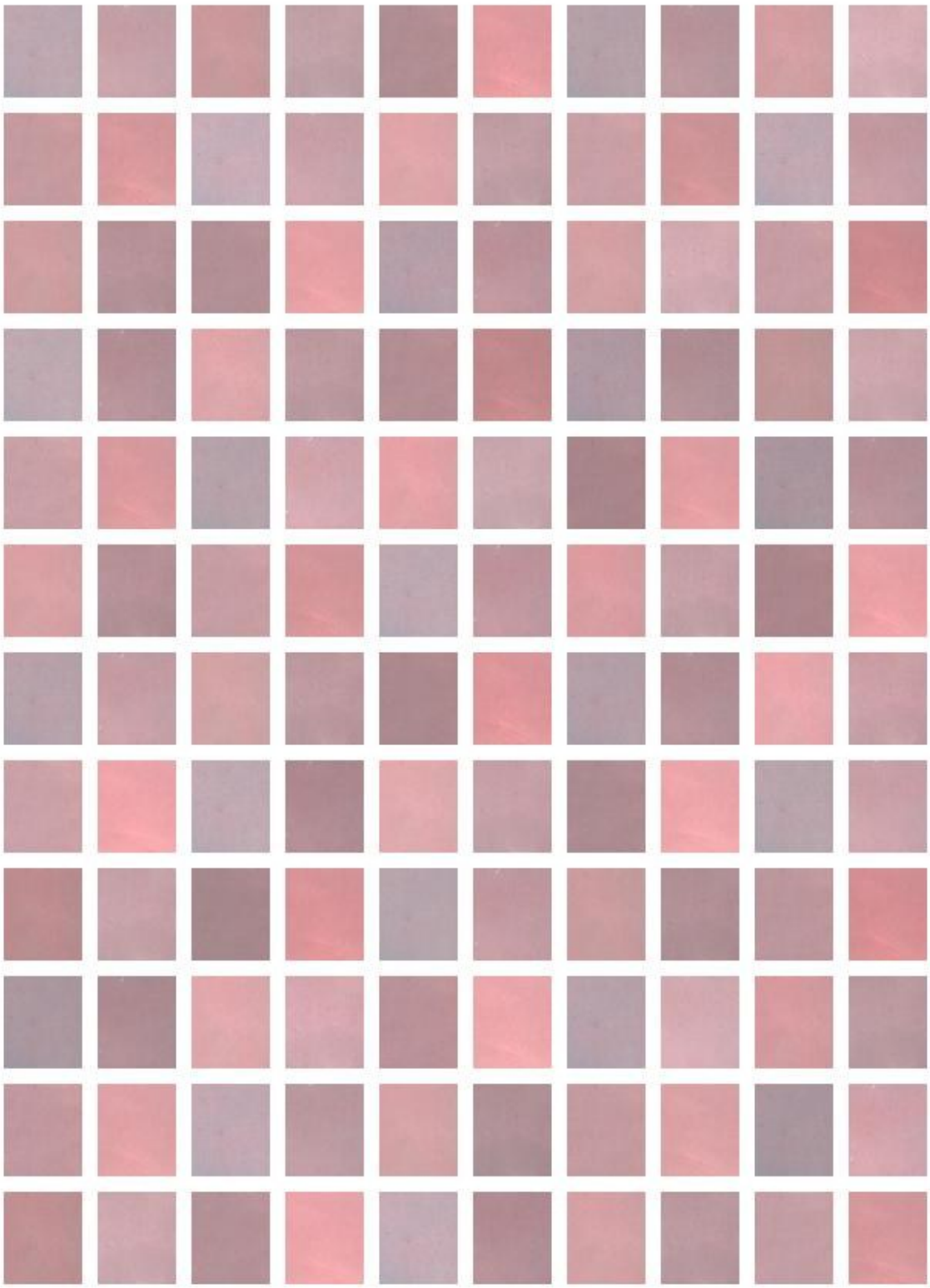

Colorimetric Response Grid - 5% PCDA

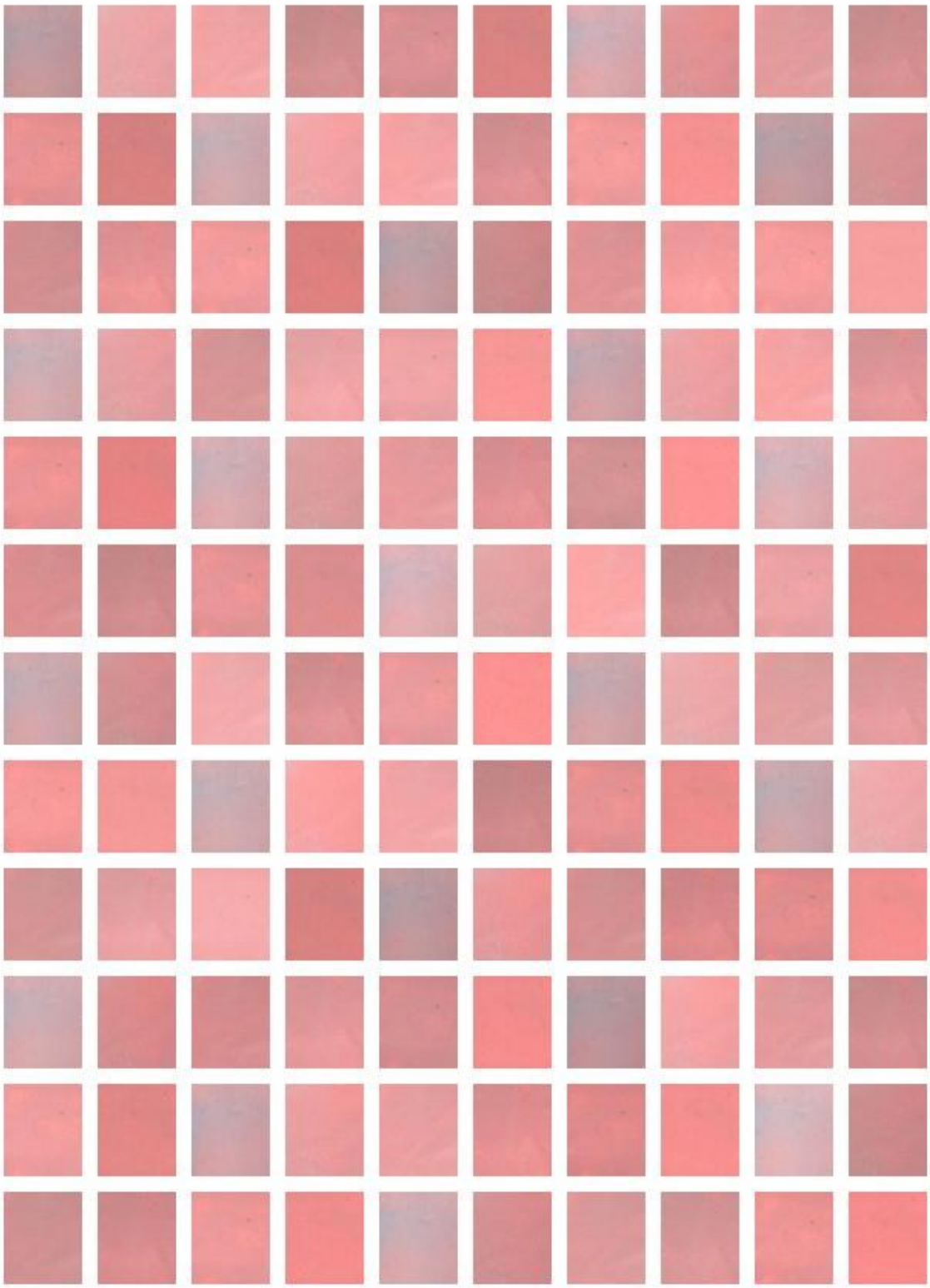

Colorimetric Response Grid - 5% PCDA

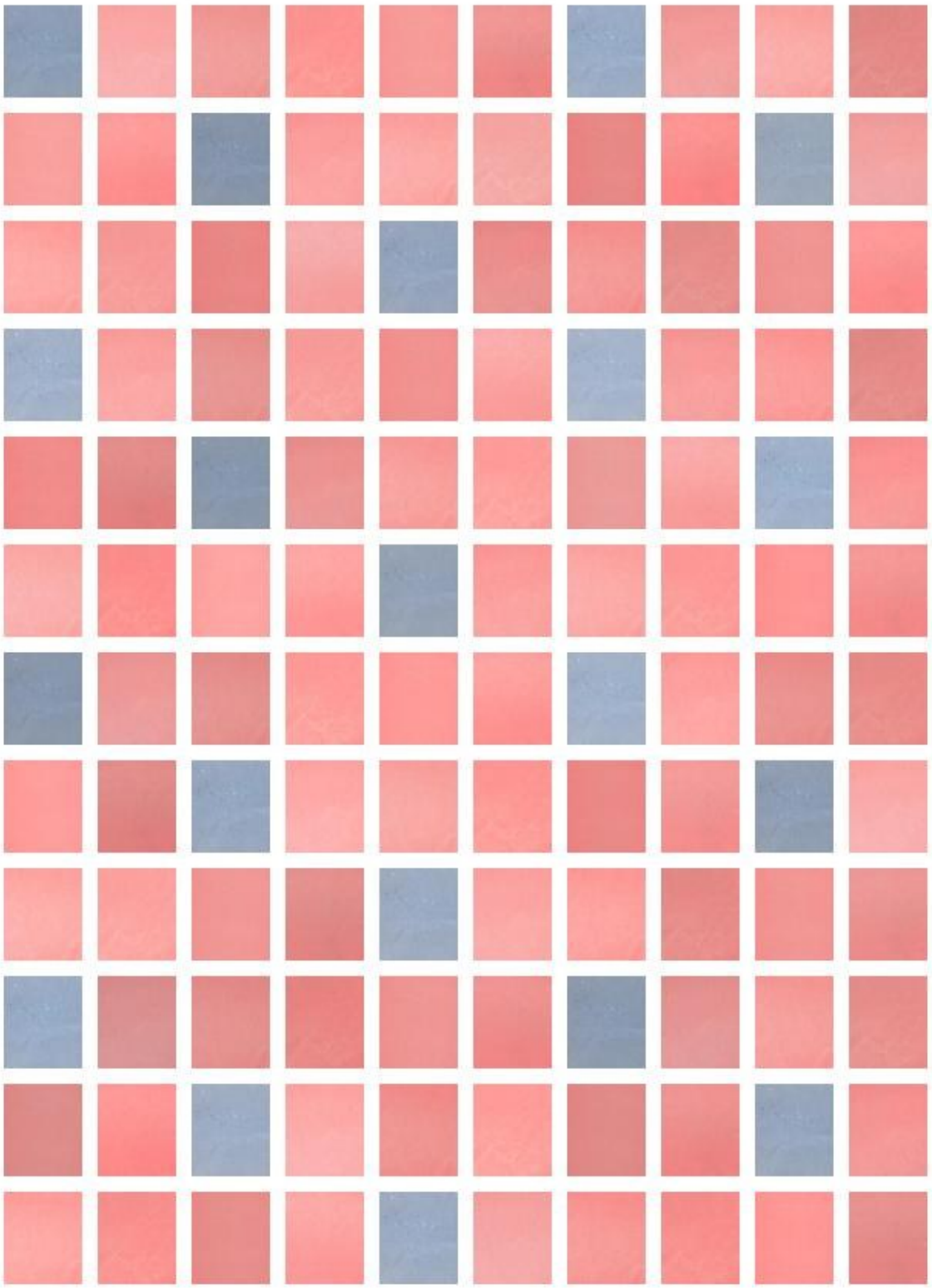

Colorimetric Response Grid - 5% PCDA

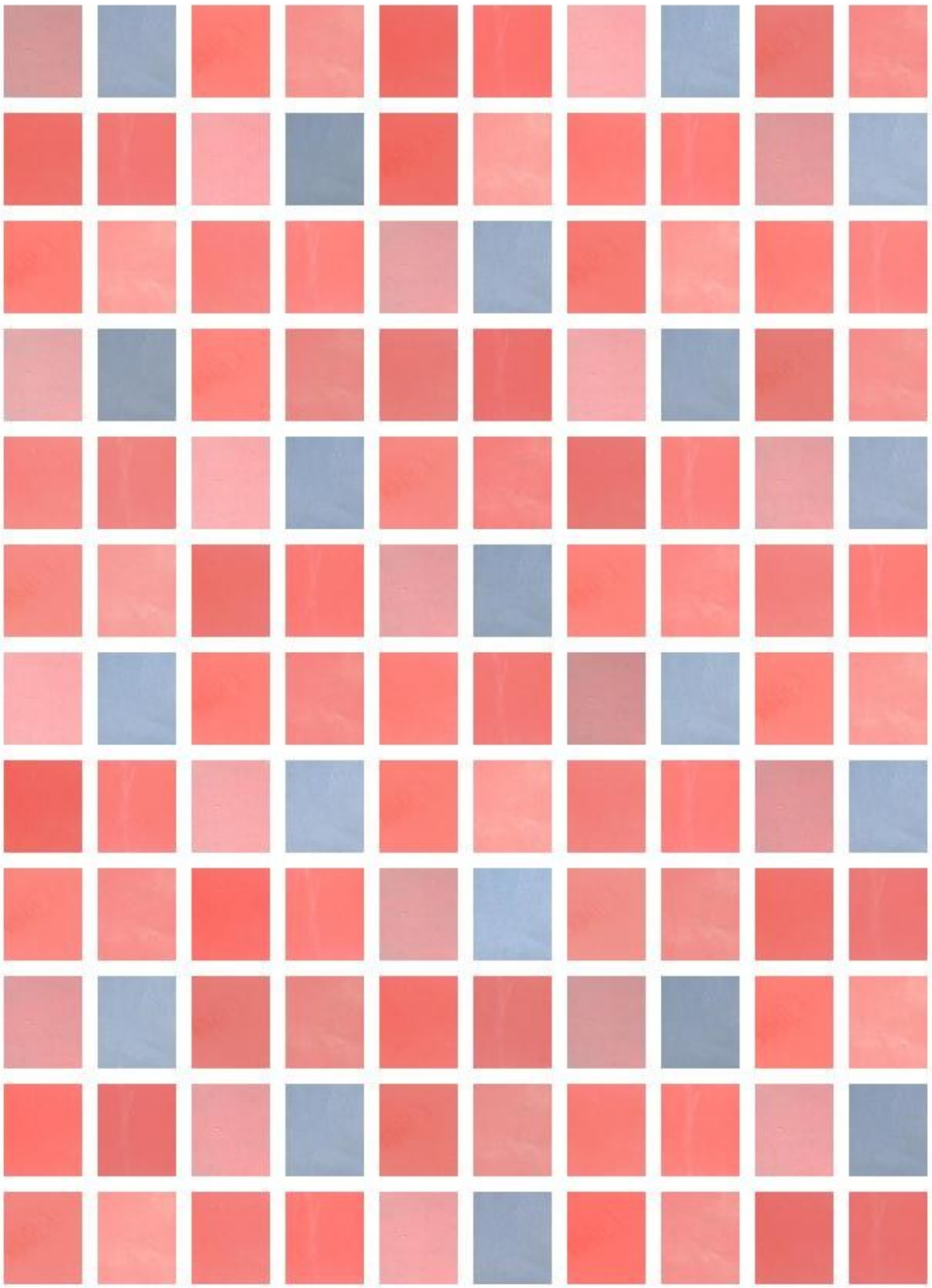

Colorimetric Response Grid - 5% PCDA

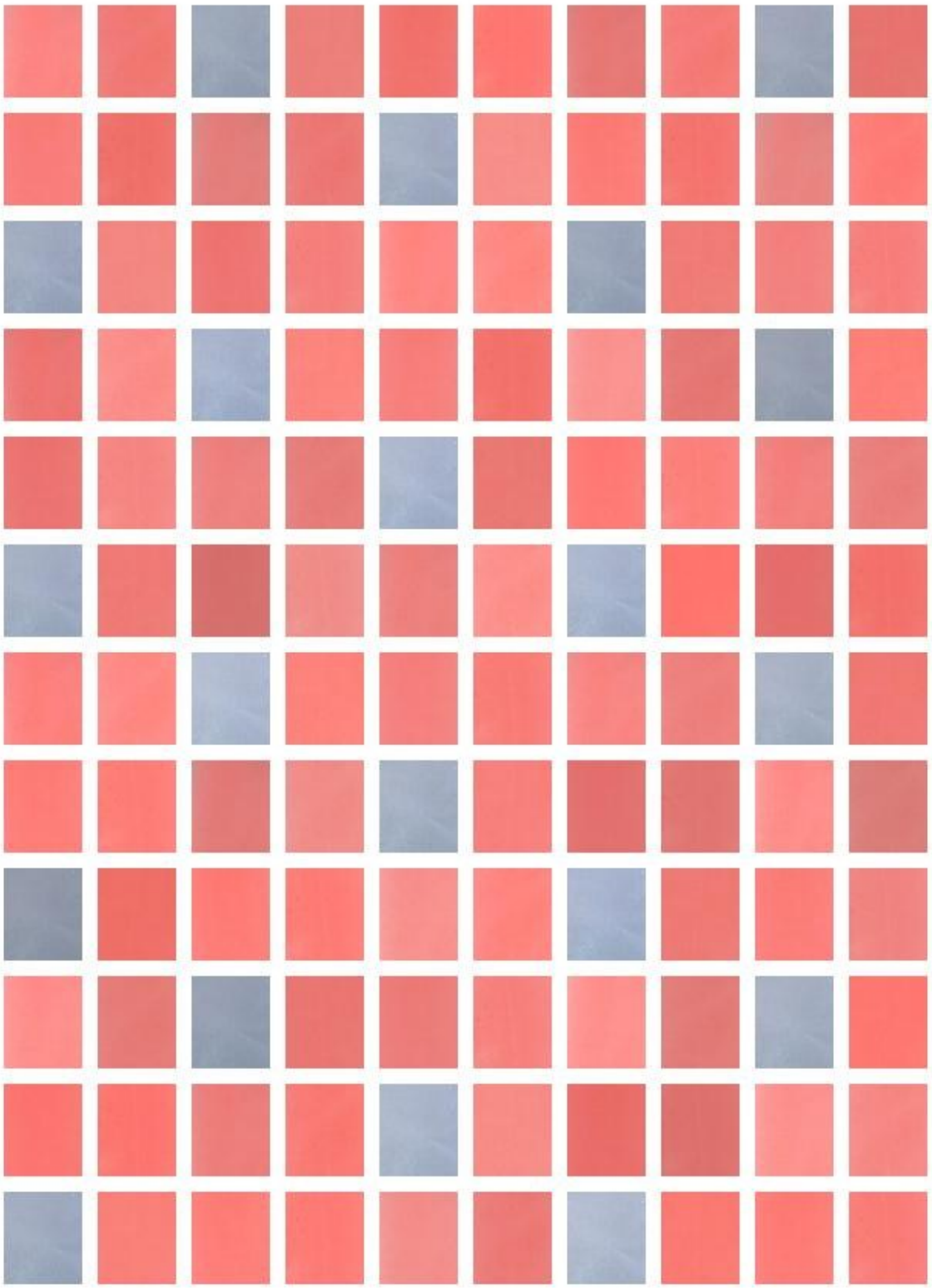

Colorimetric Response Grid - 10% PCDA

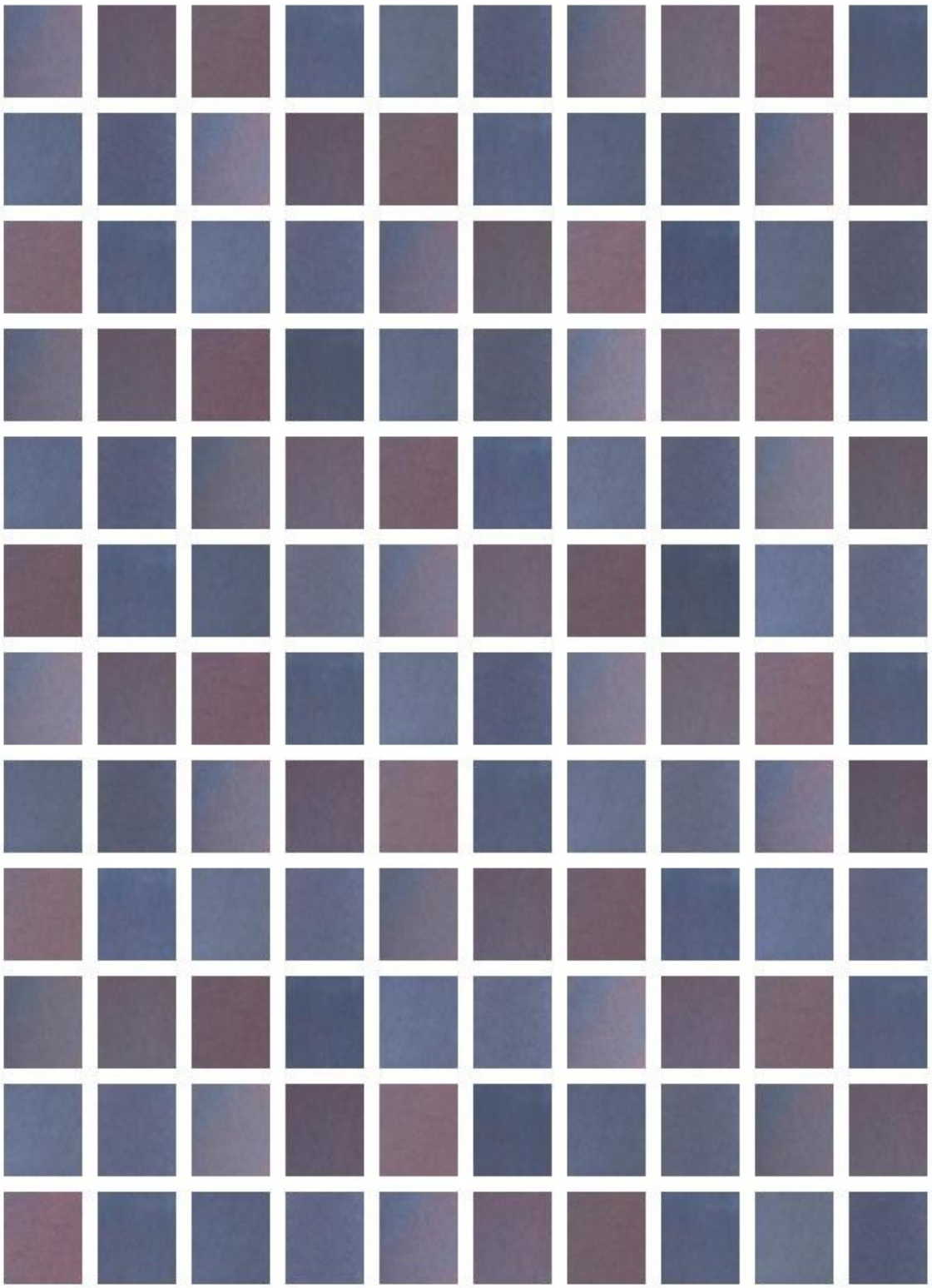

Colorimetric Response Grid - 10% PCDA

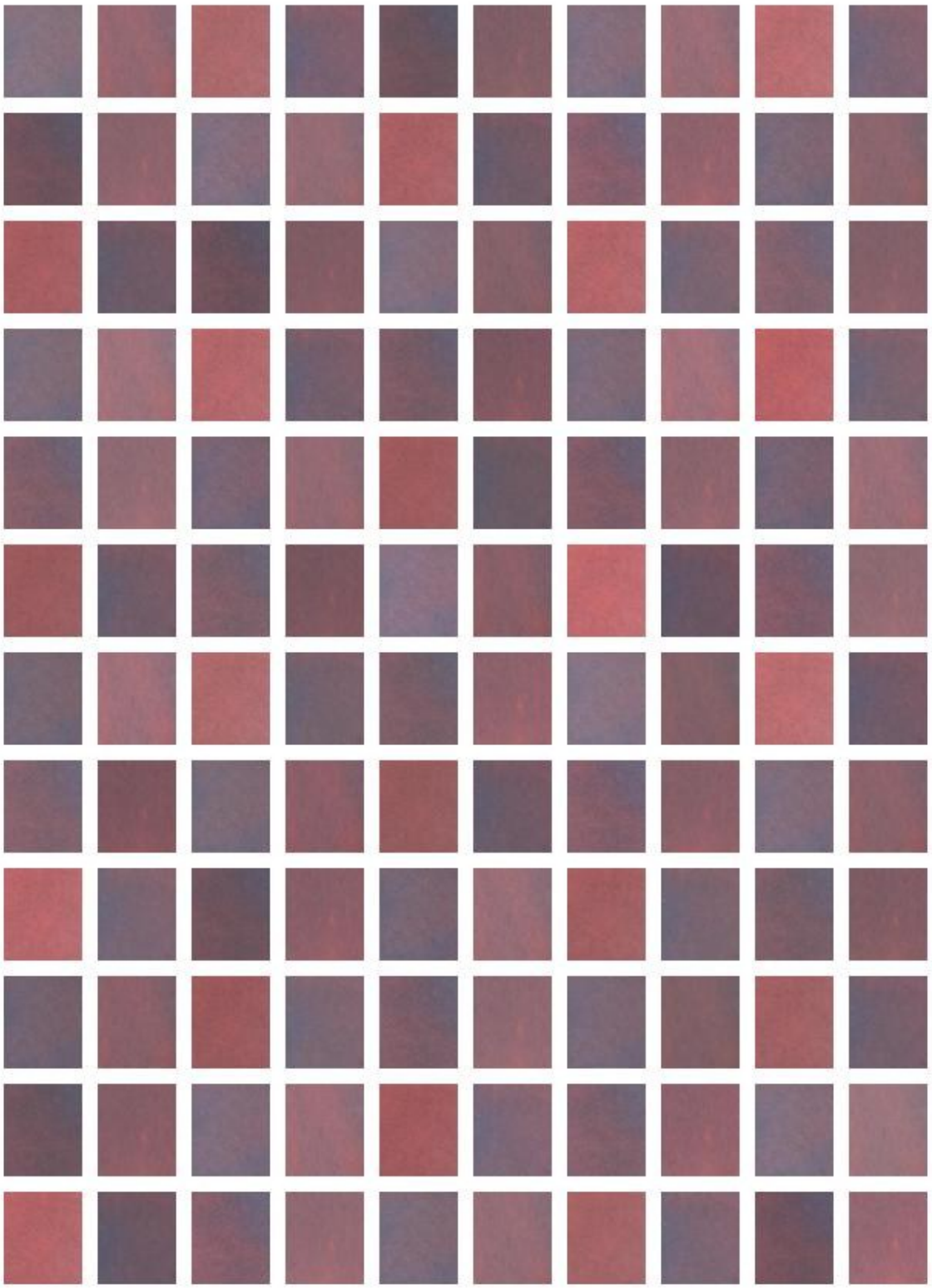

Colorimetric Response Grid - 10% PCDA

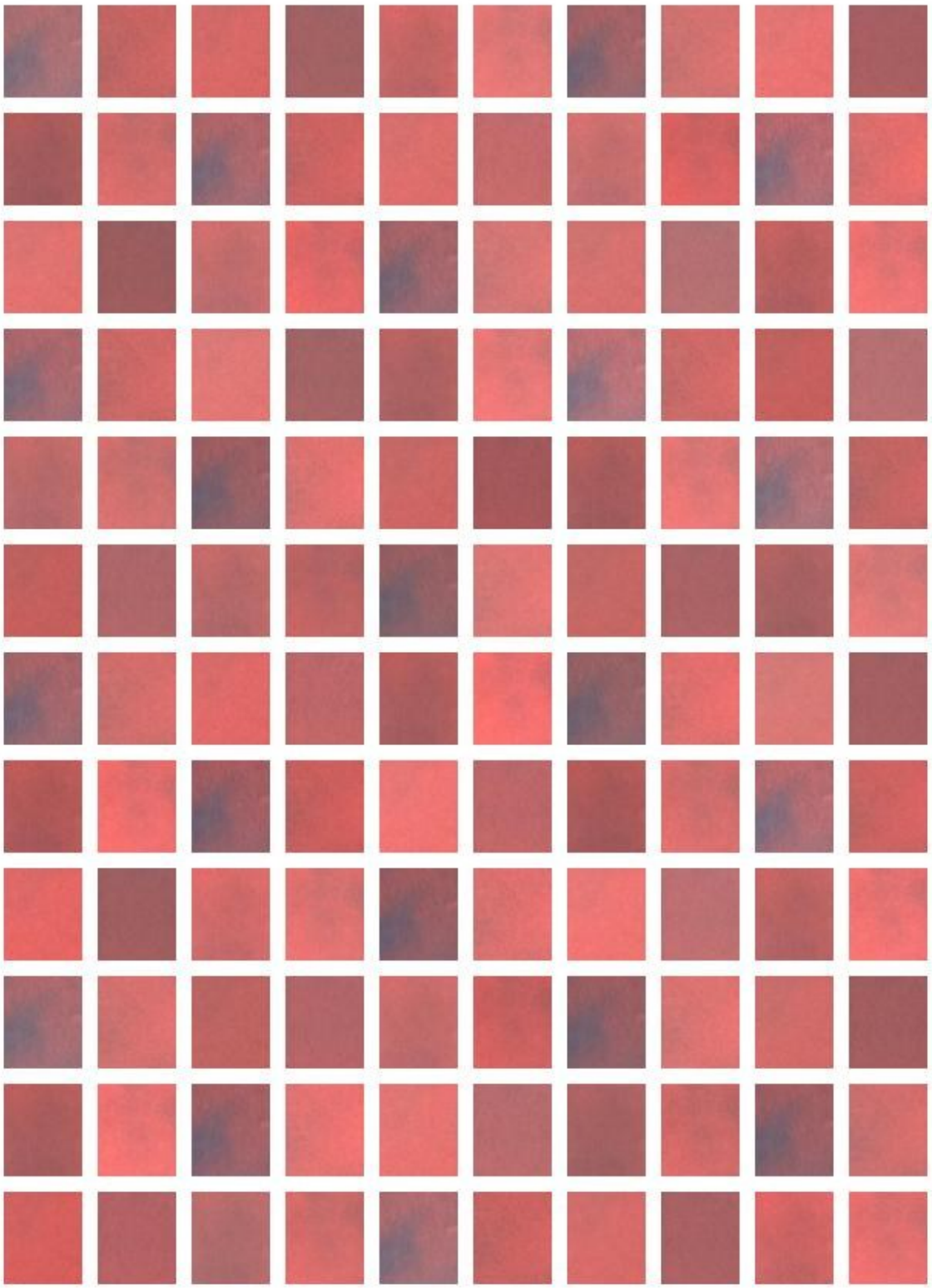

Colorimetric Response Grid - 10% PCDA

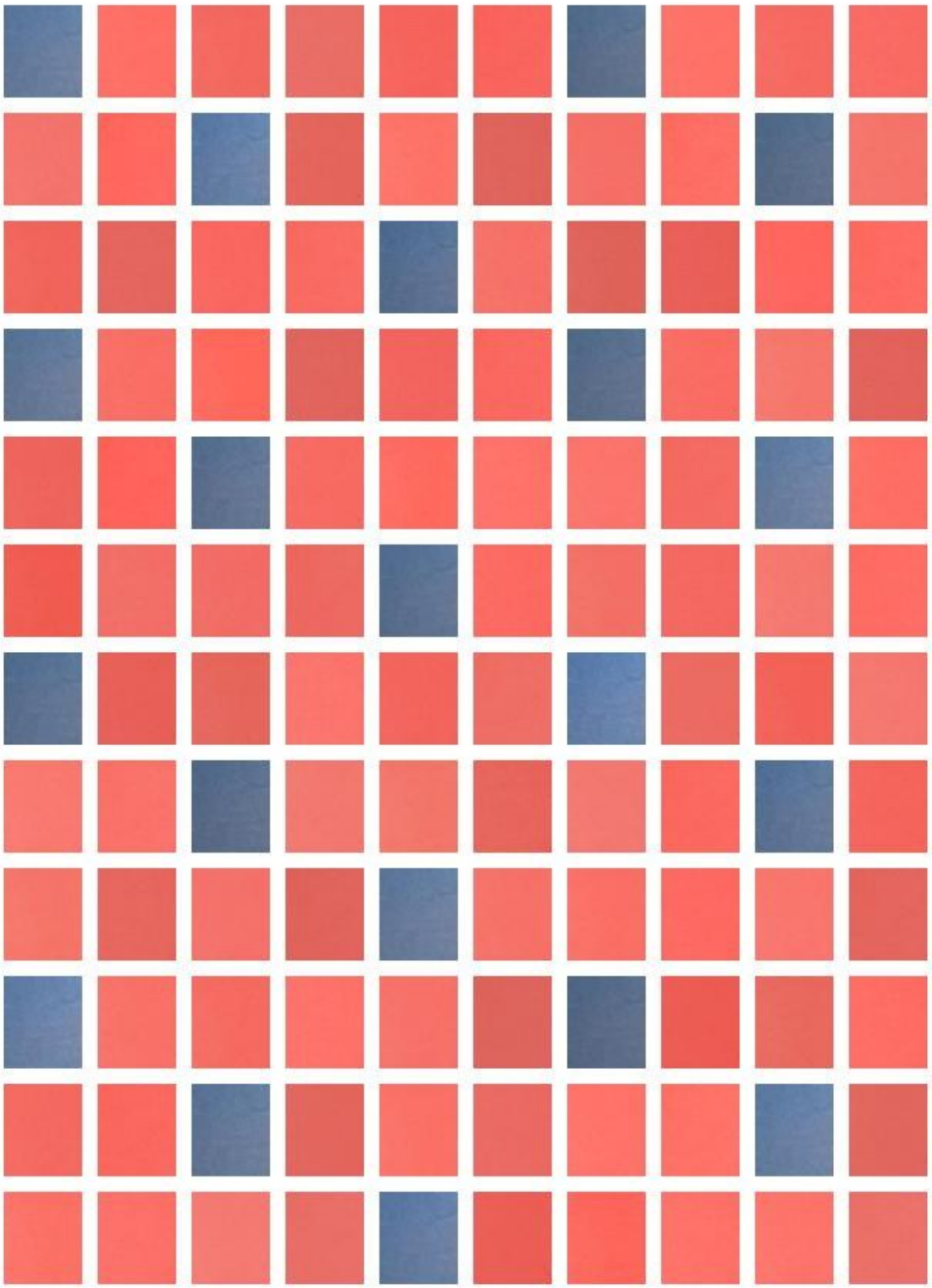

Colorimetric Response Grid - 10% PCDA

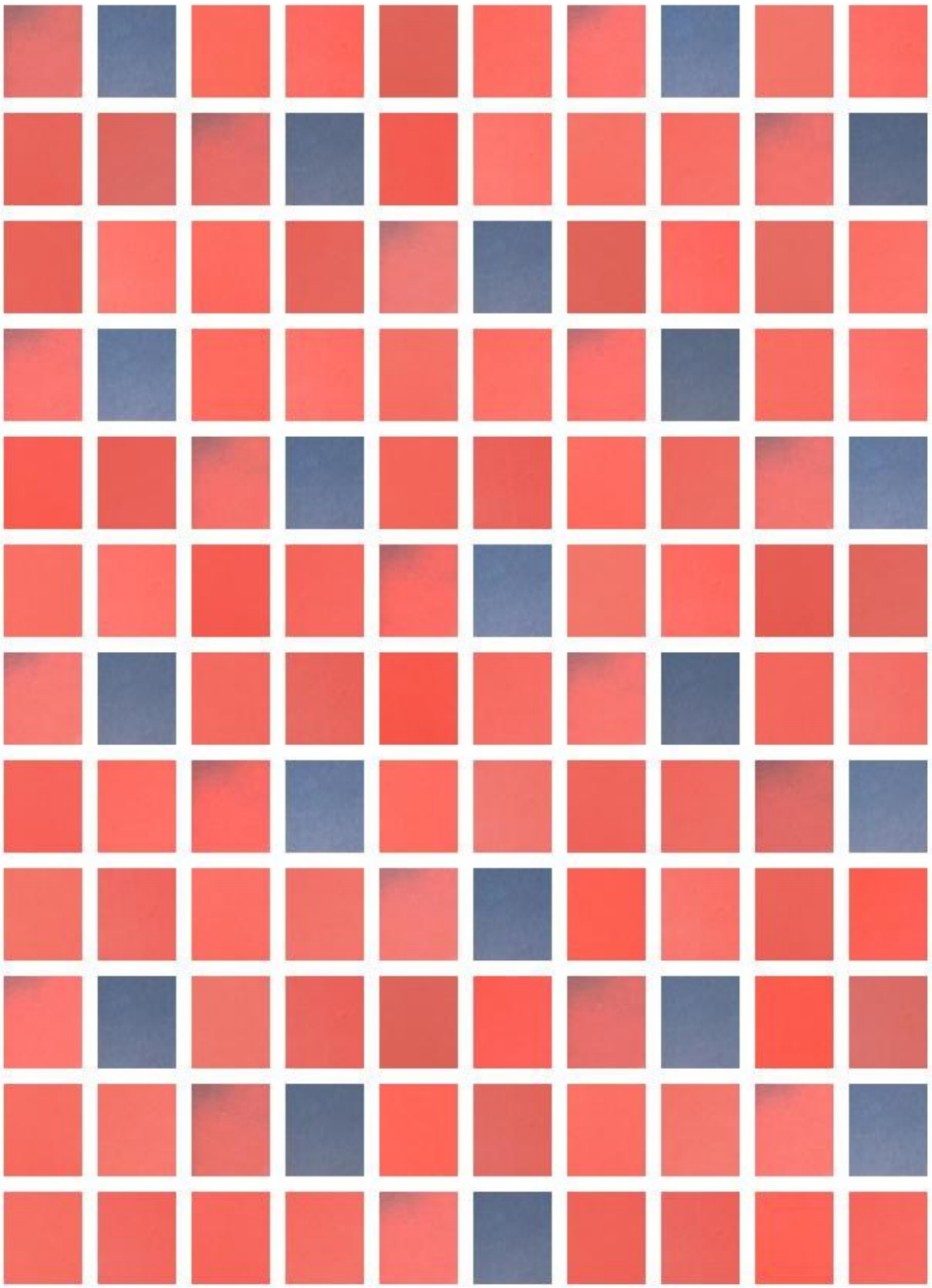

Colorimetric Response Grid - 10% PCDA

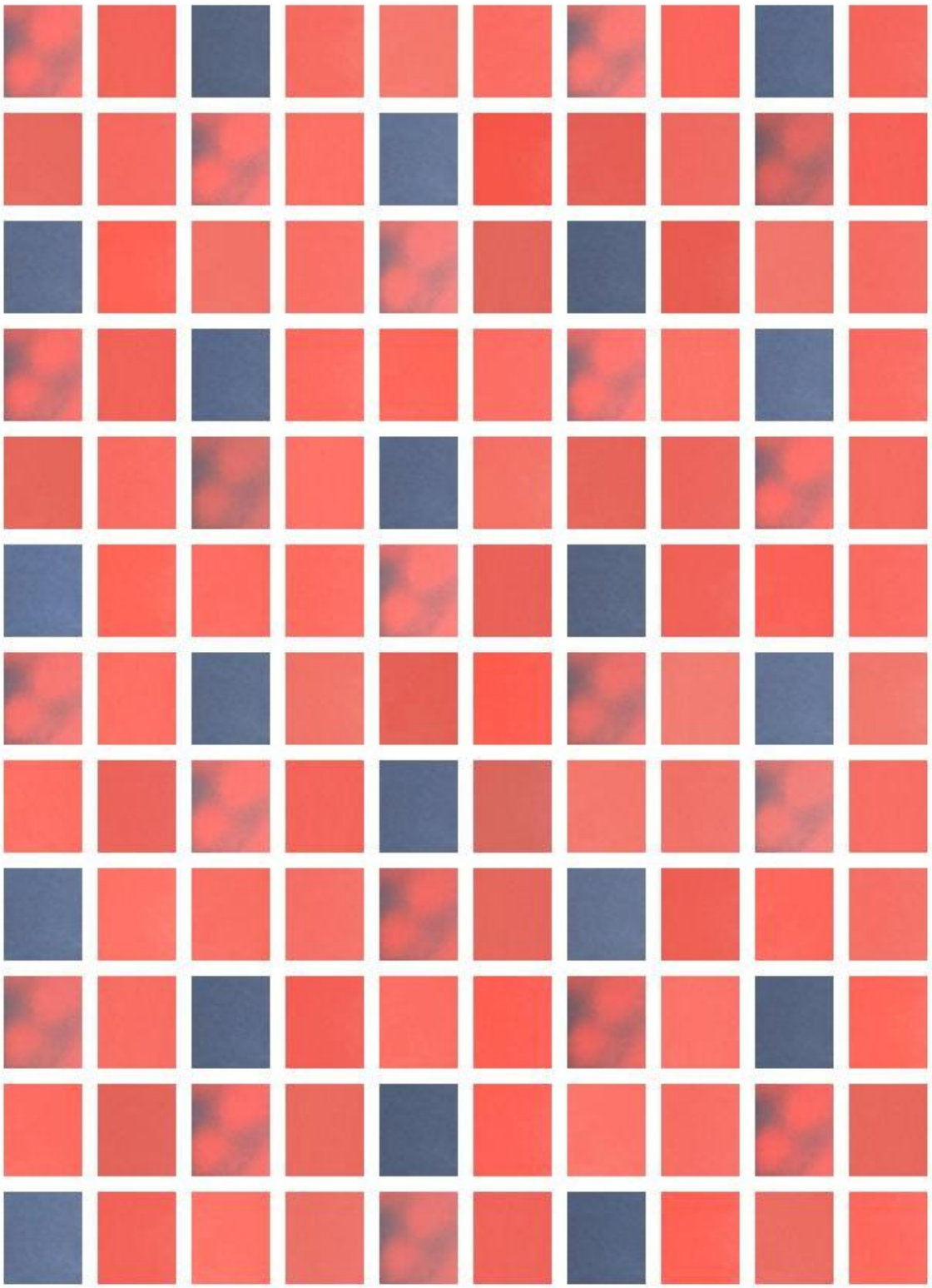

Colorimetric Response Grid - 12% PCDA

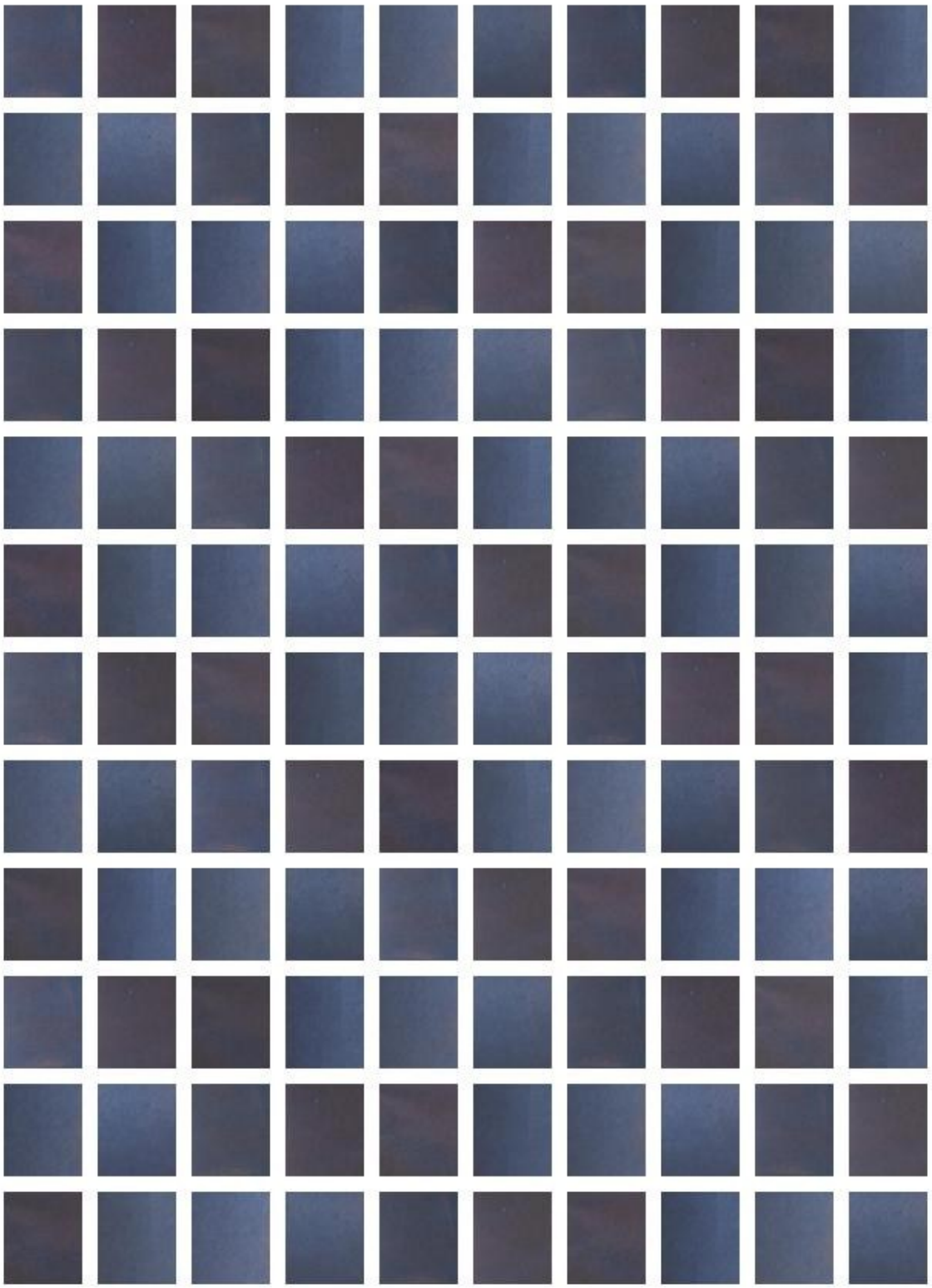

Colorimetric Response Grid - 12% PCDA

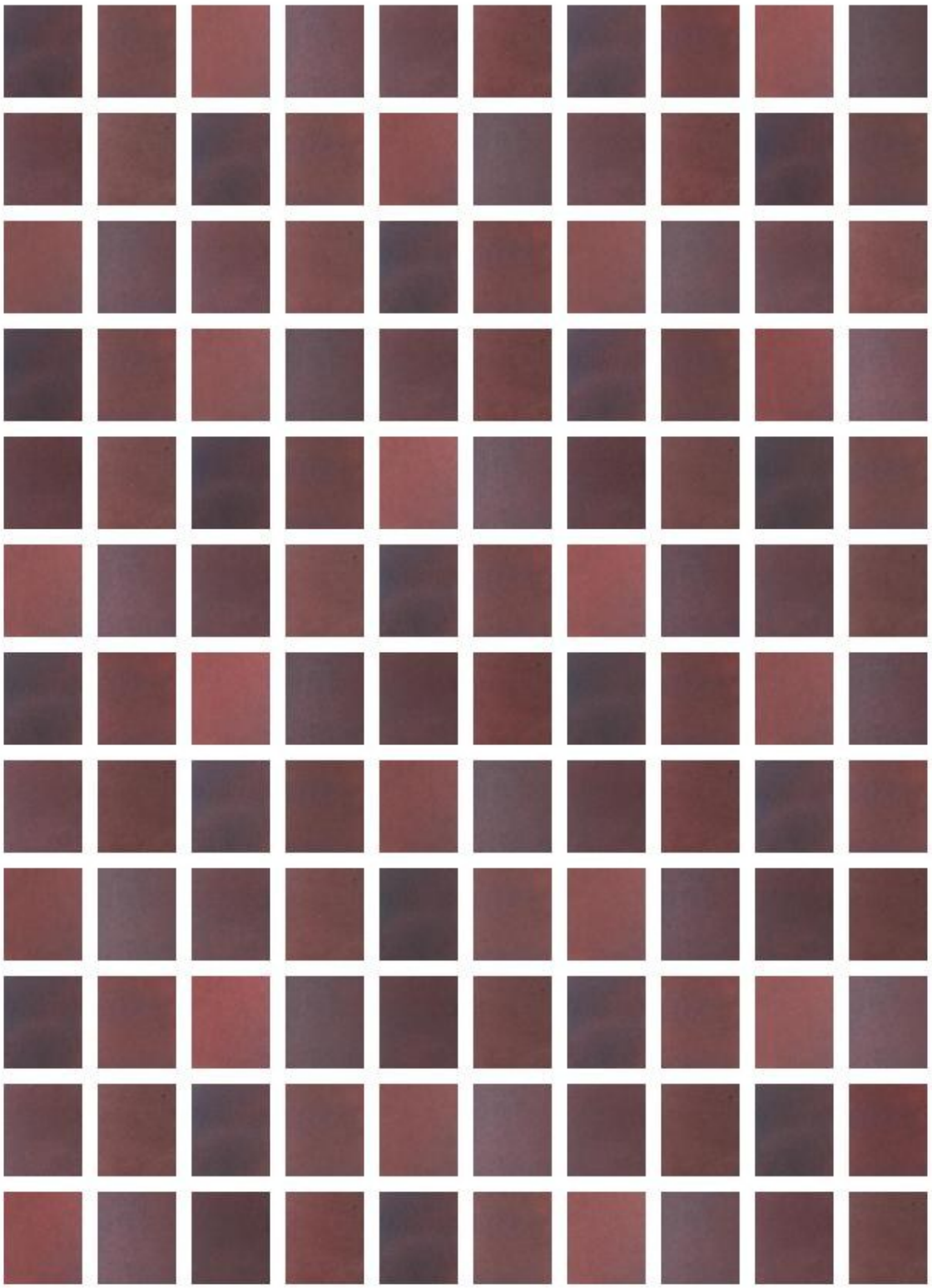

Colorimetric Response Grid - 12% PCDA

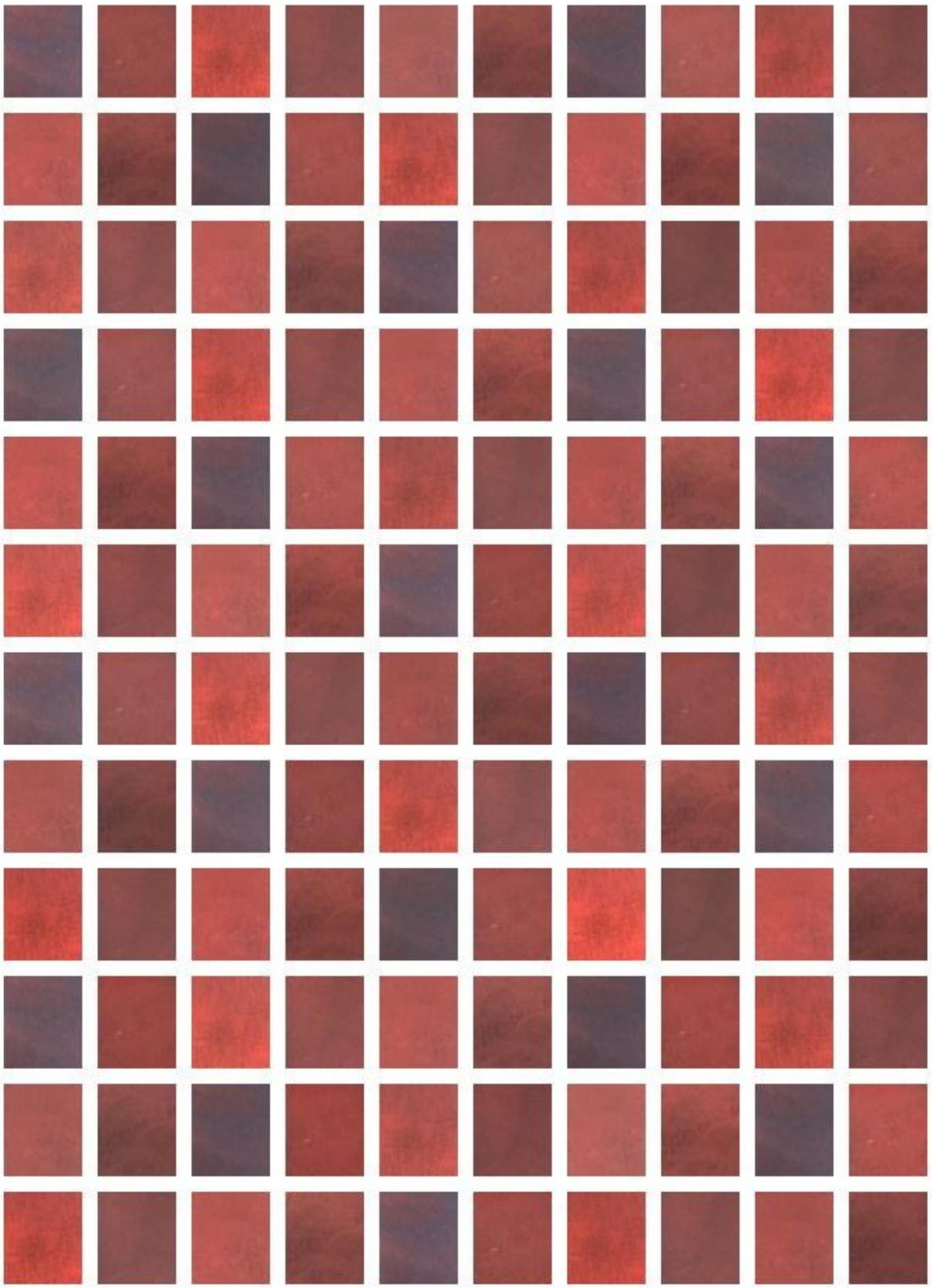

Colorimetric Response Grid - 12% PCDA

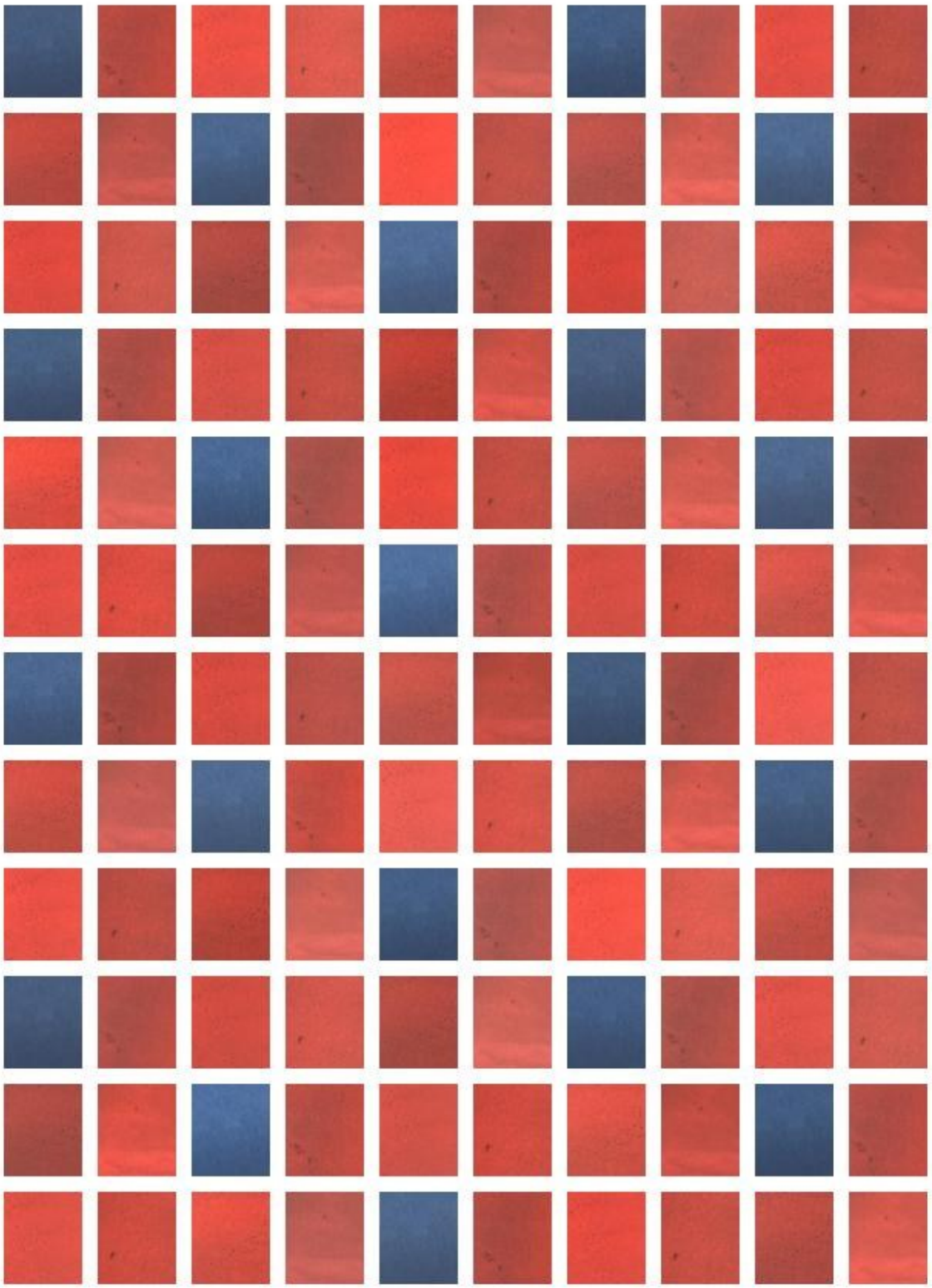

Colorimetric Response Grid - 12% PCDA

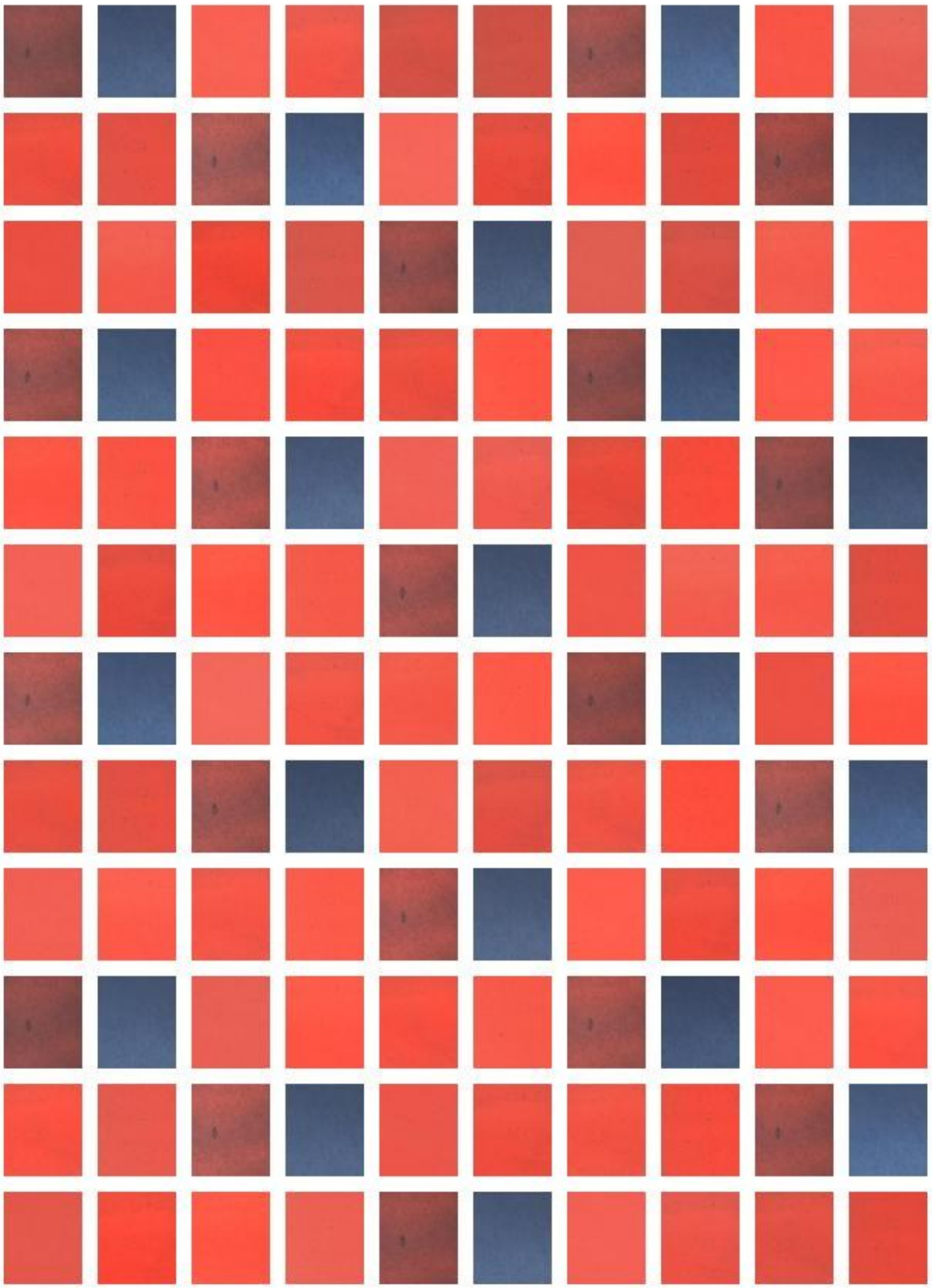

Colorimetric Response Grid - 12% PCDA

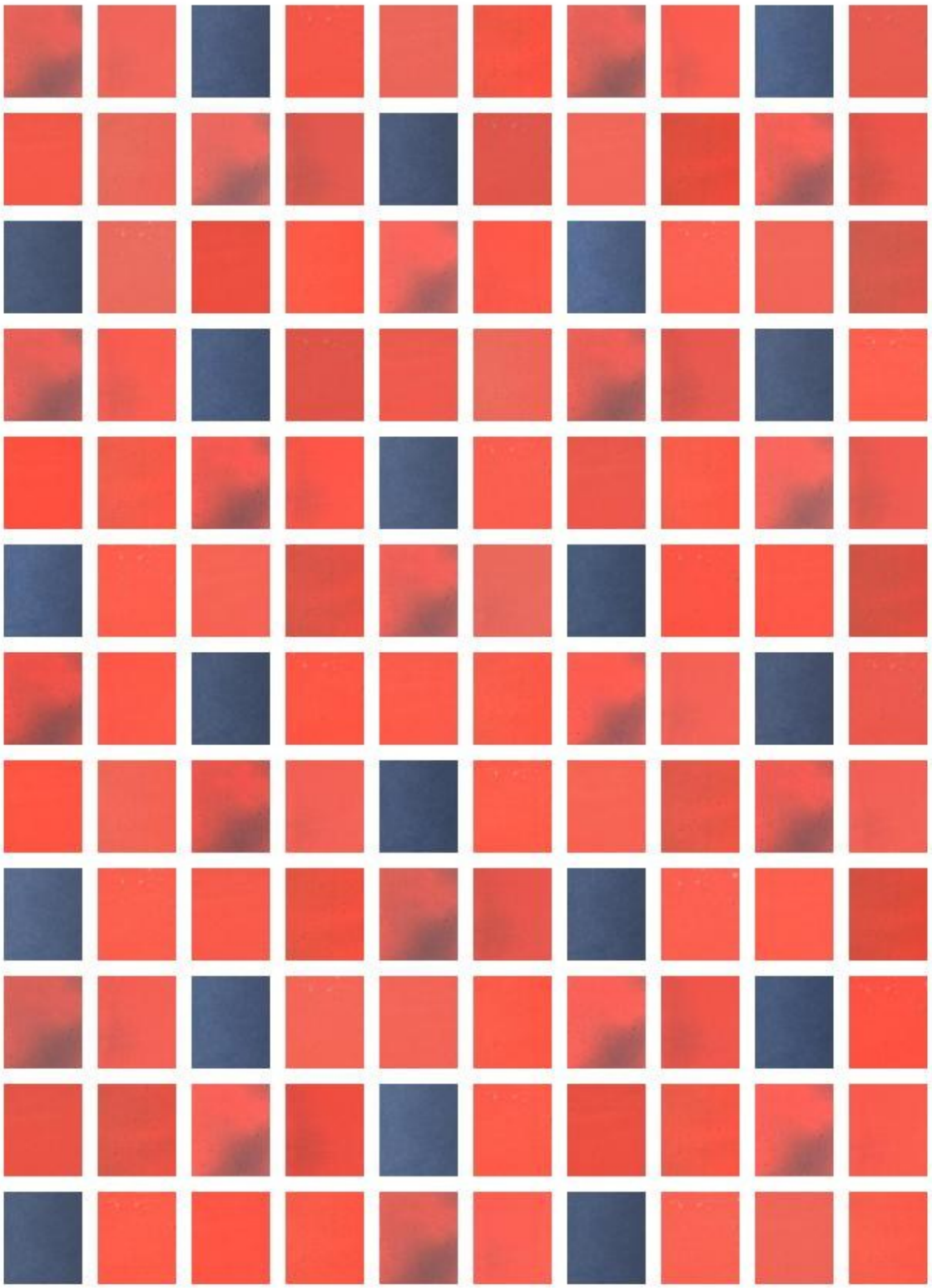

Colorimetric Response Grid - 15% PCDA

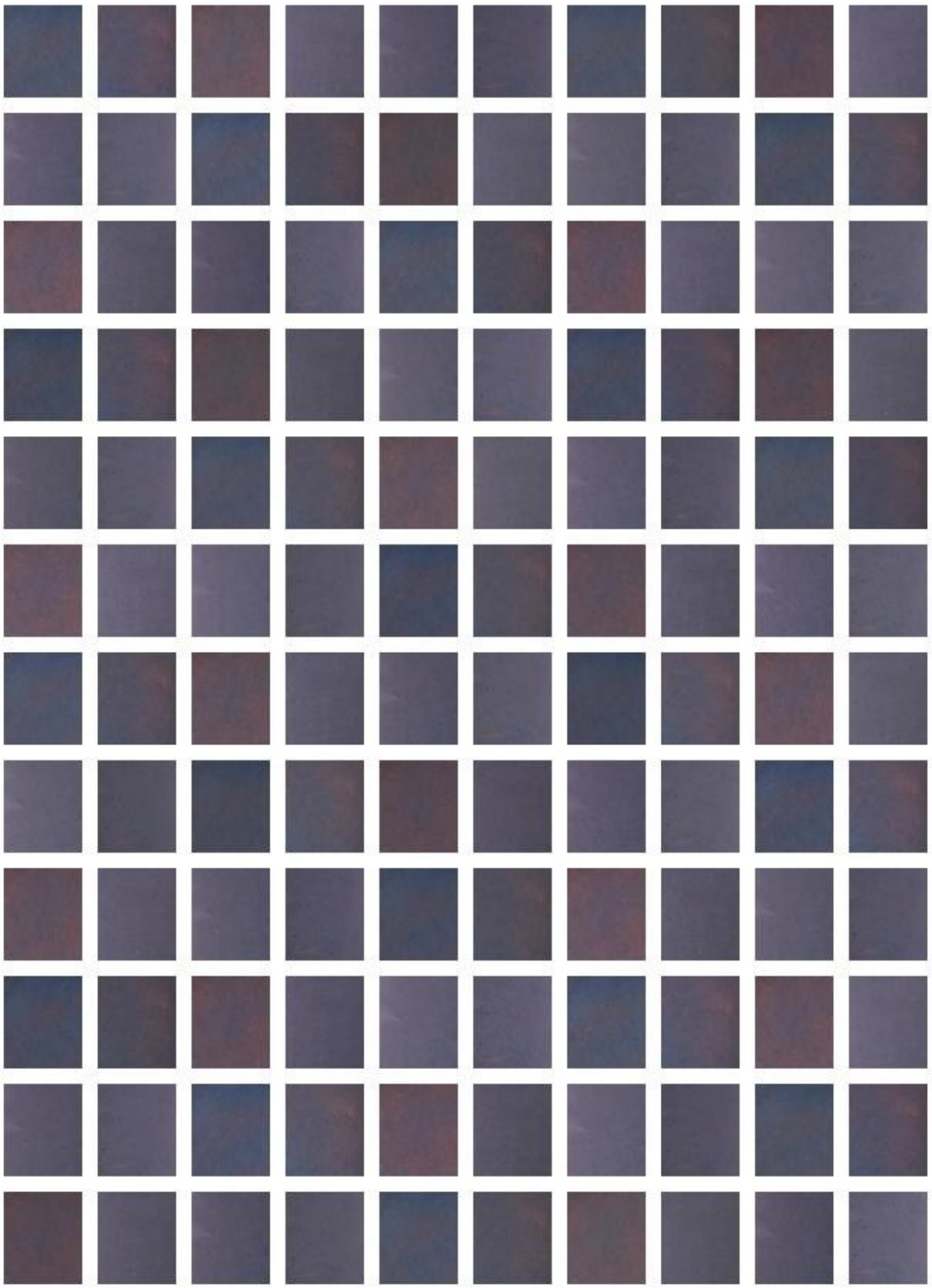

Colorimetric Response Grid - 15% PCDA

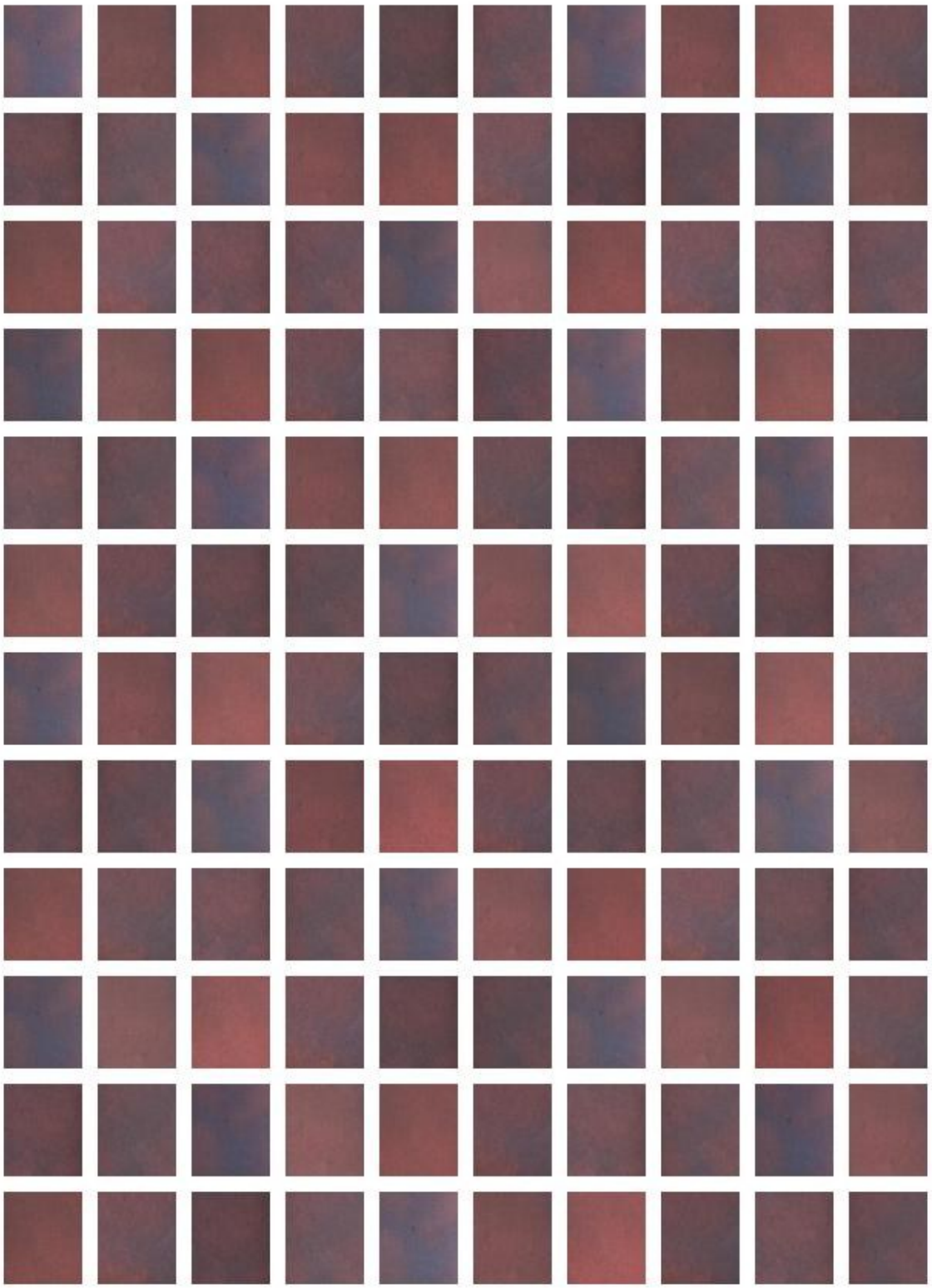

Colorimetric Response Grid - 15% PCDA

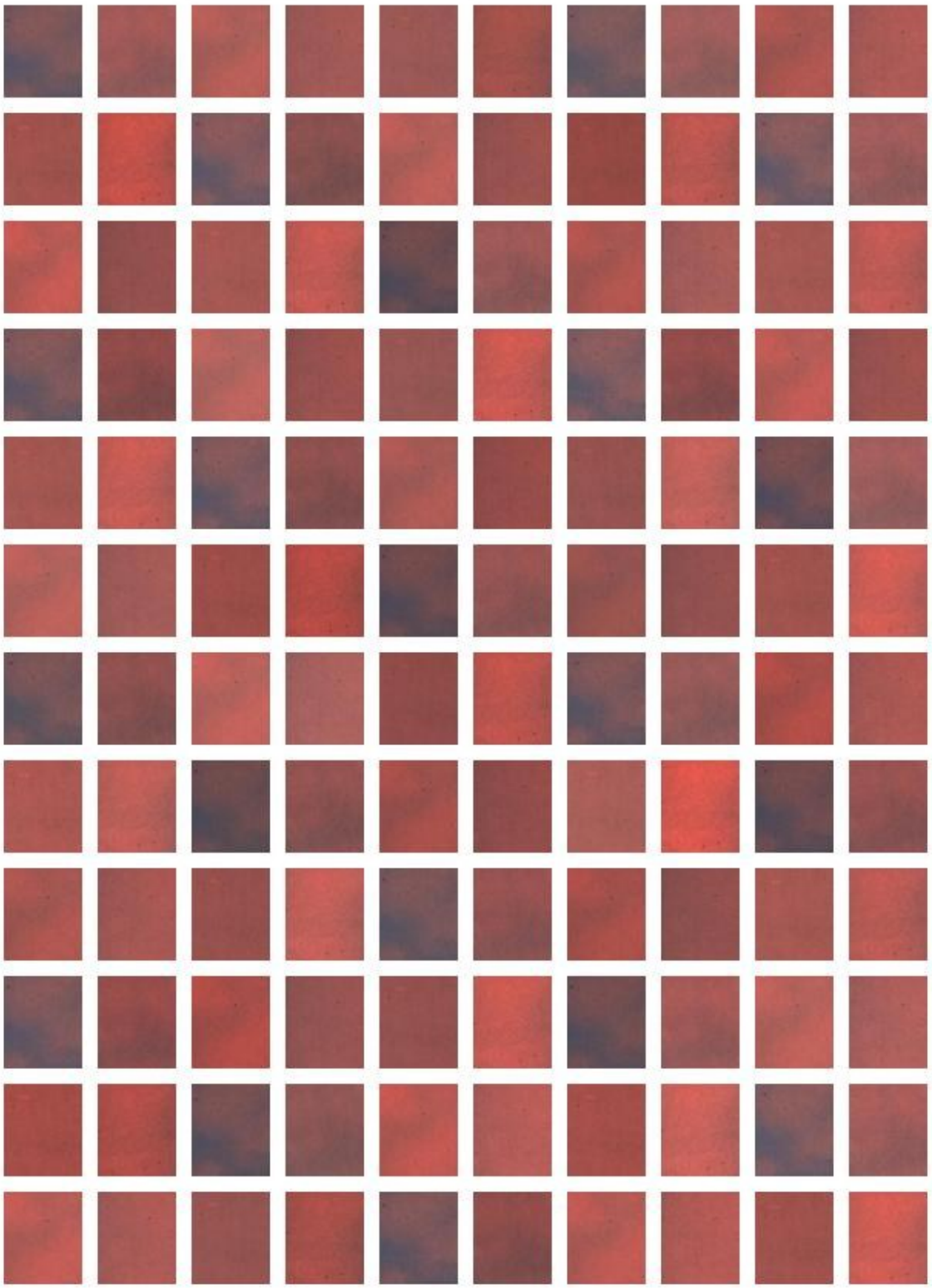

Colorimetric Response Grid - 15% PCDA

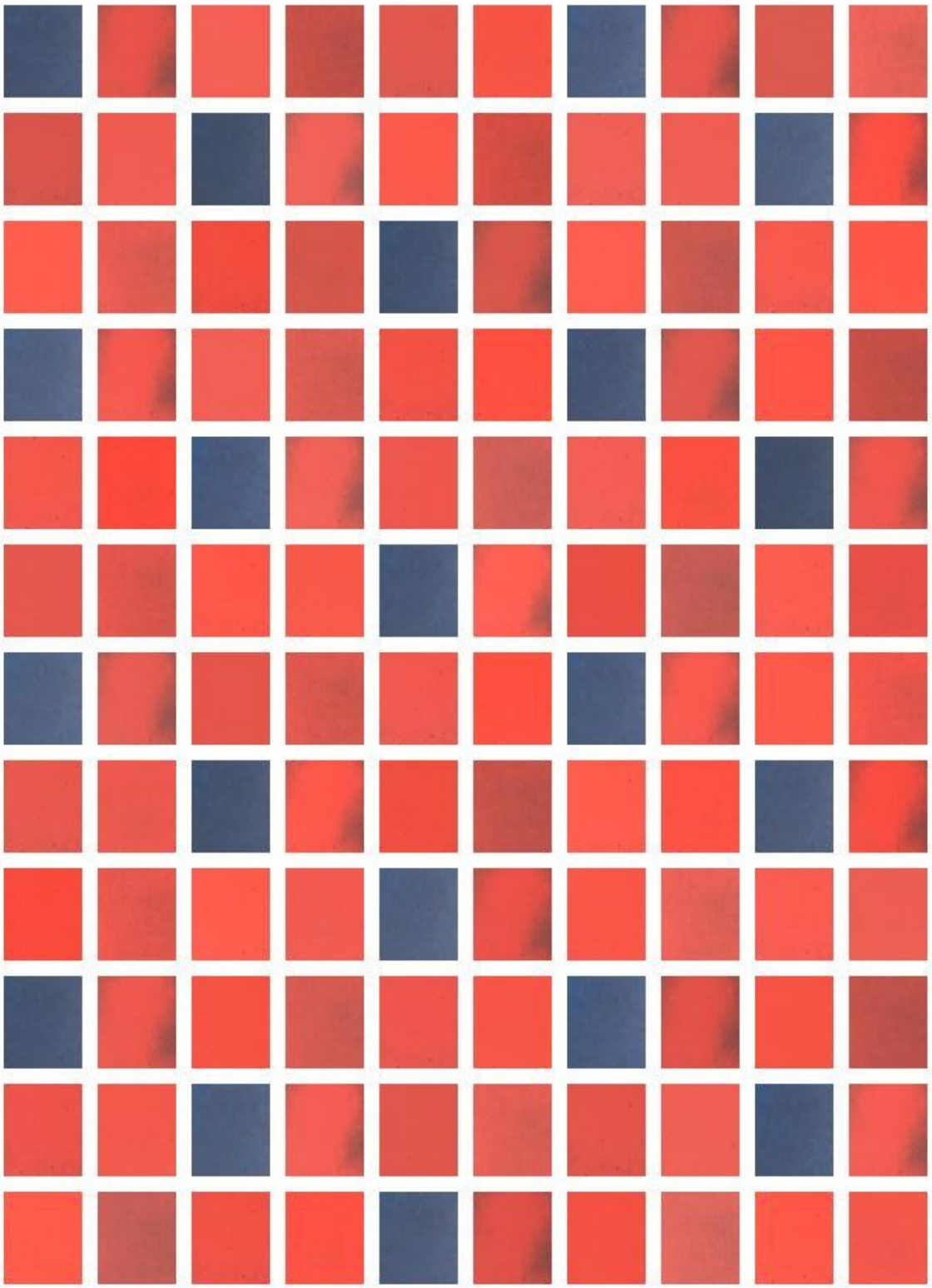

Colorimetric Response Grid - 15% PCDA

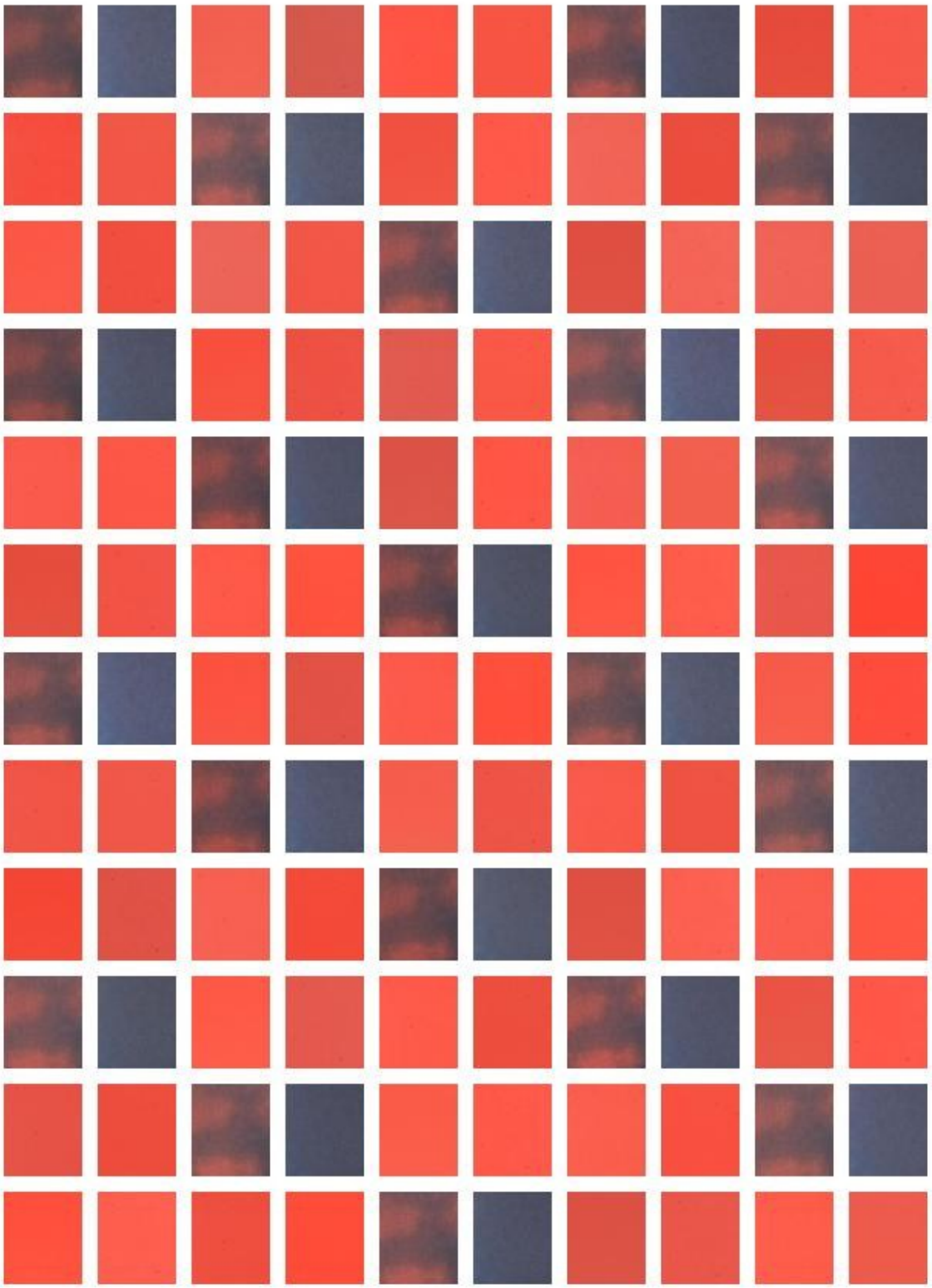

Colorimetric Response Grid - 15% PCDA

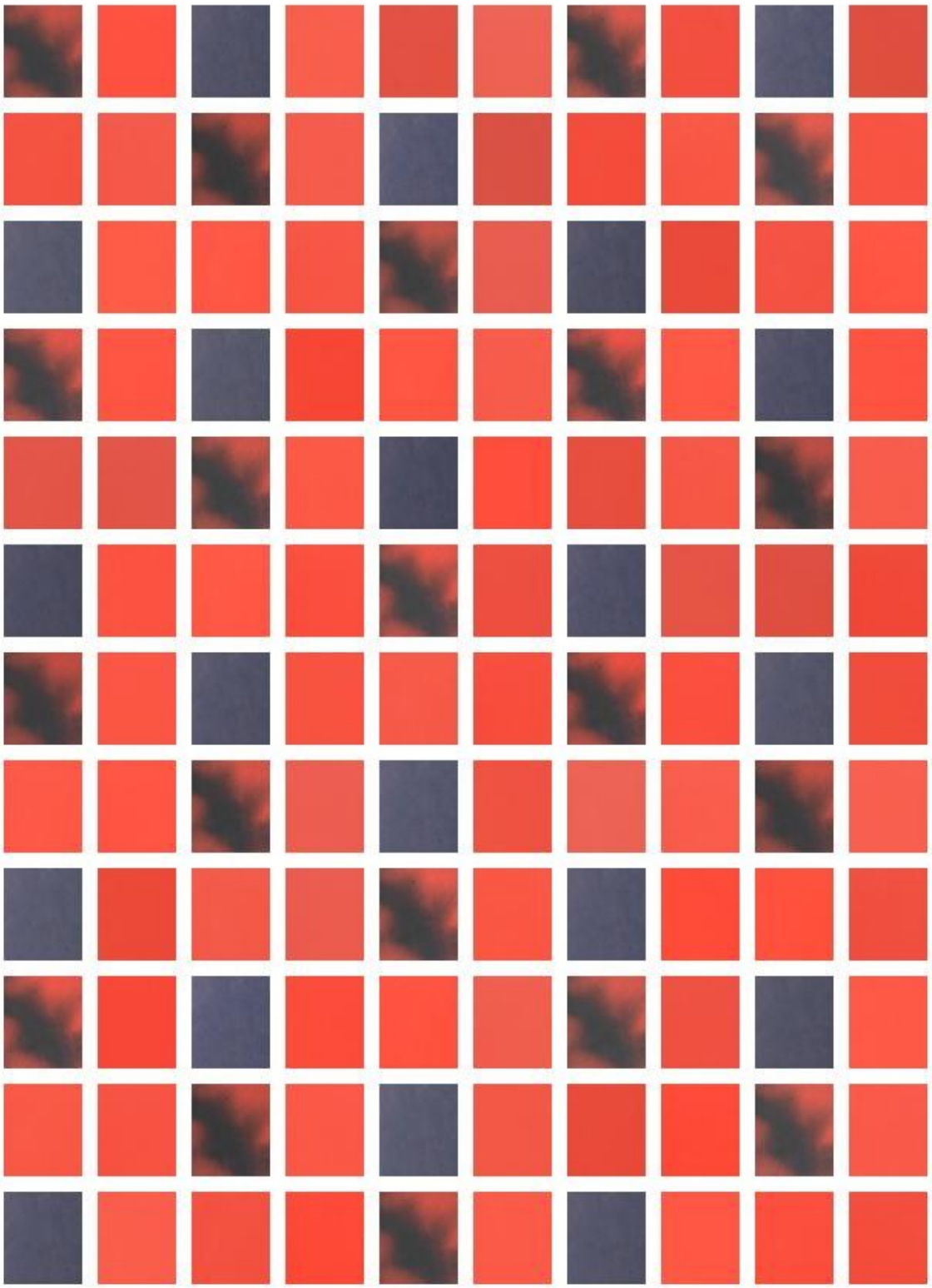

Colorimetric Response Grid - 18% PCDA

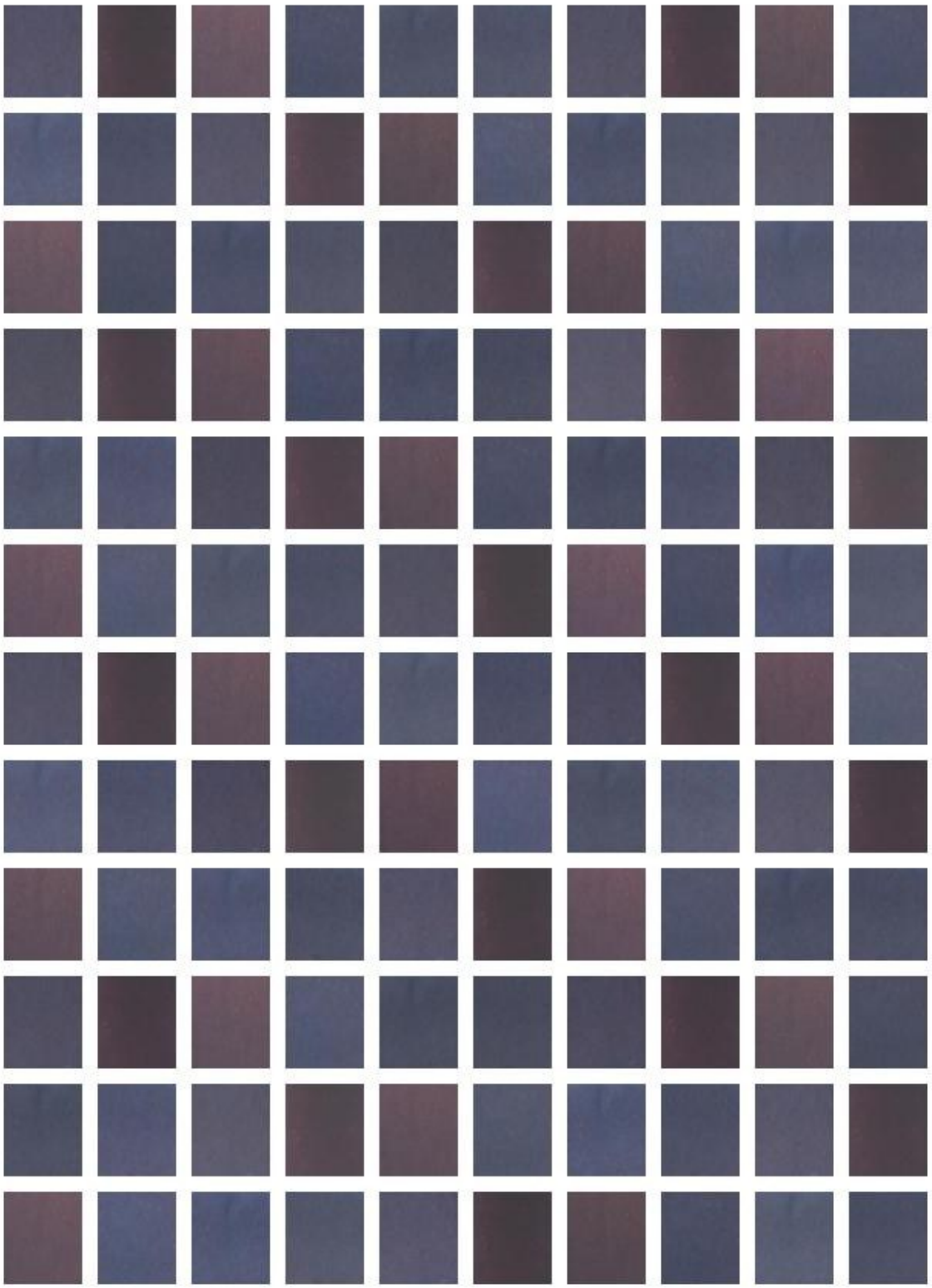

Colorimetric Response Grid - 18% PCDA

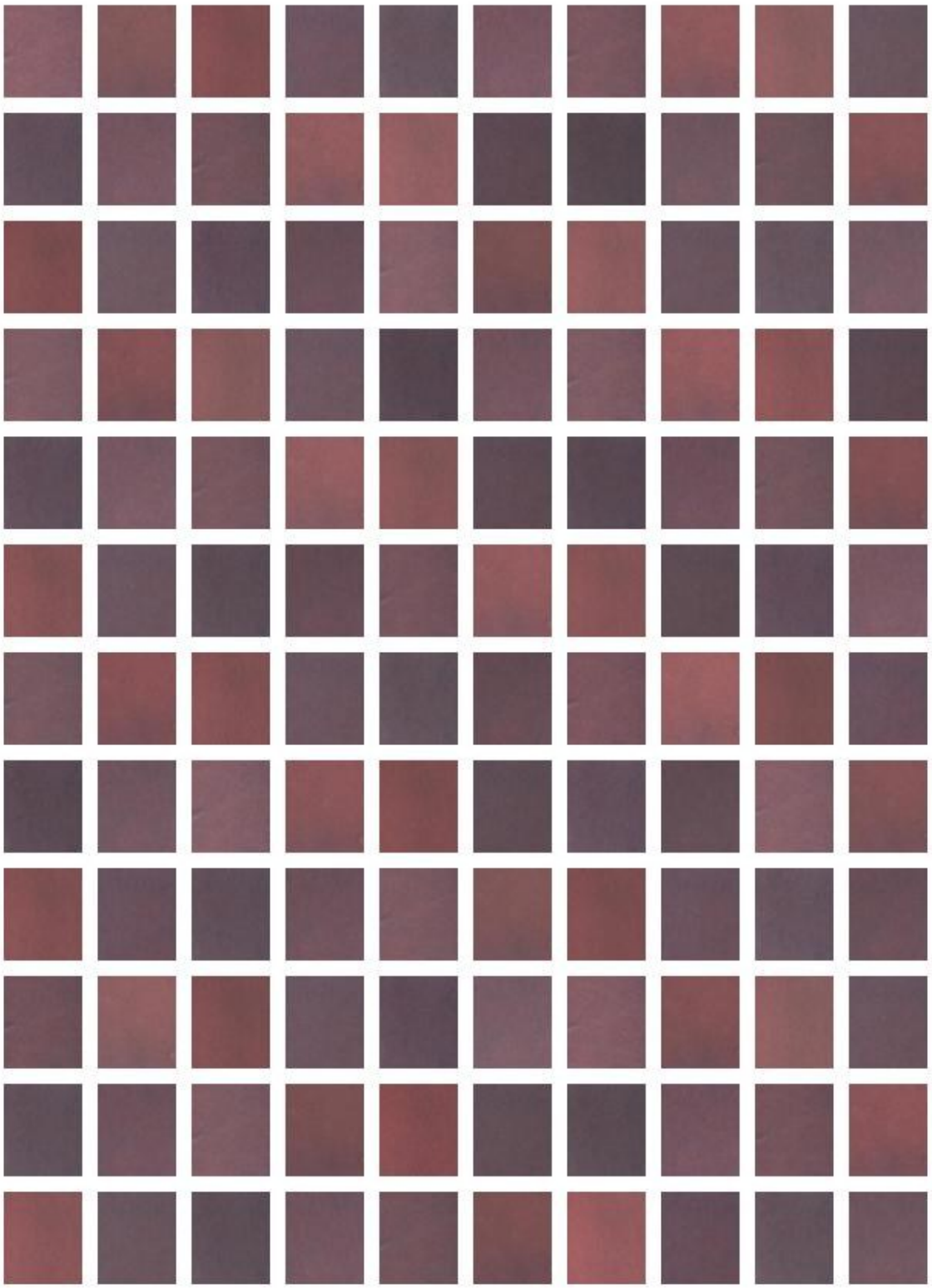

Colorimetric Response Grid - 18% PCDA

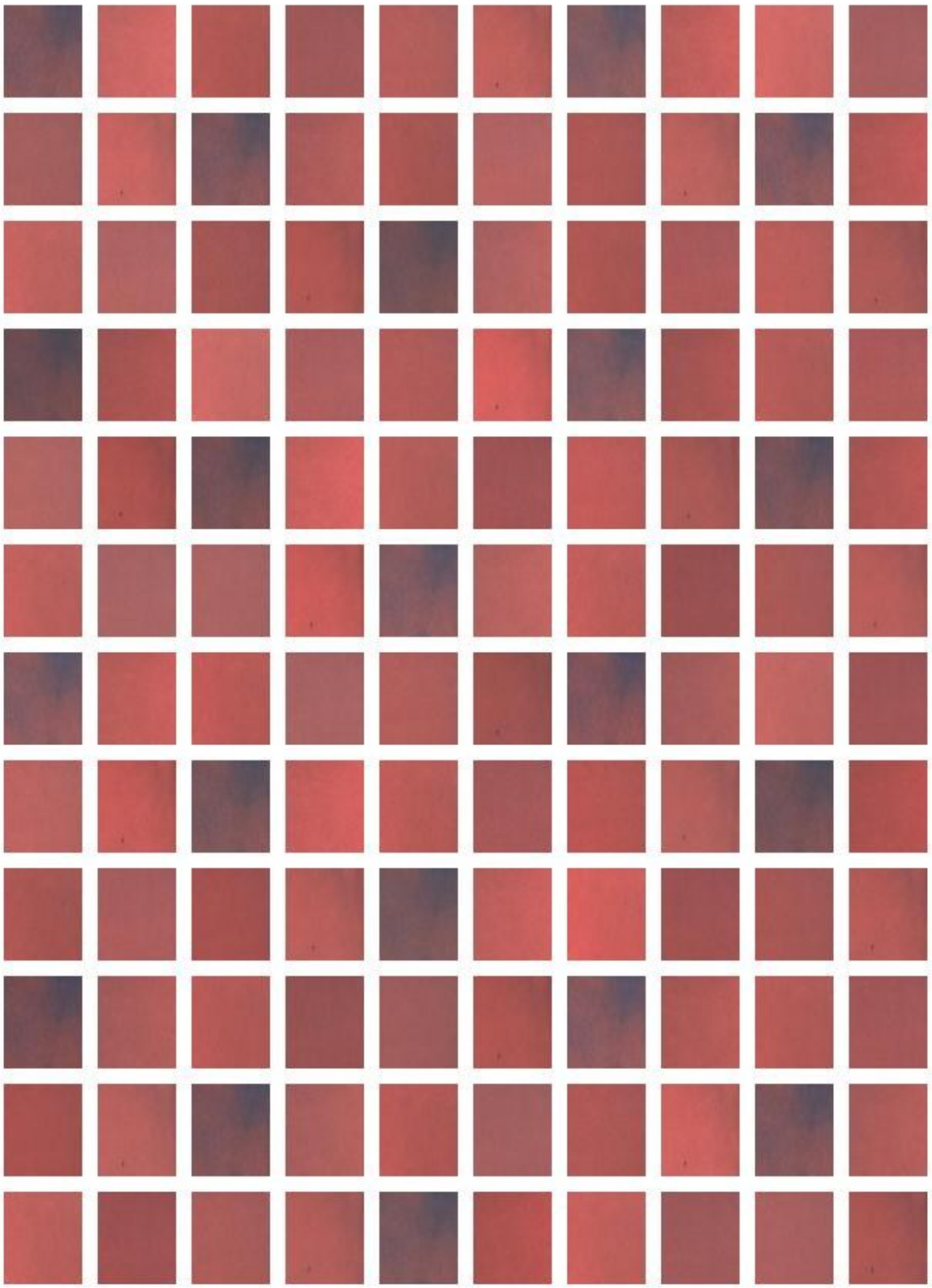

Colorimetric Response Grid - 18% PCDA

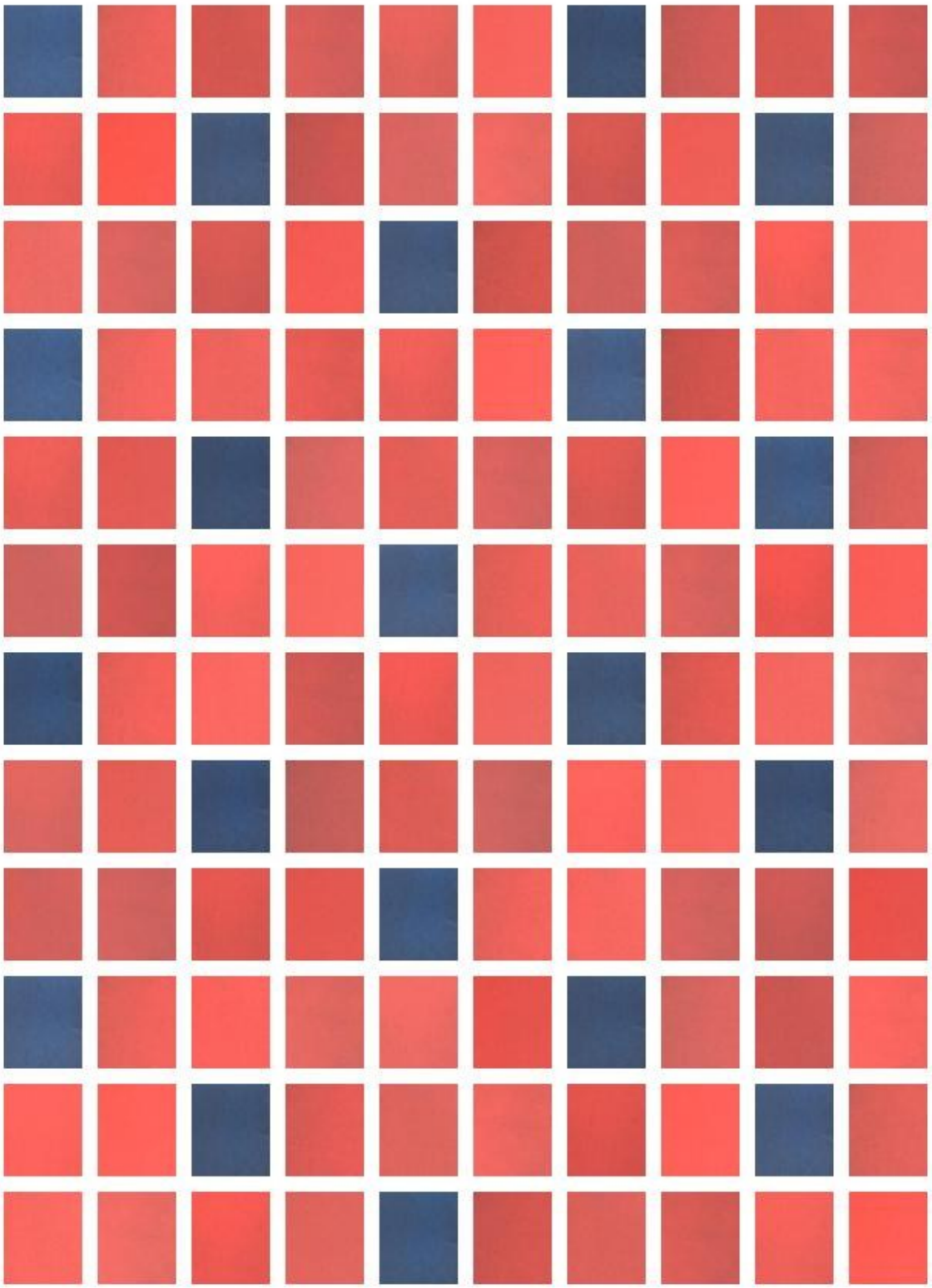

Colorimetric Response Grid - 18% PCDA

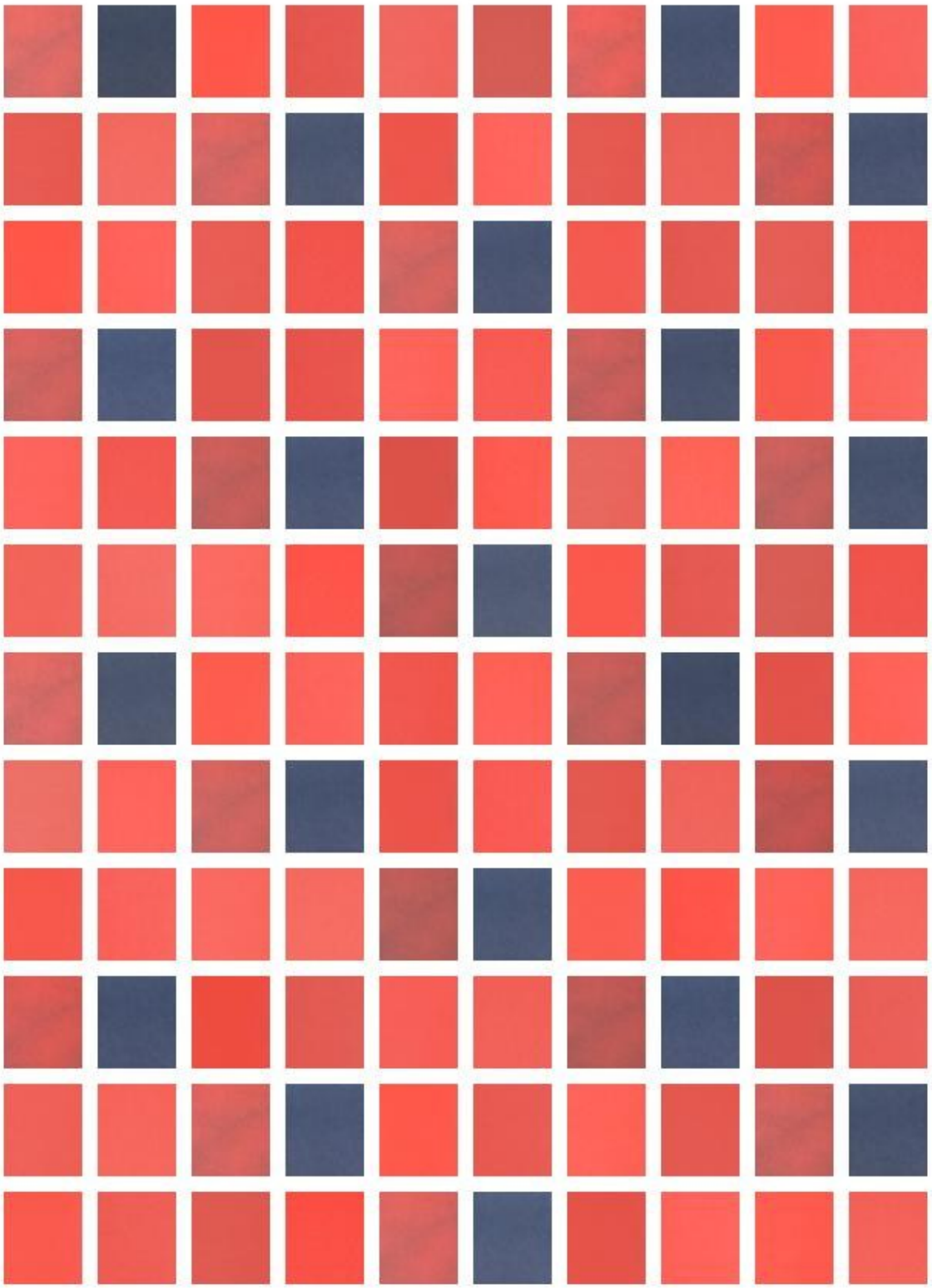

Colorimetric Response Grid - 18% PCDA

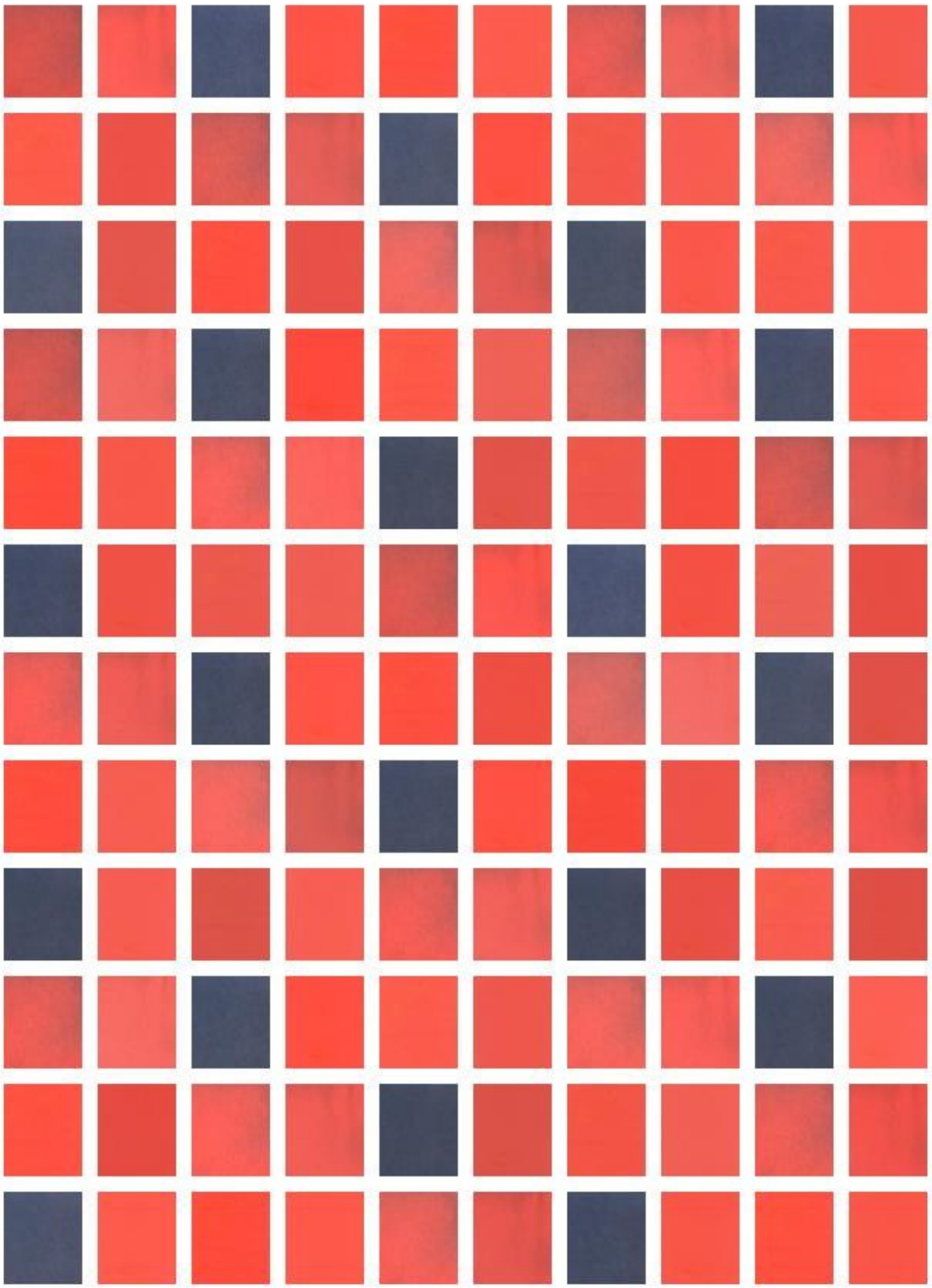

Colorimetric Response Grid - 20% PCDA

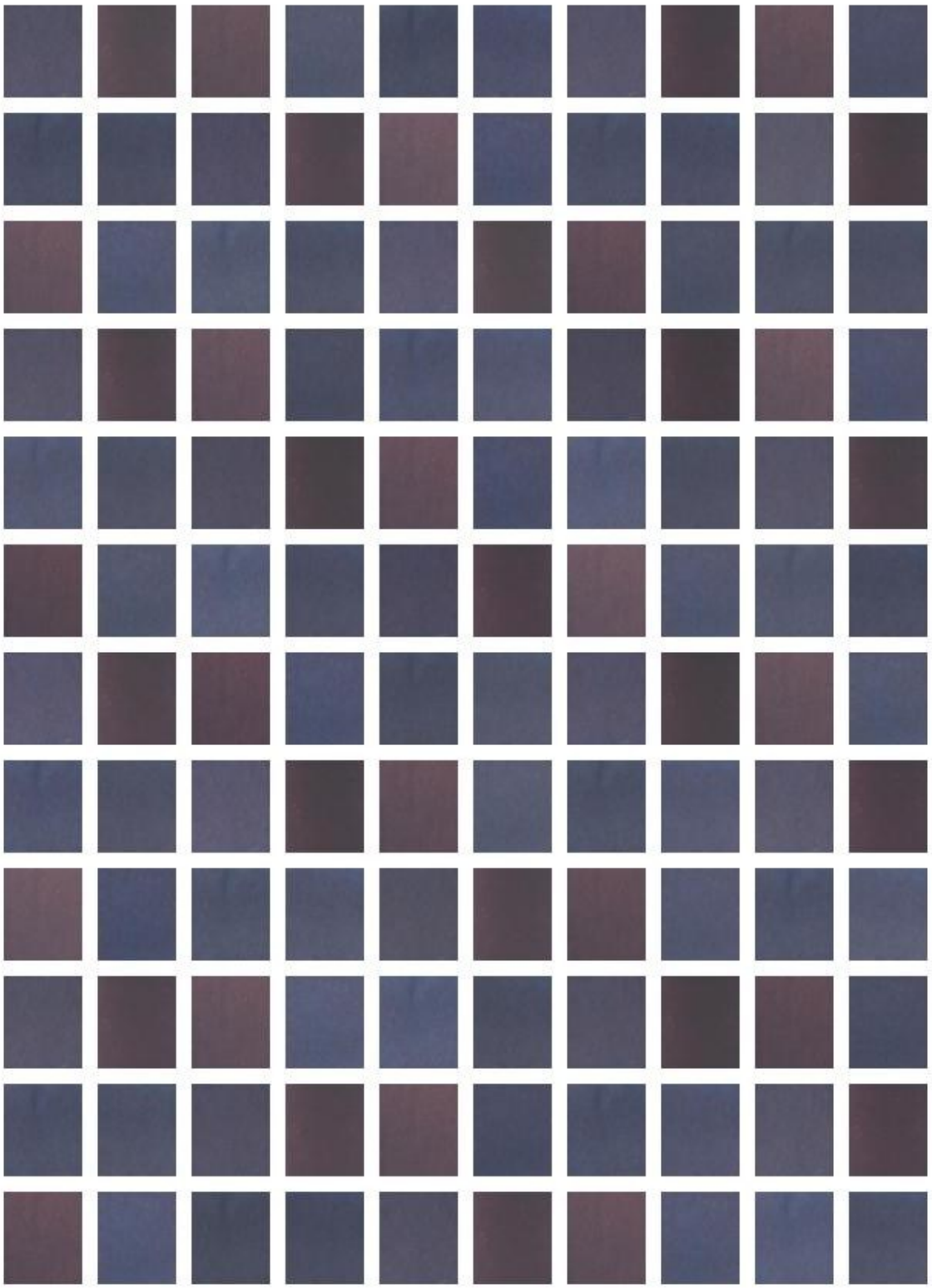

Colorimetric Response Grid - 20% PCDA

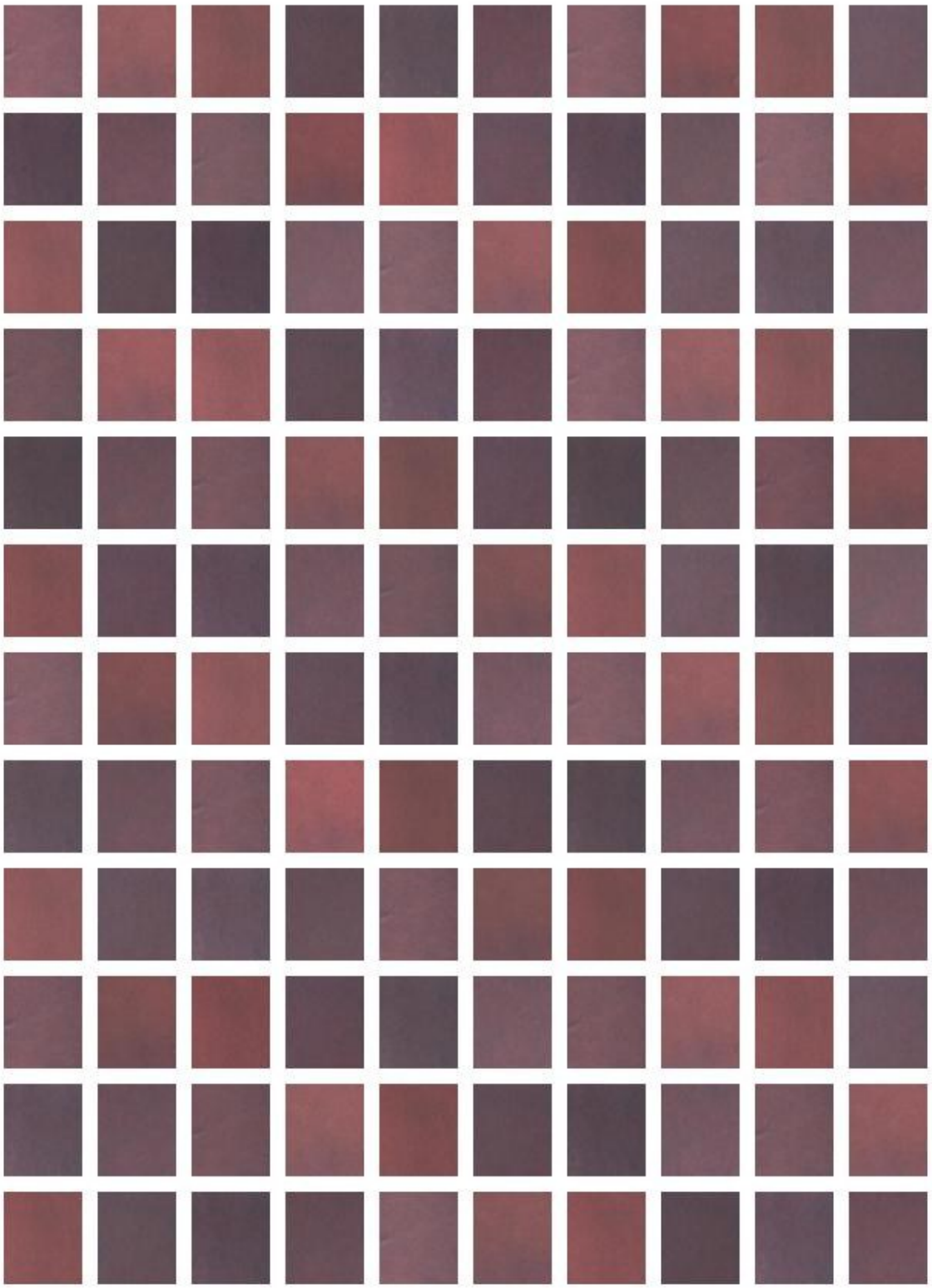

Colorimetric Response Grid - 20% PCDA

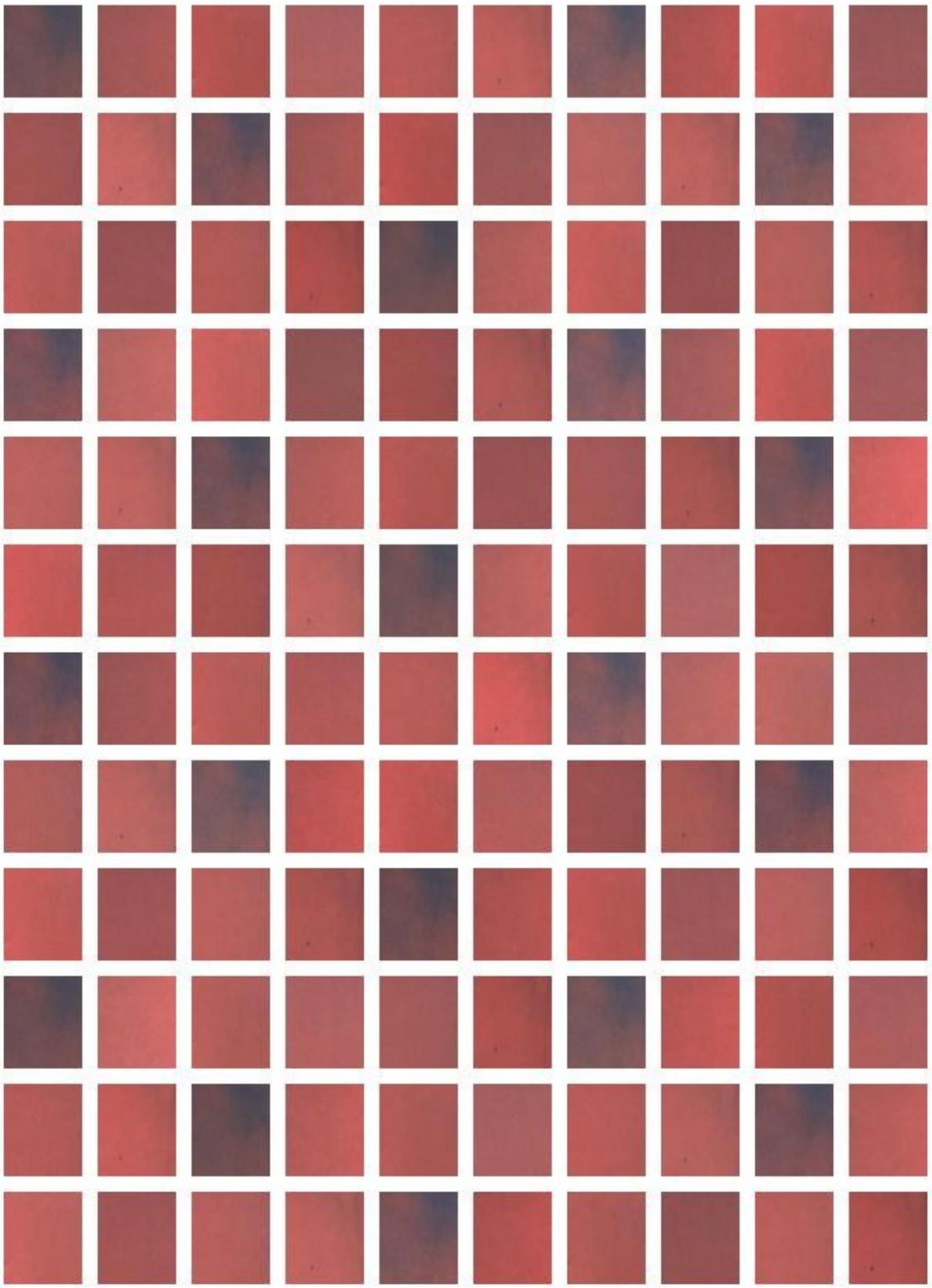

Colorimetric Response Grid - 20% PCDA

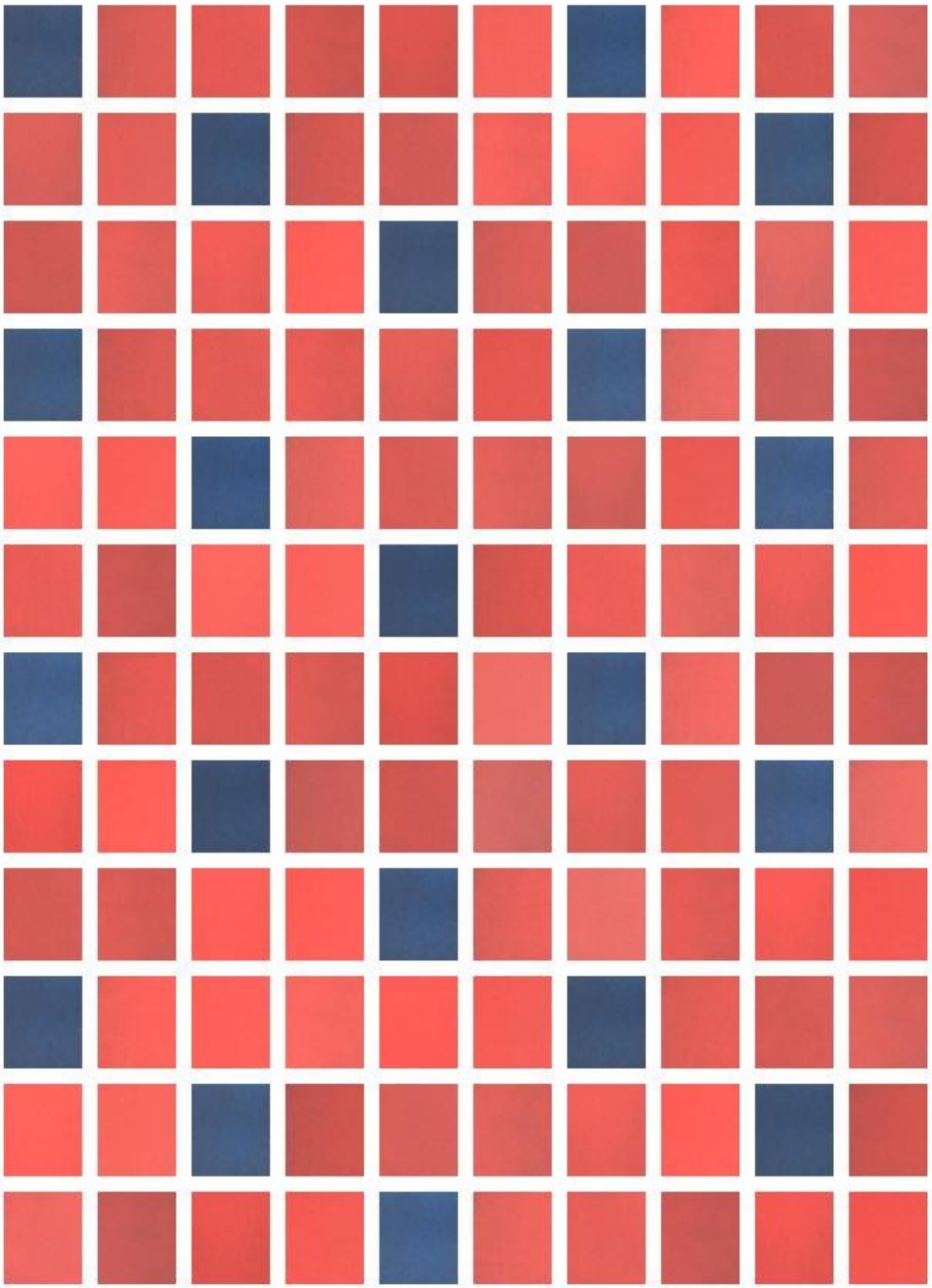

Colorimetric Response Grid - 20% PCDA

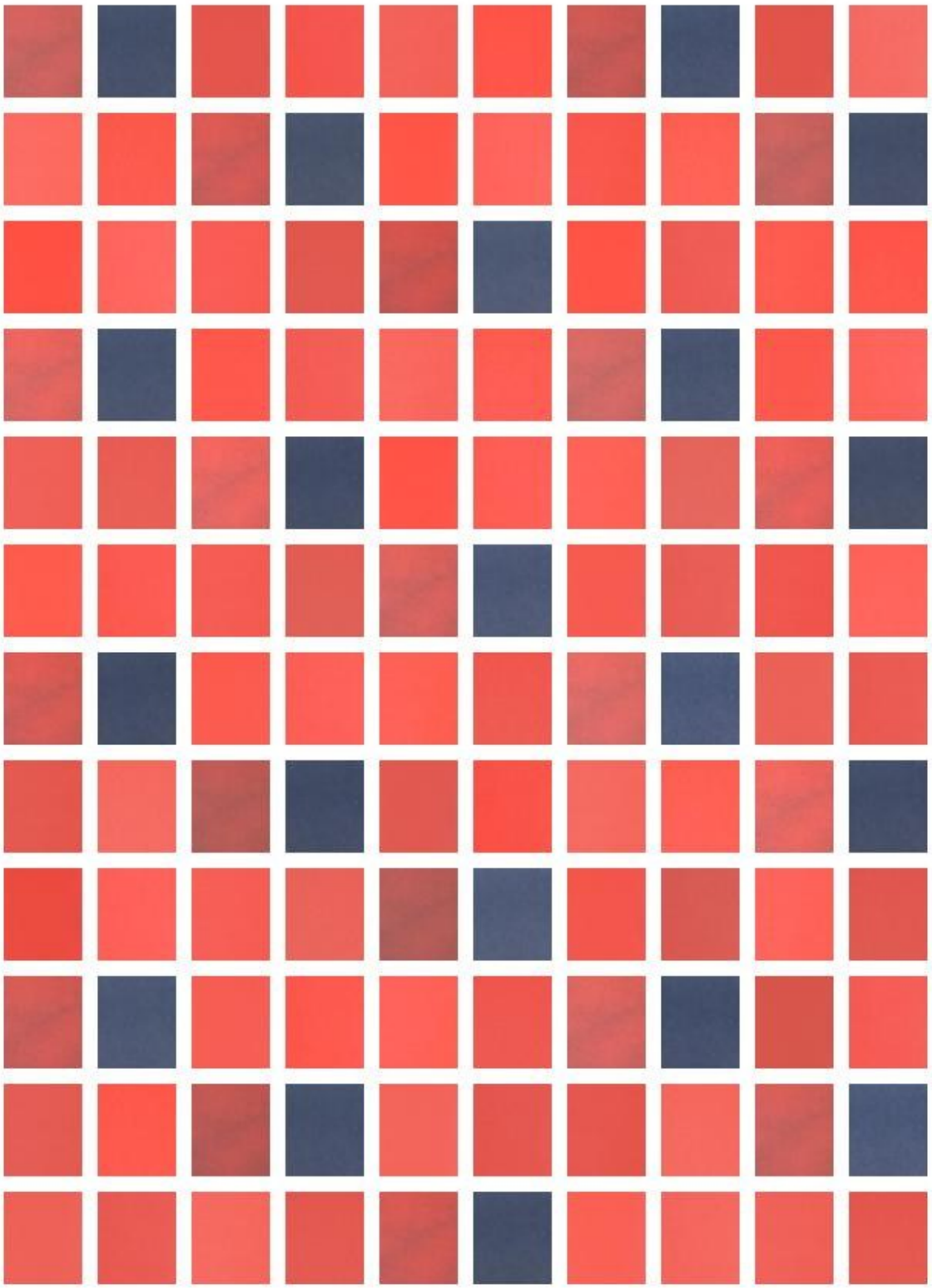

Colorimetric Response Grid - 20% PCDA